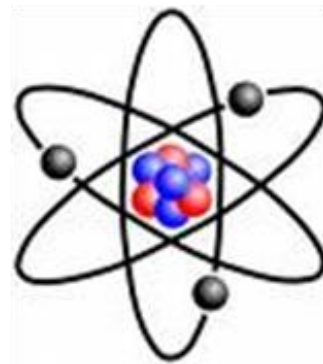


ISSN: 2167-9851

RATS



RESEARCH AND TECHNICAL STUDIES

Research and Technical Studies

Specialty Group Postprints

From the 49th Annual Meeting

Virtual Joint AIC/SPNHC Meeting, May 10 – June 25, 2021

Volume 9

2021



american
institute for
conservation

**Preserving Cultural
Heritage**

American Institute for Conservation

The Research and Technical Studies Specialty Group of the American Institute for Conservation 2021 Officers

Chair

Gregory Bailey

Program Chair

Federica Pozzi

Assistant Program Chair

Jane Klinger

Secretary/Treasurer

Courtney VonStein Murray

Publications Chair

Molly McGath

Chair Emeritus

Matthew Clarke

Research and Technical Studies Specialty Group Postprints

Abstracts, Extended Abstracts, and PowerPoint™ presentations from the 49th Annual Meetings of the American Institute for Conservation

RATS 2021 Annual Meeting Program Committee

Federica Pozzi (Program Chair), Jane Klinger and Gregory Bailey

Compiler

Molly McGath

Volume 9

2021



american
institute for
conservation

**Preserving Cultural
Heritage**

American Institute for Conservation

Volume 9 Online publication copyright © 2021. The Research and Technical Studies Group (RATS) and the American Institute for Conservation (AIC).

ISSN: 2167-9851

The manuscripts and presentations in this publication have been edited for grammar yet have not undergone a formal process of peer review. The contents of this volume were originally given as oral presentations at the Annual Meeting of the American Institute for Conservation (AIC). The materials, methods, results, and conclusions described herein are the opinion of the contributors and do not reflect the policies or opinions of AIC or RATS. All rights reserved by individual authors.

This online publication is intended for all members of AIC. Copies of this publication are available only in electronic format and may be downloaded.

American Institute for Conservation

757 15th Street, NW, Suite 500, Washington, DC 20005-1714

www.culturalheritage.org

Table of Contents

Research and Technical Studies Specialty Group Presentations: Advancement of Science and Technology.....	7
Cultural Heritage Meets Biotechnology: Nature-Science Collaborations in the Symbiocene	8
How Modern Mass Spectrometry is Reshaping What We Can Learn about Paintings, Objects and Cultural Heritage	9
Of Light and Darkness: The Use of Microfadedometry in Loan Decisions.....	11
Diving Deeper into the Origins and Intent of Organic Materials in Cultural Heritage by Combining DNA and Mass Spectrometry	12
Research and Technical Studies Specialty Group and Imaging Working Group Presentations	13
The Discovery of Community Stakeholders through the Technical Imaging Analysis of Georgia O'Keeffe's "Pelvis Series, Red with Yellow", 1946, oil on canvas, 36" x 48"	14
Building Reliable and Reusable Complex Digital Representations: The Digital Lab Notebook	16
Virtual Reality: A Versatile Tool for Historic Preservation.....	18
Recapturing Ancient Identities: Challenges and Discoveries from the Multispectral Imaging of Roman Egyptian Stelae at the Kelsey Museum.....	37
Practical LED-based Multispectral Imaging of Cultural Heritage Materials.....	67
Optical 3D Scanning System to Enable 3D Viewing, Sharing and Printing of Artworks	94
Titian's <i>Rape of Europa</i> : Artist's Pigments and Changes Revealed through Macro-XRF Mapping	96
Research and Technical Studies Specialty Group and the Society of the Preservation of Natural History Collections Presentations.....	99
Comparative Analysis of Consolidants Used to Treat Paper Shale Fossils	100
Reconstructing Asia's Ancient Ivory Trade: PCR and NGS Analysis of Elephant Tusk Sections from the Field Museum's Java Sea Shipwreck Collection.....	103
Put the Lime in the Coconut; An Investigation of the Mechanical and Aging Properties of Coconut Shell and Recommendations for Compatible Conservation Materials.....	110
Mineral Transformations on Pyrite: Microscopic to Macroscopic Perspectives.....	112
Early Plastics, Taxidermy, and Conservation at the Field Museum	114
Research and Technical Studies Specialty Group Presentations: Case Studies.....	115
The Development and Application of Instrumental Methods for the Identification of Materials and Processes used in the Manufacture of Orotone Photographs.....	116
A Low-Cost, Open Source Micro-fading Tester: Construction, Characterization, and Use.	118

Principals on Paper: Using FTIR Spectroscopy and Chemometrics for Non-Invasive Media Analysis.....	163
Elucidation of Natural Organic Red Colorants on Paper via Microsampling and Surface Enhanced Raman Spectroscopy	164

Research and Technical Studies Specialty Group Presentations: Advancement of Science and Technology

Cultural Heritage Meets Biotechnology: Nature-Science Collaborations in the Symbiocene

Theanne Schiros^{1,2*}, Helen Lu², Delfina Farías¹, Christian Joseph²,
Susanne Goetz¹, Romare Antrobus², Anne Marika Verploegh Chassé¹,
Shanece Esdaille², Yueh-Ting (Candice) Chui², Gwen (Karen)
Sanchirico¹

¹ Fashion Institute of Technology, New York, NY 10001

² Columbia University, New York, NY 10001

*Corresponding Author: Theanne Schiros, theanne_schiros@fitnyc.edu

Original Abstract

With anthropogenic activity putting Earth on course for a still avoidable mass extinction, and a global pandemic exposing vulnerabilities and systemic racism and injustices that have shaped our institutions, we seek to transform our mindset and practices to create more inclusive, critical and equitable world. This talk will explore opportunities for intersectional sustainability that combines cultural heritage with the frontiers of biotechnology to create a more equitable systems for safe, inclusive, development, through the lens of a circular materials economy. Can scientists and entrepreneurs collaborate with nature to utilize materials, energy and shared knowledge to build a resilient new normal- the Symbiocene- in which cultural diversity, biodiversity and a social justice foundation are valued and protected? Inspired by the complexity of nature and its robust regenerative potential, we harness microbial biosynthesis and adapt ancient textile techniques for the sustainable development of regenerative, high performance biotextiles. The work highlights how biofabrication and green chemistry processing, together with indigenous science and historically important textile dyes and arts, can strategically address the most damaging impacts of a linear economy, as encapsulated by the fashion industry.

How Modern Mass Spectrometry is Reshaping What We Can Learn about Paintings, Objects and Cultural Heritage

Caroline Tokarski

Original Abstract

For 20 years now, modern bio-mass spectrometry has been changing the analytical landscape of art, archaeology and cultural heritage. Alongside the technical improvements, the continuous emergence of new applications always allows improved structural elucidation of ancient components and interacting biomolecules, found in artworks and heritage objects.

Over this period, besides the effort made on sample preparation procedures, the substantial progress of mass analyzers in resolution/mass accuracy and sensitivity combined with increased capacity of fragmentation modes, have sustainably established "omics" techniques. Furthermore, these developments have confirmed mass spectrometry as a key stone to describing compounds, as varied in structure as in their complexities that are ancient lipids, sugars and proteins. From a few micrograms of precious sample from an object, and taking advantage of the computational power of new bioinformatics solutions, it is now possible to obtain protein/ tissue identity sequences and to discriminate biological species on a single amino acid basis.

In addition to this improved investigative process, enhancing knowledge of artworks and preservation approaches, we are now confronting, in heritage mass spectrometry, an even more complex issue of chemical decoding of biomolecular networks, their fine characterization, the study of cross-linking mechanisms, as well as the understanding of their modifications and interactions.

This presentation will illustrate how protein chemical signatures inform about ancient material manufacturing processes and conservation practices, and the impact of these procedures on protein structures.

In this context, the presentation will describe our latest developments in top-down and hydrogen deuterium exchange mass spectrometry to address complex questions of molecular interaction in networks in unaged and aged forms. Protein conformational changes and pigment interactions occurring during paint formulation, drying and ageing will be discussed. Analytical evidence of protein crosslinkings in historic artworks will be presented and discussed (e.g. tempera, painted leather). Other examples will also demonstrate the whole mass spectrometry capabilities in elucidating restoration procedures, based on specific chemical signature monitoring; e.g. the study of Coptic manuscripts will reveal the chemistry behind a treatment performed at the Vatican Library. Another example will show how our most recent analytical procedures for trace

level analysis based on miniaturized analytical workflow have provided insight into Thomas Gainsborough's working methods. Finally, High Resolution MALDI Imaging to decode biomolecular organization of the paint layer will also be presented. Intact material, by-products and organic-inorganic interaction examples will help to reveal evident aptitudes of this promising technique in the heritage field.

These examples will be illustrated by several outstanding cases of study from the Metropolitan Museum of Art collection and the Morgan Library.

Of Light and Darkness: The Use of Microfadometry in Loan Decisions

Emilie Cloos^{1*}

¹ The National Archives UK, Bessant Drive, Richmond TW9 4DU, United-Kingdom

* Corresponding Author: Emilie Cloos, Emilie.cloos@nationalarchives.gov.uk

Original Abstract

The museum professional knows very well of the dichotomy when it comes to light: we need it to show our collections but it is, in turn, one of the main agents of deterioration. Light is our ally and our enemy – how can we find a happy balance between displaying our collections and preserving them for the generations to come?

A few years ago, the Collection Care department at The National Archives UK acquired a Microfadometer, a scientific instrument that helps predict how certain media will react to light in the gallery environment. This talk will highlight why and how the loans team uses the technique and what its advantages and downfalls have been. When most of The National Archives' collection items fall into the 'vulnerable' and 'high' light sensitivity categories, what has microfading taught us and how is it being used alongside our lighting policy?

On the one hand, the technique allows for better light sensitivity categorization, provides empirical data to support and justify decision-making and increases material knowledge of our collection. On the other, we are faced with issues of reciprocity and reproducibility, issues with the reference standards (blue wools), as well as data interpretation and translation into real-life display solutions.

Through illustrative examples, from colorful propaganda posters to Titanic telegrams, we will discuss the ethical and technical challenges of using this instrument, as well as the steep learning curve faced by the non-scientist users.

Diving Deeper into the Origins and Intent of Organic Materials in Cultural Heritage by Combining DNA and Mass Spectrometry

Julie Arslanoglu, Christopher Mason

Original Abstract

In the early history of organic materials analysis in cultural heritage, the class of the material (oil, wax resin, protein, etc.) was the benchmark. As more advanced mass spectrometric techniques were incorporated into cultural heritage analysis, more precise assignment of specific types of materials could be distinguished (linseed oil v. poppy seed oil, beeswax v. Carbowax, egg white v. collagen, etc.). However, complex mixtures, reactions between organic material mixtures and pigments, as well as organic materials that are not in our libraries (non-European materials) can cause inaccurate identification of materials and even missing entirely some significant information. One way to address these hurdles is to expand our approach so that we are probing all aspects of organic matter (oil from seeds, proteins from tissues, gums from plants): their molecular building blocks (proteins, lipids, polysaccharides) as well as their instructions (DNA, genomics, and DNA damage rates). Mass spectrometry (LCMS, MALDI) of the molecular building blocks can be described as “-omics” and allows us to distinguish between structures that are too similar or too complex to investigate using GCMS approaches. However, DNA takes into another arena that has been little explored or correlated to MS in cultural heritage. DNA provide a unique access point into the specific species source and can often link material to a geographic area. Yet there is so much more DNA information in an art sample than just the materials used to make the artwork. There are masses of “meta data” from the DNA of microorganisms deriving from not only the moment in time when the artwork was created, but also its exposure throughout its lifetime. However, all of this information needs to be put into context: the mere presence of something does not necessarily mean that it is significant. The key is the integration and interpretation of all of this information and for that, a team with specialists in bioinformatics, historical botany and biology, human populations, material use in cultural heritage, as well as technical experts are required. The Met is collaborating with Weill Cornell Medicine and The University of Bordeaux to embark on a combined DNA and “multi-omics” approach (genome, epigenome, proteome, lipidome, microbiome) to investigate two unresolved questions: (1) the identification of Chia oil in Mexican colonial artworks and (2) distinguishing author attribution between paintings by Hokusai and his daughter, Katsushika Ōi. Here we will present the process and decisions about each of the research paths as well as a discussion of the critical role of metadata that is often discarded in our quest for a fast, accurate “answer”.

Research and Technical Studies Specialty Group and Imaging Working Group Presentations

The Discovery of Community Stakeholders through the Technical Imaging Analysis of Georgia O'Keeffe's "Pelvis Series, Red with Yellow", 1946, oil on canvas, 36" x 48"

Dale Kronkright

Original Abstract

Today, much of the documentation, analyses and characterization of the tangible evidence of fabrication, repair and re-use of heritage sites and materials is done using technical imaging. Multi-spectral imaging, x-radiography, 3D surface imaging and modeling, SEM/EDS, and scanning XRF are all examples of imaging techniques that are now part of an array of data gathering techniques used to detect, characterize and monitor the tangible characteristics of heritage materials.

Typically, prior to setting out on a course of treatment, conservators and conservation scientists analyze materials, structures, evidence of previous alterations and deterioration products, as well as archives and historic documentation to determine how a particular work was intended to look and function when first fabricated. Conservation practice has evolved further to reflect a holistic approach to the understanding of the cultural contexts and changing uses of heritage materials over time. It is increasingly common to characterize the tangible evidence of use, repair, re-use, ritual care and even disposal. In this way, conservators have a more complete understanding of changing intensions, uses, preferences, and values reflected in each fragment of evidence of alteration. Conservators now understand that any given course of treatment that removes, replaces or obscures some existing condition of a work emphasizes the evidence certain values while removing or disguising the evidence of others. Imaging documentation helps preserve the understanding of all the evidence of uses, damage, repair and fabrication, including those that might be removed or obscured as a result of contemporary conservation interventions.

Conservation has been less intentional about identifying and documenting what a heritage object or site does, culturally for contemporary stakeholders. Stakeholders are individuals, groups and even organizations whose self-identity, personal or social agency and well-being are linked to the object or site. It is uncommon for conservators to investigate what a heritage object means and does for its contemporary stakeholders, beyond the exhibition and programmatic intentions of an owner, museum or heritage agency. While this type of preservation research is gaining traction in the preservation of archaeological and Indigenous material culture, its application to contemporary art is far more rare.

This presentation illustrates how the technical characterization of materials used by the American modern artist Georgia O'Keeffe in 1946 in the canvas painting "Pelvis Series, Red with Yellow" (36" x 48", Georgia O'Keeffe Museum L.1997.3.4) helped the Museum discover and begin new dialogues with previously unrecognized stakeholders. In this abstraction of the void in an animal pelvis bone, high-key orange, red and yellow, pigments were characterized which connect the work to Veterans of World War II, Los Alamos National Lab, the Santa Fe War Relocation Internment Camp for Japanese Americans, and descendants of workers in New Mexico's uranium, coal, lead, zinc and barium mines. The discovery of possible stakeholders, as a result of technical analysis allows the descendent populations of all these groups claim a meaningful connection to painting and to the museum.

Building Reliable and Reusable Complex Digital Representations: The Digital Lab Notebook

Carla Schroer, Mark Mudge

Original Abstract

How do we capture, process, and archive digital cultural heritage data in a way that is scientific, transparent, and reusable by others, both today and in the future? How do we enable broad participation in the documentation of heritage especially for indigenous and first nations peoples? How do we separate the quality and authenticity of digital representations from the authority of who created them?

This paper will begin to answer these questions. We will explore the Digital Lab Notebook (DLN), a new set of open source software tools for the near-automatic recording and archiving of computational photography-based digital representations and their contextual and process metadata. These computational photography techniques include Reflectance Transformation Imaging (RTI), 3D Photogrammetry, Multispectral Imaging (MSI) and sets of documentary photographs.

The DLN software, currently funded by a grant from the National Endowment for the Humanities (NEH), is under development, with an expected 1.0 release in the first quarter of 2021. We will demonstrate the software, discuss its goals and future directions, and share our experience using these tools in professional training sessions. Additionally, we will share our experience working with local communities in Albania and Nigeria, the Tlingit community in Southeast Alaska, the Unangax community of the Aleutian Islands, and Maori weavers in New Zealand. The common thread running through these projects is the deep desire for local and indigenous peoples to take back the narrative of their own heritage.

Photography based imaging approaches along with tools such as the DLN can help make this a reality. The DLN serves the same function as a written scientist's lab notebook. It permits a digital representation to be qualitatively evaluated for reliability and fitness for purpose by others. This provides the opportunity for informed reuse of cultural heritage digital documentation. The DLN enables the documentary work of local cultural communities to stand toe-to-toe with the work of authoritative institutions. The quality of each community's work can speak for itself.

The talk will also explore the necessity for transparent evaluation of scientific digital representations. The goal is to establish the conditions under which a "real-world" artifact can be digitally represented as a "digital surrogate", which can reliably serve as a digital stand-in usable for subsequent scientific or scholarly examinations. The DLN dramatically simplifies the process of scientific imaging. It also manages the creation of archival

Submission Information Packages (SIPs), built in conformance with international standards (the CIDOC/CRM). The DLN's Archiver tool prepares image data, built digital representations and their scientific metadata for intake into long-term preservation environments. This simplification of scientific imaging and the dissemination of computational photography to indigenous and other local cultural communities enable people around the world to tell their own stories. Broadening participation in the creation of cultural heritage documentation can both widen the perspectives and enrich the world's understanding of how people before us have lived a human life.

Virtual Reality: A Versatile Tool for Historic Preservation

Yeneneh Terefe*

*Corresponding Author: Yeneneh Terefe, yenterefe@gmail.com

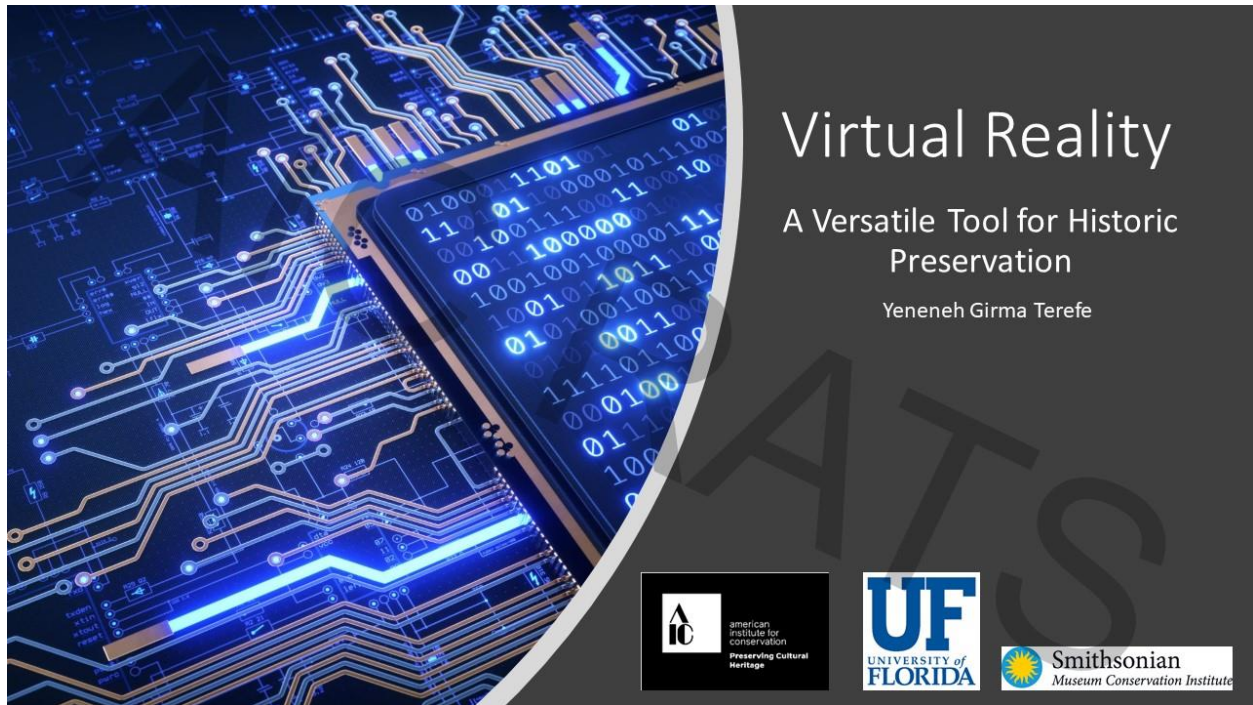
Original Abstract

Historic preservation's goal is to transfer the past to future generations by accurately documenting all the changes that occurred throughout the years. Digital technology provides accurate documentation of existing conditions and allows preservationists to accurately transfer information for future use.

Preserving the past is not simple for various reasons such as sea-level rise, natural disasters, war, and competing interests with more financial incentives like development projects. Accurate documentation and more specifically digital documentation gives preservationist a blueprint of a historic site which could be used to rebuild sites like the Bamiyan Buddha in Afghanistan and Palmyra in Syria, help in restoration projects in Notre-Dame of Paris, and serve as sea-level rise prediction model in Miami. Virtual reality offers an immersive form of digital documentation that allows users to experience the site in first-person perspective. Such perspective could potentially be used as an advocacy tool to galvanize and energize concerned stakeholders in the preservation of a historic site. Another benefit of VR is the ability to experience a historic site from the comfort of our house, especially due to COVID-19.

The goal of this research project is to create a VR application (app) that could be used as an advocacy tool in historic preservation (HP). Historic Old Mount Carmel Church in Gainesville, Florida was captured using a 360-degree camera and imported into Unity game-engine to create a VR app. The app was installed in Oculus Quest head mounted display (HMD). The future goal of this project is to determine whether VR could be used as an advocacy tool.

Annotated Slides



My presentation will be on how virtual reality can be used as a versatile tool for preservation. The presentation will provide an overview of my graduate research developing a virtual reality application and its potential as an advocacy tool for historic preservation, especially for a historic church.

Image: A blue semi-conductor picture on the left and three logos along the bottom. The logos are the AIC, University of Florida logo, and the Smithsonian's Museum Conservation Institute.



Addis Ababa, Ethiopia

Background

- Personal background
 - Born in Addis Ababa, Ethiopia
 - Interest in preservation and digital technology
- Academic background
 - BA in Business Administration, Truman State University
 - MA in Anthropology, University of Florida
 - MHP in Historic Preservation, University of Florida
- Thesis/ Master's research: "Virtual Reality: A Versatile Tool for Historic Preservation"

2

My passion for historic preservation started in my birth country of Ethiopia while on a summer historic site tour. The condition and management of these sites were poor, and I decided to pursue conservation to help preserve them. In order to do so, I envisioned combining my passion for video games and 3D technology to digitally recreate these sites for documentation and entertainment purposes. In college, for various reasons, I ended up pursuing a Bachelor's of Art in International Marketing. Unsatisfied with my degree, I pursued a Master's of Art in Anthropology focusing on cultural heritage management. After graduation, I moved to Washington D.C. and had the privilege of doing a four-months fellowship at the Smithsonian's Museum Conservation Institute with imaging scientist E. Keats Webb. As a fellow, I learned about photogrammetry and reflectance transformation imaging (RTI). Equipped with new knowledge, I decided to go back to school to study 3D laser-scanning for historic preservation, but in addition, I had the opportunity to learn about virtual reality.

Image: Image was taken in Addis Ababa, Ethiopia depicting rail tracks, buildings and an urban landscape.



Virtual Reality

Digital simulation of an environment through one or more of the senses such as sight, touch, and/or hearing.

- Display¹:
 - Head mounted display (HMD)
 - CAVE Automatic Virtual Environment (CAVE)
 - Large monitors
 - Smartphones and personal computers
- Different Immersive levels²:
 - Fully-immersive
 - Semi-immersive
 - Non-immersive

1 Wedel, M., Bigné, E., & Zhang, J. (2020). Virtual and augmented reality: Advancing research in consumer marketing. *International Journal of Research in Marketing*, 37(3), 443–465.

2 Bekes, M. K., Pierdicca, R., Frontoni, E., Malinverni, E. S., & Galin, J. (2018). A Survey of Augmented, Virtual, and Mixed Reality for Cultural Heritage. *ACM JOURNAL ON COMPUTING AND CULTURAL HERITAGE*, 11(2).

Virtual reality is a digital simulation of an environment through one of our senses such as sight, touch, and/or hearing, and sight is one of the major senses engaged during a VR experience. There are four ways in which VR engages with our sense of sight¹:

Head mounted displays (HMD) block the user's view/ environment and replaces it with a digital environment or reality;

CAVE Automatic Virtual Environment (CAVE) is a 360-degree projection in a cave-like room giving the impression that one is fully immersed in a different environment or reality;

Large monitors with stereoscopic glasses give the illusion that objects are projecting out of the screen/monitor; and

Smartphones and personal computers can be used to access and interact with virtual reality but do not provide an immersive environment.

The different displays correspond to a different level of immersion²:

Fully-immersive environments disconnect the viewer from their surroundings and fully immerses them in a virtual environment which can be done using an HMD or a CAVE.

Semi-immersive environments are often experienced through large screens or projections and can be experienced by multiple users.

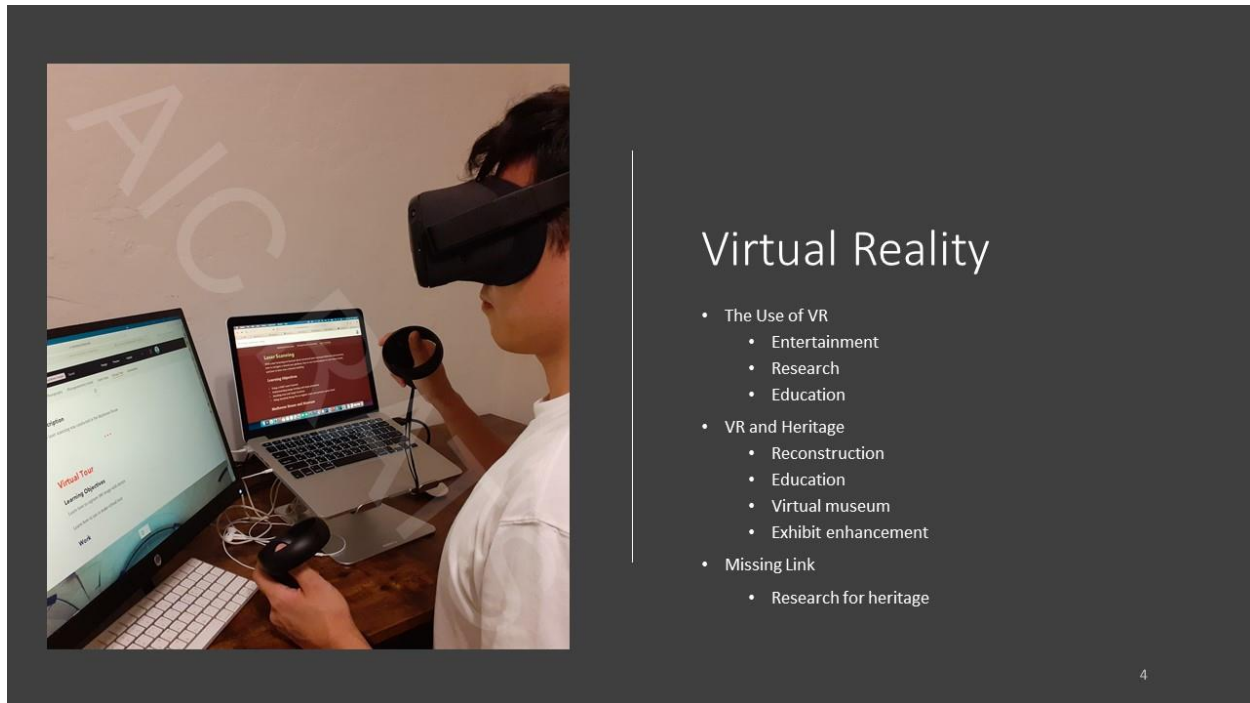
Non-immersive is the least immersive option for experiencing VR and can be viewed through a desktop computer or handheld device.

Image: A young man is wearing a head mounted display and holding controllers in each hand while seated next to a monitor and laptop on his desk.

Citation:

1 Wedel, M., Bigné, E., & Zhang, J. (2020). Virtual and augmented reality: Advancing research in consumer marketing. *International Journal of Research in Marketing*, 37(3), 443–465. <https://doi.org/10.1016/j.ijresmar.2020.04.004>

2 Bekele, M. K., Pierdicca, R., Frontoni, E., Malinverni, E. S., & Gain, J. (2018). A Survey of Augmented, Virtual, and Mixed Reality for Cultural Heritage. *ACM JOURNAL ON COMPUTING AND CULTURAL HERITAGE*, 11(2). <https://doi.org/10.1145/3145534>



VR research started in the 1960s and it was released as a consumer product in the 80s/ 90s by Nintendo, but the technology did poorly in sales. In 2010 and beyond, VR started to attract the attention of consumers and companies due to the advancement in computer graphics, animation, and artificial intelligence (AI).

Outside of the entertainment industry, VR was also attracting the attention of learning institutions, construction companies, and museums. In museums, it is mainly used in four different ways: reconstruction of past built environments, education by tailoring a unique experience for visitors through gamification, virtual museums to access the collection of the museum virtually and remotely, and exhibit enhancement to allow visitors to have a greater degree of interaction and information about a collection.

In the heritage field, VR is used to enhance visitors' experience and little as a research tool. This research aimed to offer a new perspective on the use of VR in heritage and how it could be used differently in historic preservation.

Image: A young man is wearing a head mounted display and holding controllers in each hand while seated next to a monitor and laptop on his desk.



Case Study: Old Mount Carmel

Historic church in Gainesville, FL

- Used during Civil Rights by Reverend Wright and NAACP
- Church played an important role in the desegregation of schools in the city
- Preserving Church with participation from various stakeholders
 - Black Community
 - Old Mount Carmel Congregation
 - City of Gainesville/ Planning and Historic Preservation
 - University of Florida

5

For this research, former director of the University of Florida's Historic Preservation program Morris Hylton III encouraged me to focus on an ongoing project at the time. The project was to nominate Old Mount Carmel Church in Gainesville, Florida as a historic site while simultaneously working on a renovation plan and structure report. My task was to create a VR application about the church which will be further discussed in the upcoming slides.

Old Mount Carmel and Reverend Wright played a pivotal role in the Civil Rights by hosting prominent members of the National Association for the Advancement of Colored People (NAACP), and by playing a vital role in the desegregation of schools in Gainesville, Florida. Currently, the building is experiencing structural damage due to water intrusion and termite infestation. To galvanize the community, the historic preservation program was working with various stakeholders such as the black community, past and current congregation, planning and preservation departments of Gainesville, and the university.

Image: A photo of the Old Mount Carmel Baptist Church, a Romanesque red brick-building from the mid-1900s. The picture shows the main elevation where the white double-door main entrance of the building is located.



Case Study: Old Mount Carmel

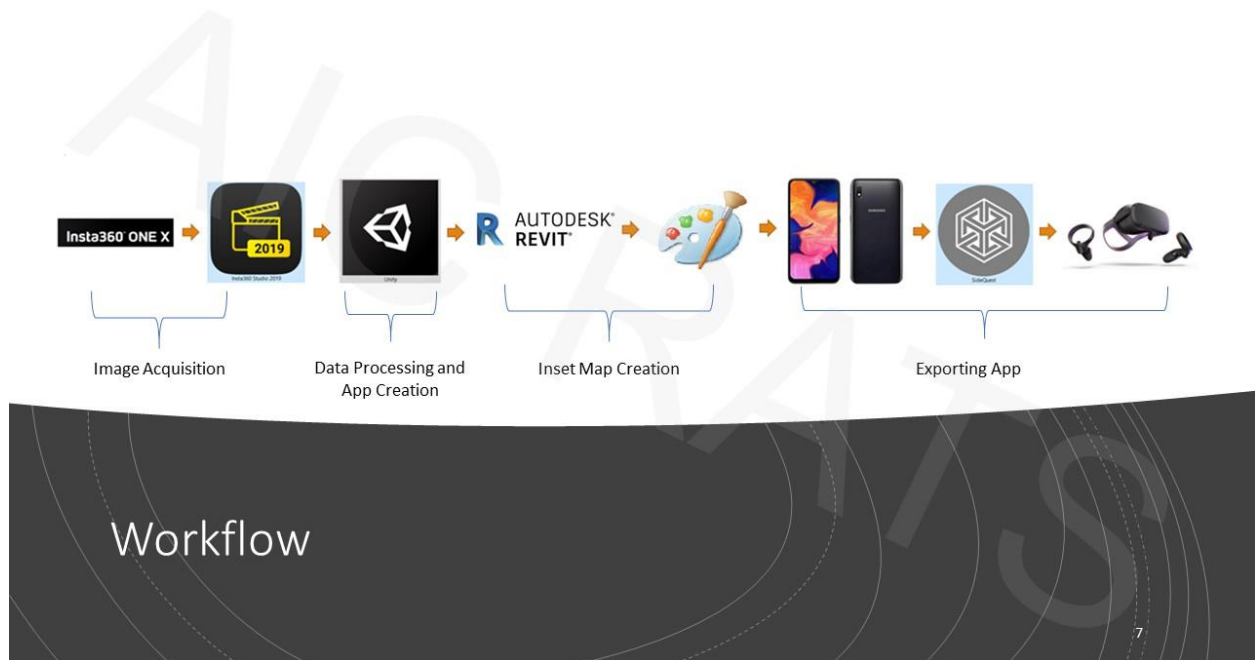
- Goals
 - Create VR app to evoke empathy
 - Share app with stakeholders
 - Test app's validity through survey
 - 30 people
 - Use app and rate its impact and accessibility

6

To create visibility and attention to the project, the department decided to create a VR application of the church and share it with stakeholders to evoke empathy and to bring awareness concerning its importance and current state. The participation of the community was an important aspect of the design plan since the goal was to empower the community by giving them a voice to tell their own story.

The prototype application was to be shared with thirty people or more through a short anonymous survey at the townhall meeting. A station with an Oculus Quest HMD and a survey-form would have been available so volunteers could try the VR app and rate their experience. I would have been on-site to help first-time VR users and troubleshoot in case of technical difficulties. The survey collected would have informed me on new features to implement and fixes to make for the next version of the app. During the last townhall meeting, the new improved VR app would have been presented to the community before making a final revision of the app.

Image: A photo of the Old Mount Carmel Baptist Church, a Romanesque red brick-building from the mid-1900s. The picture shows the main elevation where the white double-door main entrance of the building is located.



The following slides will look at the methodology used to create the VR app. To build the prototype, there were four steps involved:

- Image acquisition
- Data and image processing in Unity game engine
- Implementing features by using other programs such as Revit and Microsoft Paint
- Exporting/ mirroring the application to Oculus Quest HMD.

Schematics: This slides shows the workflow for creating the VR app by including icons of each software for the four steps involved in the creation of the app.


 Insta360 ONE X


Image Acquisition

- Opted for photo-realistic experience
- Used Insta360 OneX to take pictures:
 - Captured the main entrance elevation
 - Ground floor hallway with new sanctuary
 - Second floor hallway with historic sanctuary
 - Inside of new Sanctuary
- Used Insta360 Studio 2019 to process the panoramic photos in jpg format

8

To evoke empathy, photorealism was chosen instead of 3D reconstruction. The data was acquired through Insta360 One X panoramic camera, and the photos were processed in Insta360 Studio 2019 software and saved as JPEGs.

A total of 41 panoramic pictures were taken. This is due to the assumption that acquisition of panoramic pictures are like photogrammetry with 60 % of overlap between pictures to capture a single-room and stitch them together, but this assumption was incorrect and discarded because one panoramic picture is all that is needed during data processing. Instead, only five pictures were selected showing the main entrance elevation, first floor hallway, current sanctuary on the first floor, second floor hallway, and the historic sanctuary on the second floor.

Image: Top left is the logo of Insta360 One X camera and on the middle is the logo of Insta360 Studio 2019



Data Processing and App Creation

- Unity software is a video game engine
 - Built-in VR integration for Oculus Quest and Google Cardboard
 - User-friendly
 - Free
- Importing 360-pictures in Unity
 - Using a game engine to create an interactive 360 panoramic view for heritage
 - Each picture corresponds to a different view of the building (exterior of building, first floor hallway...)

9

To use the panoramic pictures in VR, they should be imported in Unity. Unity is an open-source and user-friendly game engine, and it allows functionality and features to panoramic pictures otherwise challenging to do so without a game engine. Unity has a built-in Oculus integration to create an interactive VR experience for Oculus Quest HMD. The integration can be found in Unity's asset store for free, and once installed in the project, a VR setting is enabled without additional scripting and streamlining the process as a result. Unity's documentation and other online resources are available for additional information on tools and scripting.

Once the VR environment was set in the project, the JPEG photos were imported in Unity to create an interactive VR experience in Oculus Quest. Each photograph represents a different section or room of the building. These images replaced the default skybox in Unity, and new scenes (frames) were created for each panoramic photo, so a total of five scenes (frames) were built. Each room/ section of the building is connected as it would be on-site. For example, to access the second floor, it must be through the first floor hallway stairs.

Image: Logo of Unity on the left corner of the screen.



Inset Map Creation

- Floorplans of building lost
 - Laser-scan imported in Revit
 - Create floorplans
 - Screenshot exported to Paint
 - Added scan location in Paint to indicate the camera/ user place
- Image added as an inset map to indicate user's location for desktop and VR app

10

Floorplans are important visual indicators to show a building's layout. Unfortunately, the Mount Carmel original floorplans were lost, and the department did not reproduce the floorplans from the laser scan data at the time. The church's floorplans are an integral part of the VR app, so I had to recreate them in a short period of time and integrate them as a feature in the app.

I obtained the point clouds from the laser scan and imported them to Autodesk Revit. The generated cross section in Revit from a top-view perspective was used to create the floorplans. Due to time constraints, the generated section was not traced in AutoCAD, and the point clouds' cross section was used as the final floorplan of the project. Next, the results were screen-captured and imported to Microsoft Paint to add graphical information to indicate the camera/ user's location on the floorplans. Five different pictures were created with different camera positions to produce five different inset maps for each scene. Finally, the Microsoft Paint JPEG files were imported in Unity to create the inset maps.

Image: Logo of Autodesk Revit and Microsoft Paint on the left corner of the slide.



Mirroring Application

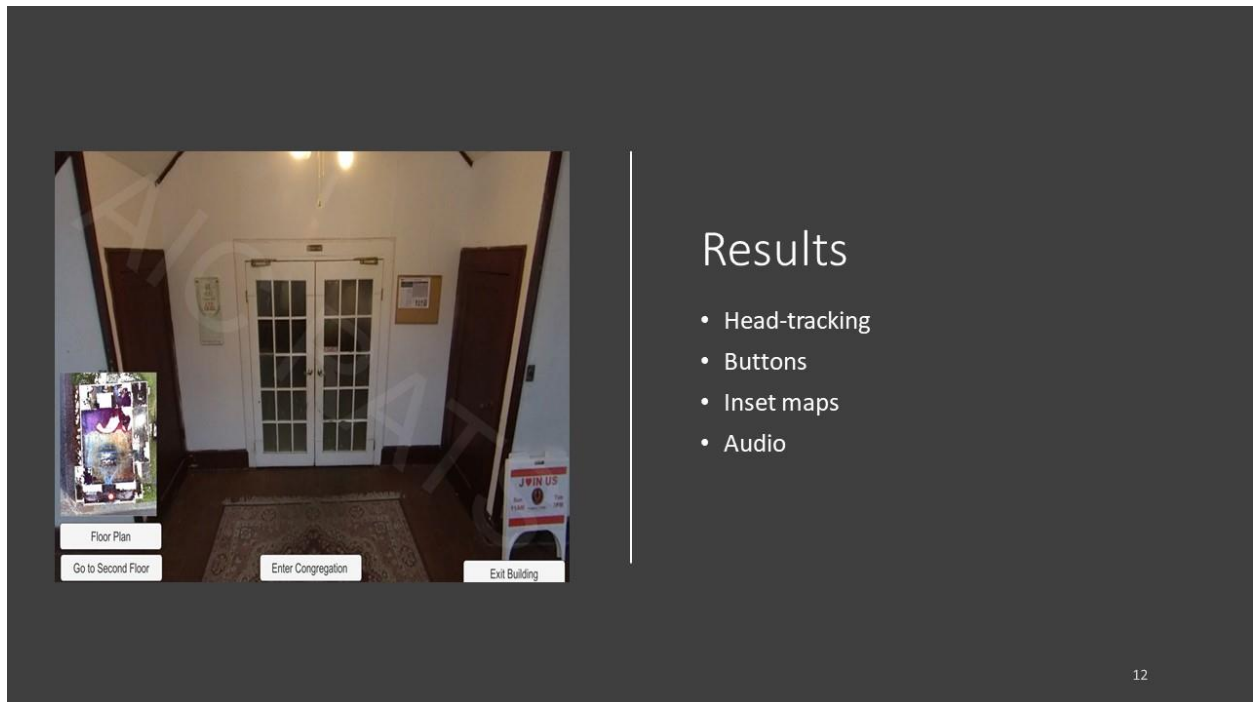
- App intended to be used for Oculus Quest
- App optimized for Android phones
- To use app in Oculus Quest, Android file must be mirrored in SideQuest

11

The Oculus Quest app was built for an Android-based device, but it is not possible to directly install the file in Oculus Quest's internal memory since Oculus is not an Android-based device.

SideQuest, a mirroring software, is needed to resolve this issue by connecting the software with the HMD. Any file that is added in SideQuest will automatically be installed in the Unknown Source subfolder in Oculus Quest. The file could then be accessed and run in Oculus Quest.

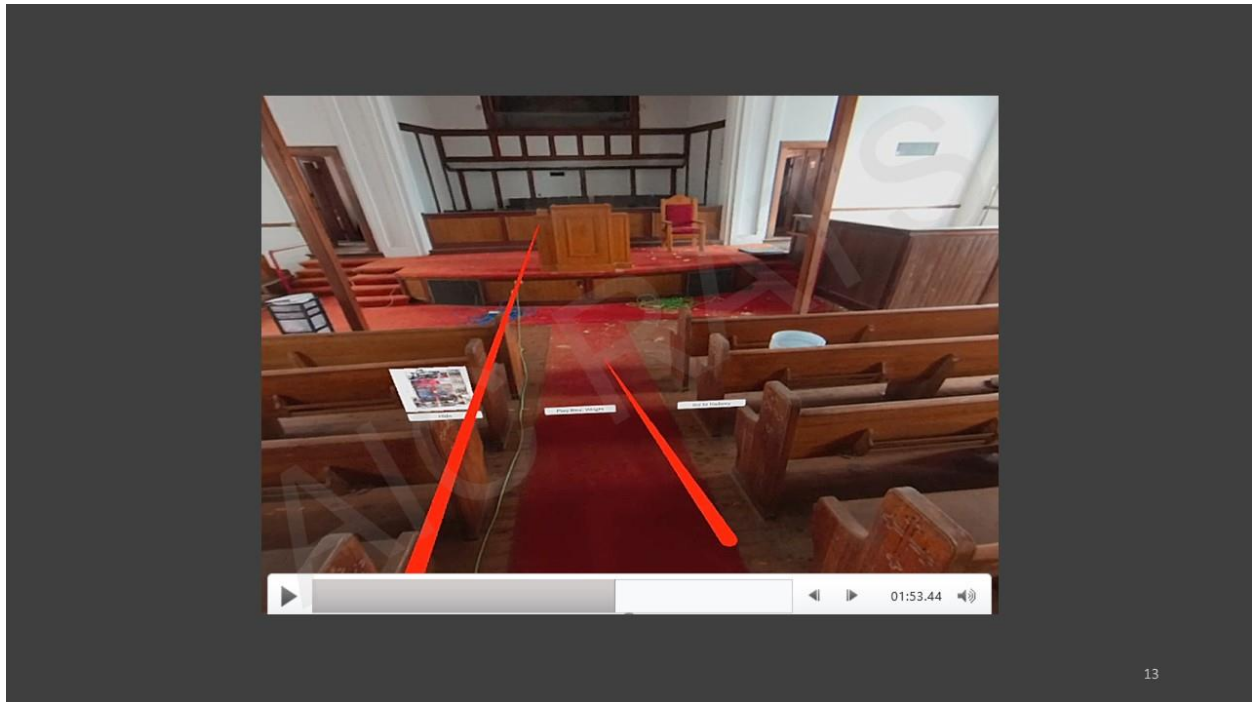
Image: On top left corner of the slide, there is a picture of a Samsung Galaxy A series Android smartphone, the logo of SideQuest is in the middle, and a picture of an Oculus Quest HMD is at the bottom.



The last several slides have looked at the process of creating the VR app, and now we can look at the resulting prototype application. This is a screenshot from the prototype showing some of the features. The user can observe the church with head-tracking features allowing an immersive experience, but movement is limited since it is not a 3D reconstruction. The user could not move in real-time or interact with objects such as doors. The user must rely on the interactive buttons to travel to a different room, access the inset maps, and play the audio file recording of Reverend Wright.

To access the buttons a red raycast from each controller is projected in the virtual world, and when the raycast detects a button, it will change its color from red to white, indicating that it can be pressed with the trigger button on both controllers.

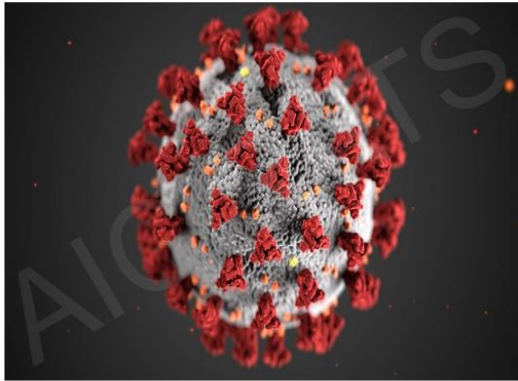
Image: A screen-capture of the app when the user is located inside the church, with a double-door in the center and two single-flush doors on each-side. There is an inset plan with floorplan and two user-interface buttons on the bottom left-corner of the screen, a single button in the bottom center, and another button on the bottom right-corner.



A video of the prototype application was shared during the presentation. The full video can be accessed on YouTube <https://youtu.be/vT0s39DdzNA>

This short video capture using the Oculus Quest shows what the VR app looks like. The video shows a quick walkthrough inside the new and old sanctuary. It also shows different features such as accessing the inset maps, clicking on the navigational buttons, and listening to the audio recording of Reverend Wright.

Image: Screenshot from the video of the prototype application showing the interior of the sanctuary and the red raycasts used to navigate the application.

Centers for Disease Control¹

¹ Center for Disease Control. (2021). Coronavirus Disease 2019 (COVID-19) [Image].
<https://www.cdc.gov/dotw/covid-19/index.html>

Challenges

- First person to attempt a VR project in my department
- COVID-19
 - Project delayed
 - App could not test empathy and stakeholder participation
 - Surveys not administered

This project was my first attempt at creating a VR application, thus there are some shortcomings in the application. For instance, I did not use a remote-clicker to take the panoramic pictures, instead I held the camera on a selfie-stick. As a result, I appeared in all the scenes and had to create a plane to hide myself. This created an artificial plane that is distracting to VR users. In addition, the camera was held high so in the VR app it feels like one is floating instead of being at floor-level.

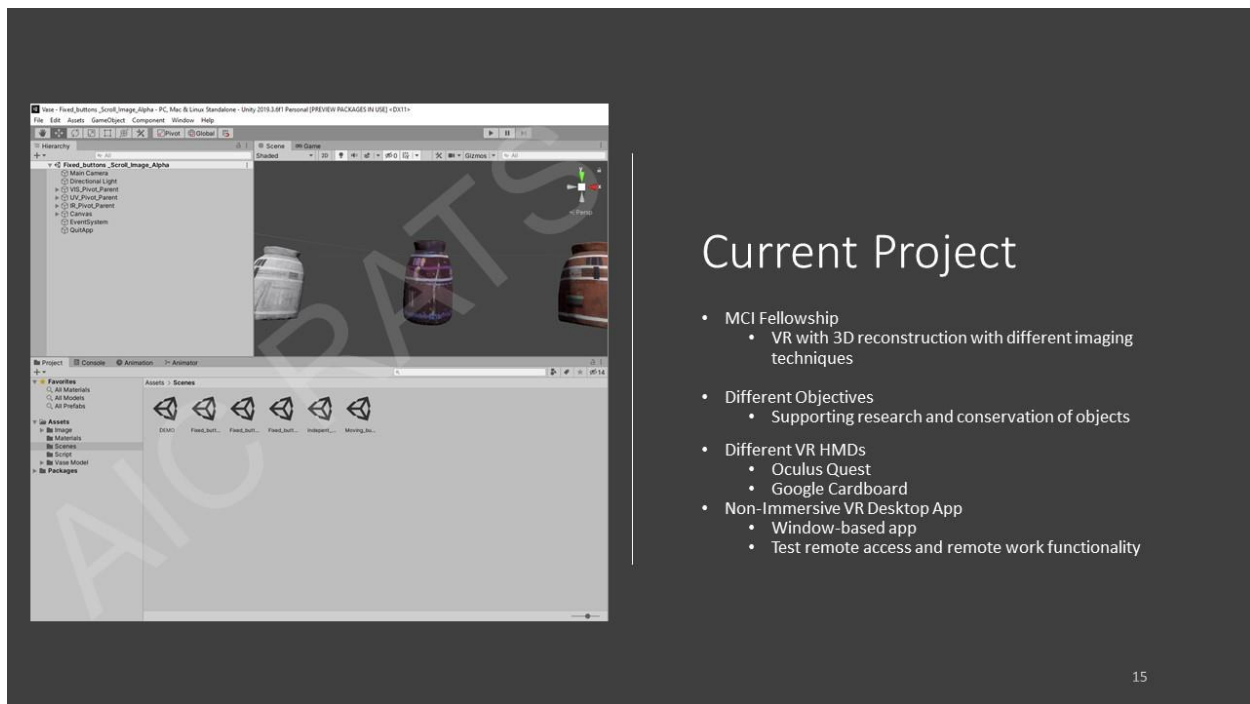
The inset map loads when the app is booted, and this was not by design. The original intent was to have the maps appear after the user clicks on the button. Another issue is with the button layout, there was no clear design choice but a random placement.

Unfortunately, the second townhall meeting was canceled due to COVID-19, and the app was not shared with the community, the project got delayed, and I did not get the opportunity to revise and address these shortcomings. A second take would have given me a chance to fix these issues. Also, it was impossible to test if the VR app is a tool to evoke empathy and galvanize the community for historic preservation.

Image: An illustration of COVID-19 virus.

Citation:

1 Center for Disease Control. (2021). Coronavirus Disease 2019 (COVID-19) [Image].
<https://www.cdc.gov/dotw/covid-19/index.html>



These setbacks limited testing the potential of VR as tool to evoke empathy for historic structures, but I had the opportunity to continue exploring the potential of VR as research tool at MCI.

A new research project was undertaken at MCI as fellow to demonstrate VR's versatility as a research tool in heritage. Imaging is used to assess the condition of an object, inform the care and treatment, and increase understanding of the materials and manufacture. The new research is to determine if VR could allow the integration of imaging and analytical data in a way that allows dynamic visualization and investigation of the physical object and digital data to gather new information for conservation.

The research includes looking at different options for displays for VR applications since there are different barriers and limitations with the different options. To remedy this issue, the research will look at building a Window-based desktop app as well as a Google Cardboard version to offset cost and allow more users to experience the VR app based on their budget.

Image: Screenshot of VR app being developed in Unity to integrate imaging results from different techniques of a vase.

Conclusion

- Advantages of VR
 - Versatile
 - Immersive
 - Excellent tool for teaching and learning
 - Allows “virtual mobility”
- Limitations of VR
 - Expensive
 - Could create divide between people with various computer literacy
 - Sanitary issues
 - Potential mental health issues
- Tool for empathy
- Remote access to heritage
- Virtual exhibition
- Research

16

VR has a long history and only recently experienced resurgence due to technological advancements. The video game industry made a big investment and it is paying dividends. Institutions such as museums also started investing in VR for education and entertainment purposes, and some allow their visitors to visit their galleries remotely through VR. The aim of this presentation is to show the versatility of VR as one of its strengths by allowing different immersion levels based on the user's needs, facilitating learning, and providing an option for remote access. While there are many advantages for VR, there are also a handful of limitations. These limitations include cost, sanitation, mental health impacts, and access relating to computer/ technology literacy.

To conclude, I was able to demonstrate the versatility of VR in historic preservation throughout different projects. Although there were some minor setbacks due to unforeseeable circumstances, it would have been interesting to test the legitimacy of VR as a tool to evoke empathy by working closely with a community. Furthermore, there is ongoing research to determine the potential of VR as research tool in conservation by dynamically visualizing different imaging techniques to assess the condition and surface information of an object.



Acknowledgments

- University of Florida
 - Morris Hylton III, Program Director of Historic Preservation
 - Jason Meneely, Associate Professor, Department of Interior Design
 - Ralph Tayeh, PhD Candidate, School of Construction Management
- Smithsonian's Museum Conservation Institute
 - Robert Koestler, Director
 - Paula DePriest, Deputy Director
 - E. Keats Webb, Imaging Scientist
- Funding
 - MCI Fellowship is generously supported by Smithsonian Museum Conservation Institute Federal Appropriation.

17

I would like to acknowledge and recognize the people that helped me along my journey to explore and learn about VR. My gratitude goes out to Morris Hylton III, former Program Director of Historic Preservation UF; Jason Meneely, Associate Professor, Department of Interior Design UF; and Ralph Tayeh, former TA and PhD, School of Construction Management UF.

This opportunity would have not been possible without the support of MCI, and I would like to express my deepest appreciation to Robert Koestler, Director at MCI; Paula DePriest, Deputy Director at MCI; and E. Keats Webb, Imaging Scientist at MCI.

Image: A photo of a white cat sleeping on a window-sill.



Image: A blue semi-conductor picture on the left and a "Thank you!" note

Recapturing Ancient Identities: Challenges and Discoveries from the Multispectral Imaging of Roman Egyptian Stelae at the Kelsey Museum

Caroline Roberts^{1*} & Suzanne Davis^{1*}

¹ Kelsey Museum of Archaeology, University of Michigan, 434 South State Street, Ann Arbor MI 48109

* Corresponding authors: Caroline Roberts cirobert@umich.edu, Suzanne Davis davissl@umich.edu

Original Abstract

This paper discusses the initial outcomes of a project to document the polychromy of a group of limestone funerary stelae from the Roman Egyptian city of Terenouthis. In 1935, the University of Michigan led excavations of the necropolis at the site. The ancient cemetery, dating from roughly the 2nd to the 4th centuries CE, had hundreds of small pyramid and barrel vaulted tombs. Each included a carved and painted limestone funerary stela, or grave marker, with a depiction of the deceased. Many of the tombs also had plastered and painted forecourts. When the excavation concluded, 194 stelae and some of the painted plaster fragments were brought to the University's Kelsey Museum of Archaeology as part of an agreement with the Egyptian government. Although the salt-laden objects have deteriorated since their excavation, many retain some of their original pigment.

The stelae and their painted tombs present an opportunity to reconstruct ancient paint schemes and color use in Roman Egypt, a unique period of cultural exchange in antiquity. Using multispectral imaging (MSI), conservators at the Kelsey have started to document and characterize pigments found on the stelae. Thus far, rose madder, Egyptian blue, and green earth (celadonite) have been identified. These pigments point to connections between Terenouthis—a small provincial city in the Nile Delta—and a broad network of trade that spanned the Roman Empire.

Our paper also discusses challenges we have encountered in studying in the stelae's remaining color. These include deteriorated and disrupted surfaces; damage from historic, aggressive conservation treatments that included repeated cleanings and coating applications; and, more recently, problems with collections access and image capture due to COVID-19. Confronted with an uncertain research timeline, we developed a condensed MSI protocol to map color and gather data for subsequent analysis.

While conducting MSI, we also made an unexpected discovery: painted images and inscriptions only visible in ultraviolet-induced visible luminescence (UVL) images. These


newly revealed images include Anubis figures, fringed shrouds, and inscriptions written in Greek on seemingly blank registers below the individuals' carved portraits. The images are not mentioned in previous publications on the stelae; however, black and white photographs taken shortly after the stelae's excavations suggest they may have been visible at the time of the objects' discovery nearly ninety years ago.

Our initial pigment data, coupled with these re-discovered decorative elements, are creating new insights about the lives and choices of ancient people, using legacy excavated materials. This imaging project has also produced compelling new visual information from the collection, a valuable tool in our Museum's efforts to reach students and scholars remotely. From archival photographs to newly captured digital data, this research reminds us of the power of images to preserve and reconnect us with the past.

Annotated Slides

Recapturing Ancient Identities

Challenges and discoveries from the
multispectral imaging of Roman Egyptian stelae
at the Kelsey Museum



Caroline Roberts and Suzanne Davis

IWG/RATS Session, AIC Annual Meeting
Wednesday May 26, 2021

I wanted to start by acknowledging the historical origins and present location of the Kelsey Museum of Archaeology, which as part of the University of Michigan is located on the traditional lands of the Anishinaabeg and Wyandot. These lands are still home to many indigenous people, and I honor and respect their present and ancestral ties to this land. I also want to acknowledge that the Kelsey's collection, likewise, originates in the removal of

cultural resources from indigenous and local communities in other parts of the world. As museum staff, we can't change this past, but we can think critically about the research we do and the efforts we make to distribute this knowledge widely, and these can be small steps toward a reparative type of conservation practice.

I am excited to share with you today some initial outcomes from a research project I'm conducting with my colleague Suzanne Davis. We are documenting and analyzing the polychromy of a group of limestone grave markers (or funerary stelae) from the Roman Egyptian city of Terenouthis. By studying the stelae we hope to answer two key research questions: First, how was color used in Roman Egypt? For example, what pigments are being used and how are they being applied? And second, how does this compare to color choices seen in dynastic Egyptian art? We've started to answer these questions with the help of our lab's low-tech multiband imaging setup, which has allowed us to map and begin characterizing specific pigments on the stelae. MBI also led us to an unexpected, significant discovery – a partial name on a stela we had believed to be uninscribed. In addition to sharing our findings I'll talk about the challenges we faced while imaging the stelae during the pandemic. By reflecting on what we've learned so far, we hope to demonstrate the value of adaptable imaging methods, and the benefit of looking carefully at old archaeological collections with new, accessible technologies.

The Terenouthis stelae

- Ancient city in the Nile Delta
- Discovered in 1935
- Necropolis / cemetery



The subjects of our case study are the limestone funerary stelae of Terenouthis, an ancient city in the Nile Delta. The stelae were excavated in 1935 by a team led by archaeologists from the University of Michigan, who carried out a salvage expedition on the last remaining corner of what was once vast necropolis, or cemetery. The artifacts recovered from the site date to the late second through early fourth centuries CE, a few hundred years into the Roman occupation of Egypt.

The Terenouthis stelae

- Mudbrick tombs
- Evidence of ancestral worship
- Stelae found in niches



The necropolis was filled with hundreds of mudbrick tombs built in various shapes – from small pyramids to barrel-vaults. Many of the tombs were fronted by forecourts, a sign of their function as venues for familial worship of the dead. A niche was built into the center of each tomb's façade, and inside these arched recesses sat a carved, painted, limestone stela.

The Terenouthis stelae

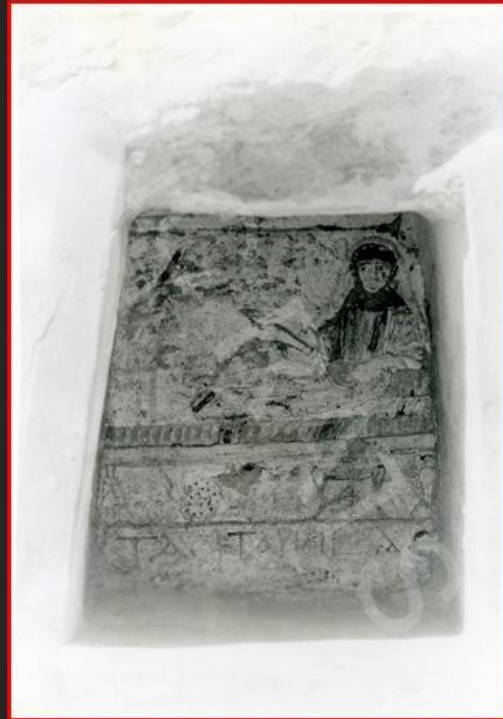


Clockwise from upper left:
KM 21130, 21057, 21186,
and 21036

The stelae are carved with images of the deceased person. Most individuals appear either standing with raised arms - an ancient prayer position - or reclining on a couch with a funeral banquet placed before them. Many of the stelae are inscribed in Greek with names of the deceased, along with their age at death and, in some cases, a comment on their life or character and sometimes a message of comfort to the mourners. Many people are accompanied by jackal and falcon figures – symbols of the Egyptian gods Anubis and Horus, associated with the afterlife and rebirth. The stelae are multicultural, with inscriptions in Greek, clothes and furnishings that are stylistically Greek and Roman, Egyptian religious symbolism, and Greek and Egyptian hybrid names. The stelae are also rare in that they come from a documented, archaeological context. They offer us a glimpse at regular people in the ancient world, and tell us something about their beliefs and values.

The Terenouthis stelae

- Nearly 200 stelae + archival photographs
- ~136 have polychromy



In addition to nearly 200 stelae, the Kelsey Museum of Archaeology preserves excavation archive photography from Terenouthis. In some cases, these images have allowed us to reconstruct exact find spots and to understand how the stelae functioned in their funerary contexts. What these images do not capture, however, is the richness of the stelae's polychromy...

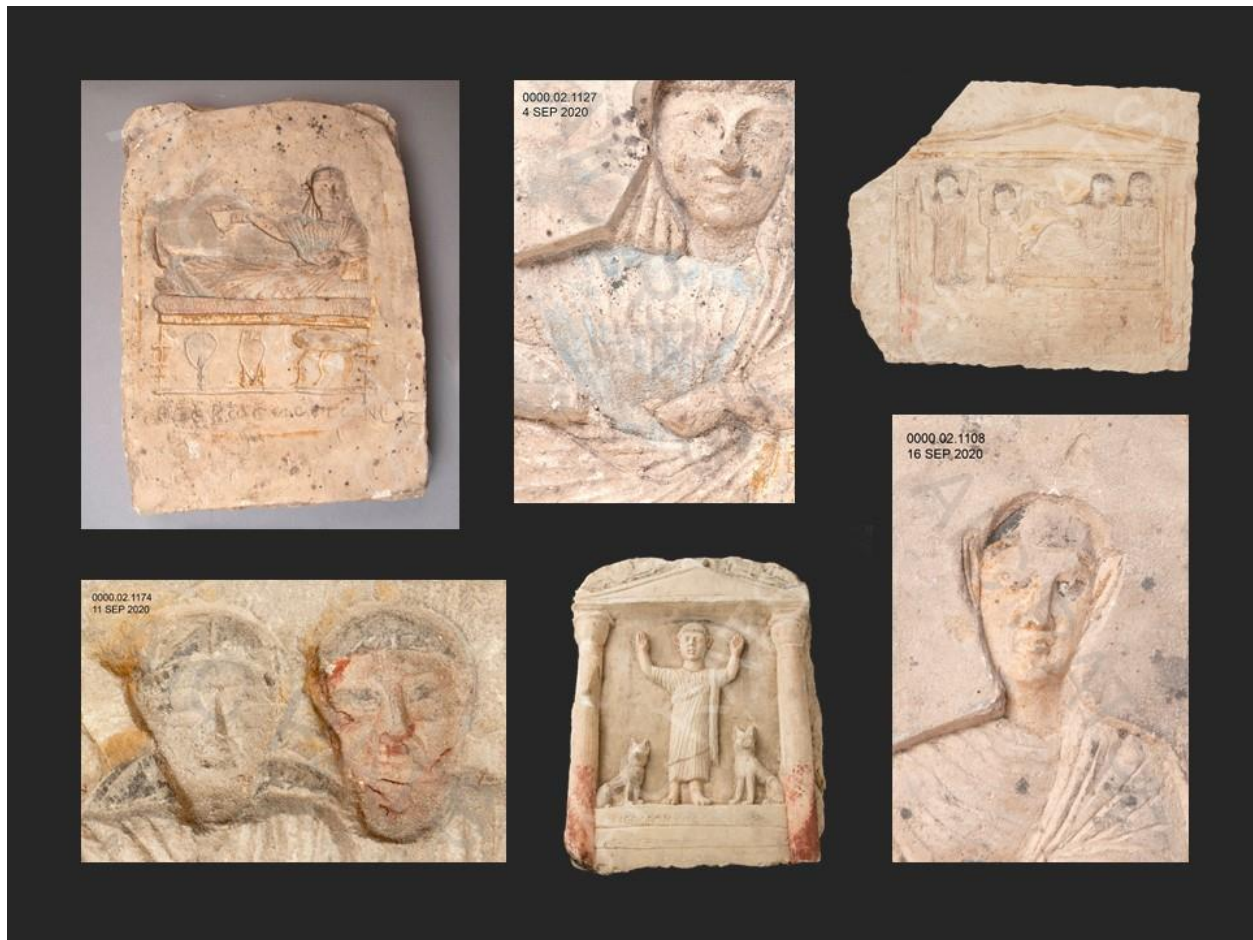
Stelae polychromy



Stela of Tasitarion, 21169



...some degree of which remains on more than half of these grave markers.



Although the stelae have been catalogued, their inscriptions translated, and their imagery analyzed, no one has comprehensively studied their paint surfaces.

Stelae polychromy

RESEARCH QUESTIONS:

- *How was color used in Roman Egypt?*
- *How does this compare to color choices seen in dynastic Egypt?*

OBJECT PHOTOGRAPHY

MULTIBAND IMAGING

- Modified Nikon D80
- PECA #916, 914 and 904 filters
- Impact VC-500LR, Blak-Ray 100W longwave and Z96 LED lights



Fayoum portrait of a woman, KM 26801

This reflects a much bigger trend in the study of Egyptian polychromy, which has traditionally focused on artifacts from earlier periods of Egypt's history. But this is starting to change with recent advances in technical color research on Fayoum portraits – including this one, preserved at the Kelsey – and on Roman Egyptian funerary artifacts. The Terenouthis stelae offer us a chance to contribute to this growing Roman Egyptian color dataset, and explore what these data can tell us about color use during this later period.

We started our research with a photographic sweep of about 50 stelae that had polychromy, capturing detailed photographs of their paint surfaces. We then selected a smaller number from this group for multiband imaging using our lab's modified Nikon DSLR camera, a set of PECA lens filters, and various light sources including Impact monolights, a Blak-Ray longwave UV lamp and a Z96 LED light array for infrared luminescence imaging. Our aims were to map out where specific pigments were being used, to begin characterizing the pigments with imaging, and to plan for future scientific analysis.

Stelae polychromy

COVID CHALLENGES

- Limited time at the Museum
- Limited collections access
- Difficulty with handling



ADAPTED METHODS

- British Museum Technical Imaging capture and post-processing
- Limited to UV-induced visible luminescence (UVL), Infrared reflectance (IRR) with IRR false color, and visible-induced IR luminescence (VIL)
- Single light sources for UVL and VIL
- No flat fielding

Then COVID hit, adding significant challenges to the project. When Suzanne and I packed up our desks in March 2020, we expected to be back at work within a few weeks or so. We didn't re-enter the building until late August, and COVID-related safety concerns have limited the number of staff who could work on site at any given time. This made it difficult to access and move the stelae, which are heavy and require more than one person to handle them.

But we didn't want to lose momentum on this project, so we had to adapt our imaging protocols for safety and efficiency. We decided to use a familiar technique (the British Museum's Technical Imaging guidelines), but with some adaptations:

- We limited the techniques we used to those that targeted the types of pigment responses we were anticipating
- We used single light sources for UVL and VIL imaging
- And we opted not to flat field our images

I'll discuss how these decisions impacted our outcomes later on.

Stelae polychromy



But first let me share some of our imaging results.

VIL imaging revealed that Egyptian blue was used in select areas, including women's tunics, couch cushions, and in green and blue objects as a representative color for glass.

Stelae polychromy



We know that Egyptian blue was used on art objects from the early dynastic period through the Roman period in Egypt, where we find it on a variety of artifact types from mummy portraits, to sculpture and wall paintings. So its use on the stelae is not a surprise. What is interesting is how selectively it is used: we found it on only 25% of the stelae we imaged.

Stelae polychromy



In some cases, other bluish pigments—like the green earth we see in this woman's garment and in the waves beneath her funeral boat—were used instead of Egyptian blue. The reasons for this aren't entirely clear. There were multiple production centers for Egyptian blue throughout the Roman Empire, and according to the 4th century Edict of the emperor Diocletian, its price point would have been relatively low around the time the stelae were painted. But its selective use on the stelae suggests that while people could buy the pigment, it might have more expensive than other blue pigments, or that it might not have been as readily available in the local area.

Stelae polychromy



Another pigment we were able to characterize was rose madder, whose characteristic orange-pink visible florescence was captured in UVL images. We found madder pigment in women's garments, on columns and column capitals, and in register lines around inscriptions.

Stelae polychromy



Madder root would have been available throughout the Roman Empire and it could be used to produce either a pink dye or a pink lake pigment. Unlike Egyptian blue, rose madder wasn't used with much frequency until the Ptolemaic period, which is the period preceding the Roman occupation of Egypt. Before this, the color pink was achieved by mixing red earth pigments with white pigments like calcite, huntite or gypsum.

Stelae polychromy



We see madder frequently on contemporary artifacts like mummy portraits, but we know less about its use on sculpture and architecture from the period. On this stela, madder is being used in the incised architectural framing line, in the figure's tunic, and in a cluster that may represent writing in the center of the background.

Stelae polychromy



On one stela, Egyptian blue and rose madder were used in combination. Their luminescence in the same locations on this woman's dress suggests a deliberate mixture or layering of the two pigments to create purple. Purple textiles were symbols of luxury in Roman Egypt, in part because of their association with the 'imperial' purple dye produced from the murex snail. In 1st-century CE Rome, a pound of Tyrian purple dye cost 100 denarii - about half a Roman soldier's annual salary. But a number of other options - plant-based purple dyes, for example - were available to produce 'purple' textiles, and the color would not have been completely out of reach for the people of Terenouthis. We see purple depicted frequently in women's garments, and—as we see here—red and blue pigments could be combined to create the color.

Stelae polychromy



Another pigment we've been able to characterize is green earth, which appears in IRRFC images as a blue color typical of Cyprus green earth. Previous XRD analysis of the background color on the stelae shown here helped us confirm this characterization. Green earth is used frequently on the stelae - in backgrounds, in clothing, and to represent water for stelae that depict boats. Like madder, green earth is rarely seen in Egypt until the Ptolemaic period. Copper based greens were used more frequently in dynastic Egypt, but during the Roman period pigment choices expanded to include green earths, indigo-orpiment mixtures, and other pigment combinations. In addition to new options for the color green, the pigment minium or red lead also appears in Egypt starting in the Roman period, expanding the palette for red as well.

Inscriptions



We've also learned something new about the woman with the purple garment. While imaging her pigments, we made an unexpected discovery. In the UVL image on the right you may be able to see a dark figure to the right of the woman. Look closely and you may also be able to see something hanging from her left hand. And below her feet, we can just make out a few Greek letters. None of these painted images or inscriptions are apparent in the image on the left.

Inscriptions



UVL – red channel

The UVL image's red channel isolates these features better. The figure to the woman's right is a reclining jackal, while the item hanging from her hand is in fact a fringed shroud that is draped over both hands. The text below her is also more visible.

Inscriptions



—ΩΝΑΜΟΥΝΙΚΩ—ΛΙΘ

Our colleague Caroline Nemecheck translated the ancient Greek text that was revealed by the longwave UV light. The letters at the beginning are lost, but the remainder reads: “—onamounis, about 19 years old.” The “..amounis” part of this woman’s name was popular in the Greek and Roman east, and evokes the Egyptian sky god Amun. So, thanks to the imaging, we now know the woman’s partial name and her age at death.

Inscriptions



1935 division album photograph



The images and inscriptions on —onamounis's stela were visible at one time. The stelae were photographed shortly after their excavation as part of the process of 'dividing' finds that would travel to Michigan from those that would stay in Egypt. These early photographs serve as snapshots of each stela's state of preservation at the time. You can see that —onamounis's inscription would have still been somewhat legible in 1935. By 1961, when the stela was re-cataloged, archaeologist Finley Hooper noted that it had no inscription. The letters had faded or been worn away. The stela did go through multiple treatment campaigns in the early- to mid-20th century to remove soot build up from the coal fires that were used to heat the Kelsey Museum, so it's possible that these episodes of cleaning eventually wore away the already faint traces of pigment.

Inscriptions



UVL – red channel

I still have a lot of questions about this – like what really caused the pigment to fade or erode? What is the pigment? And why is UVL so good at revealing it? My current theory is that the pigment – or what's left of it – is blocking or quenching the natural luminescence of the limestone. But I really don't have an answer yet. Any thoughts or theories from the audience on this are more than welcome!

Inscriptions



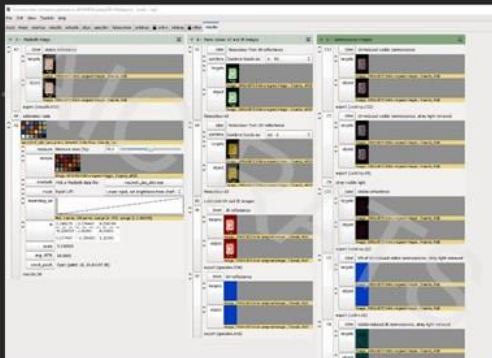
UVL – red channel

But the most important takeaway from this discovery is the possibility that many other funerary stelae are inscribed, and this is a potential most scholars probably don't realize. Since we have only imaged about thirty stelae so far, we suspect more faded images and inscriptions will be discovered. We've already found one other faded image on stela 21162, on the right. I hope that you can see the banquet objects coming into view beneath the reclining figure, and a couple of the letters in the inscription below.

Lessons learned

Incorrect exposures

- VIS and IRR images
- Impacted processing in Nip2



Even while we were able to gather useful imaging data – and make useful discoveries in the process – we encountered quite a few challenges while trying to do this work during COVID. Some of these were simple mistakes that we might not have made under normal circumstances. For example, there were a few batches of images which the Nip2 software couldn't process properly – they kept turning out overexposed in the workspace. After troubleshooting, I discovered that the VIS and IRR images in these batches were very underexposed in a few cases. Had I checked the exposures of each image, we would probably have avoided this problem. But we were rushed, and didn't check the RGB values on the ColorChecker in all of our images.

Lessons learned

Flat fielding

- Problematic for stelae with hidden inscriptions



We also ran into some problems with uneven illumination of the stelae. We opted not to flat field because we felt it would save time, but another reason is that we frequently forgo flat-fielding while imaging objects in our lab – most of which are small enough that we can normally ‘get away’ with bypassing this step. But in the case of the stelae, which are about a foot square and relatively flat on their relief faces, we probably should have flat fielded. The uneven illumination is pretty apparent in some of the UVL and VIL images (these are the worst of the worst), and while this didn’t prevent us from locating madder and Egyptian blue, it did complicate visualizing the inscriptions under UV.

Lessons learned

“Better is the enemy of good”
– Bruno Pouliot



Ultimately, we were able to capture the color data we needed in spite of these problems. I've found that the British Museum protocols can be adapted to different situations and research questions, which speaks to its value as a research tool. And in cases where we ran into trouble in the post-processing stage, we were able to use guidelines published in the AIC's Guide to Digital Photography as a backup. We want to capture images that will be useful and comparable to others, but also want to be flexible enough to adapt to different situations and working environments. As my mentor Bruno Pouliot liked to say: “Better is the enemy of good,” and these words have taken on a new meaning for me as we've worked through the challenges of this past year.

Summary

POLYCHROMY

- Color palette expands during the Roman period

INSCRIPTIONS

- More stelae may be inscribed than scholars realize

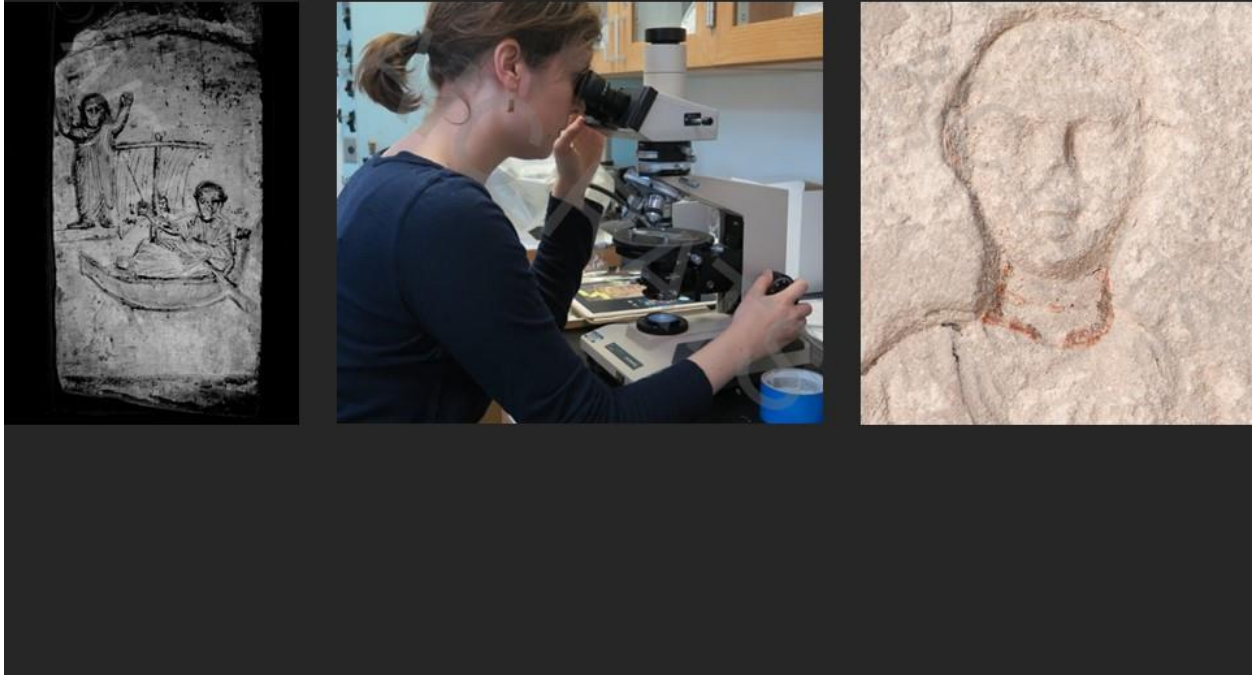
IMAGING

- Check exposures and flat field whenever possible
- Combine processing methods if needed



Although we still have questions about the stelae, our technical imaging has revealed a lot of new information about these objects and their polychromy. We have new evidence of pigment mixtures, and new data about color choices made by regular people in Roman Egypt. These new data contribute to our knowledge of Roman Egyptian color use, and of the expanding palette of colors that were available to artists and craftspeople during this period. We've also discovered images and inscriptions on the stelae that we could not see, which has big scholarly research implications for these objects. And we learned a few things in the process of capturing these images. We recommend checking exposures as you go and to flat field whenever possible – or at least make a rule to do it if your object is flat or larger than a square foot in size. And finally, don't be afraid to combine (and of course document!) different processing methods if you need to.

Continued research



As we move forward with this project, we hope that we will find more hidden inscriptions and to optimize our methods for revealing them. We will also work on confirming our initial pigment characterizations using our lab's new handheld XRF spectrometer, along with PLM, and other instrumental techniques available to us here on campus. I'm especially interested in analyzing the red pigments we've seen on the stelae, some of which look like they could be something other than red ochre. The presence of pigments such as cinnabar or red lead could have significant implications for where and how the stelae's pigments were sourced, and would provide more evidence for their use on Roman Egyptian sculpture.

Acknowledgements

- IWG/RATS session chairs and moderators
- Joanne Dyer
- Staff & students at the Kelsey Museum of Archaeology, especially Sebastian Encina, Michelle Fontenot, Caroline Nemechek, and Terry Wilfong



I'd like to thank my co-author and research partner Suzanne Davis, who's attending the session today and can help answer questions. Thanks also to my colleagues back in Michigan and elsewhere for their support of this project. Special thanks to the session chairs for organizing this great program of talks, and my thanks to all of you for your attention.

Practical LED-based Multispectral Imaging of Cultural Heritage Materials

Olivia Kuzio¹ & Susan Farnand^{1,*}

¹ Rochester Institute of Technology, 1 Lomb Memorial Drive, Rochester, NY 14623

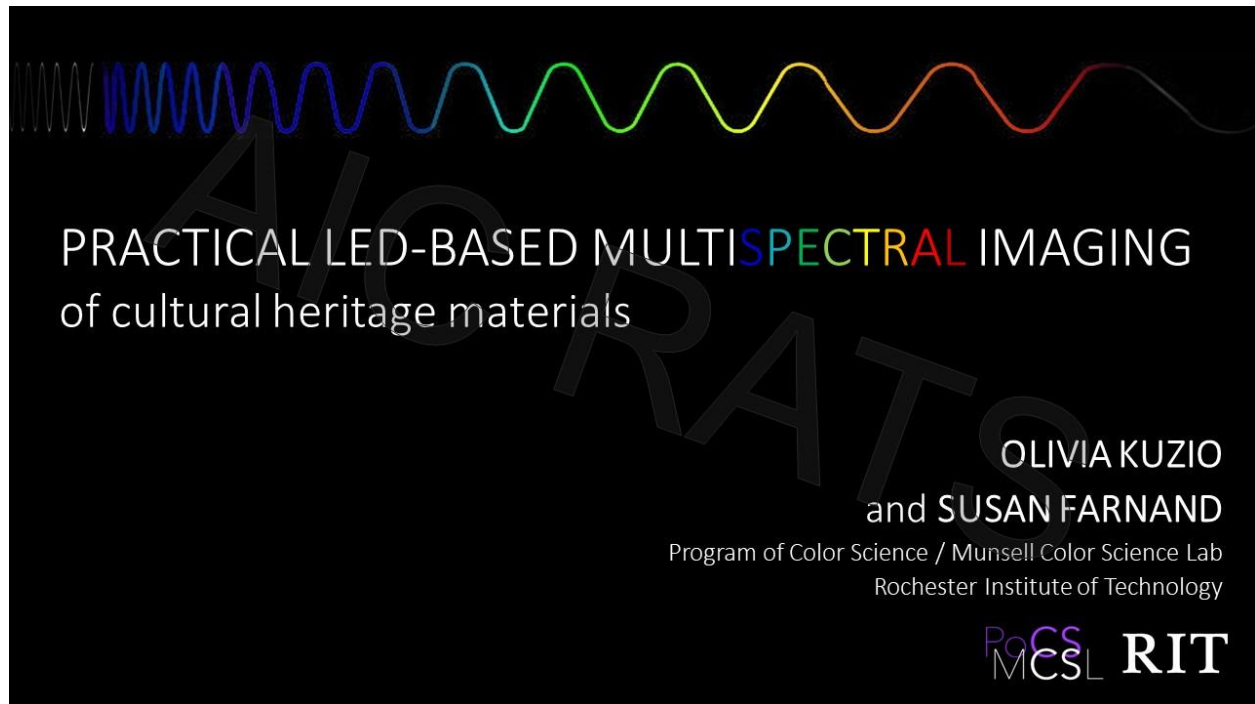
* Corresponding author: Susan Farnand, susan.farnand@rit.edu

Original Abstract

Multispectral imaging (MSI) is a powerful tool for documenting cultural heritage materials. In the context of this research, MSI refers to the capture of 6 to 10 images within select wavebands spanning the visible spectrum and spaced at relatively regular intervals. Coupled with computational image processing techniques, this capture strategy enables the estimation of a reflectance spectrum at every pixel of the image. In part, a reflectance spectrum describes both the color and material nature of an object. An image-sized collection of the spectral reflectance across the surface of an object provides dense information about the object's physical characteristics and their spatial variation. Furthermore, spectral estimation also enables improved color reproduction. These characteristics of MSI render it a more comprehensive technique than conventional RGB imaging.

While commercial systems have been developed to take MSI from a lab-based analysis to a studio-friendly capture technique, these systems may prove prohibitively expensive for exploring MSI. Furthermore, when the advantages of routinely using MSI are not clearly articulated, it is less likely that the curious will invest in costly systems for independent experimentation with the technique. In recognizing these barriers which currently limit the accessibility of MSI, this research demonstrates a lower-cost MSI system alternative that is still studio-friendly and affords high spectral and color performance. The system incorporates multichannel, narrow-waveband LED lights, and otherwise requires only equipment already found in most imaging studios. We have developed capture and processing strategies practical for the studio environment, and we will present these workflows along with the color reproduction and spectral accuracy they afford. We aim to emphasize the utility of MSI for color-critical imaging of cultural heritage materials and to demonstrate an accessible, needs-based strategy with which it can be implemented.

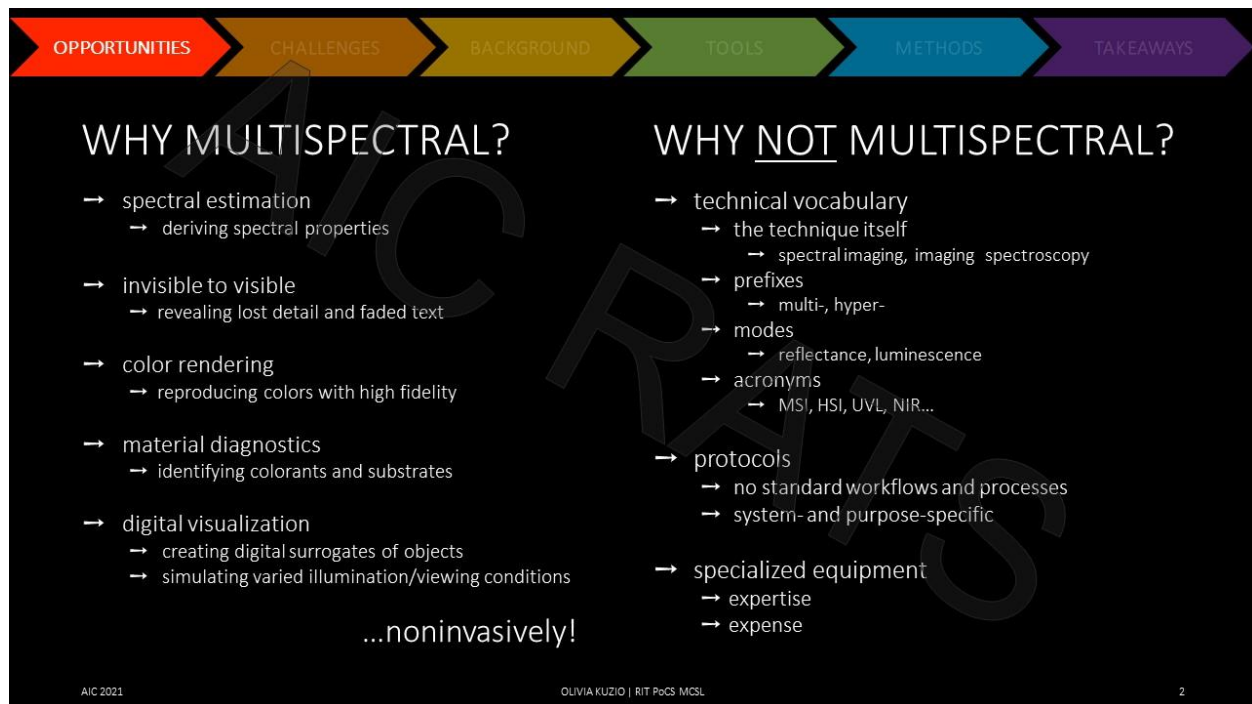
Annotated Slides



Outline of presentation:

- 1) Review of advantages and challenges associated with spectral imaging
- 2) Development and evaluation of practical methods for implementing multispectral imaging

Goal of the research: development of a simple multispectral system and workflow that is more available at a more accessible level to more institutions



Multispectral imaging: a hot topic because it's so versatile

Name is derived from the key "spectral" aspect of the imaging

Why use multispectral imaging?

- Invisible → visible, i.e. revealing faded/degraded details
- Rich spectral information enables renderings with higher color accuracy than conventional color imaging
- Material classification; e.g. pigment identification and mapping
- Creation of digital surrogates
 - E.g. visualize what an object looked like pre-degradation and estimate what it will look like if degradation continues
 - E.g. visualize how an object appears under different illumination conditions (i.e. daylight vs. tungsten illumination)
 - This is impossible with RGB images, so this is a particularly powerful feature of spectral images
- Imaging is inherently noninvasive
 - Analysis with no physical cost to the object
 - Often used in an initial survey of an object to identify areas to study more closely

Challenges associated with multispectral imaging

- Lack of a consistent vocabulary
 - What is the technique itself called? → different groups call it different things
 - Distinctions based on...
 - Number of bands
 - Type of radiation recorded
 - Numerous acronyms
- Lack of standard protocols

- System- and purpose-specific
- Expertise is often necessary to operate and communicate about specialized equipment
- Specialized equipment is expensive



Tendency toward “more is better” has led to the development of spectral imaging systems that look, and are, complicated

- Many are scientific instruments that enable work at the cutting edge of noninvasive technical examination of cultural heritage objects
- Such spectral imaging systems have limited accessibility (in terms of cost and complexity) to non-experts

WHY IS MULTISPECTRAL IMAGING SILOED IN SCIENCE LABS?

COMPLEXITY \neq ACCESSIBILITY

Consider...

→ HOW GOOD IS GOOD ENOUGH?

→ WHAT ARE THE NECESSARY EFFORTS?

concept
practice
cost-benefit

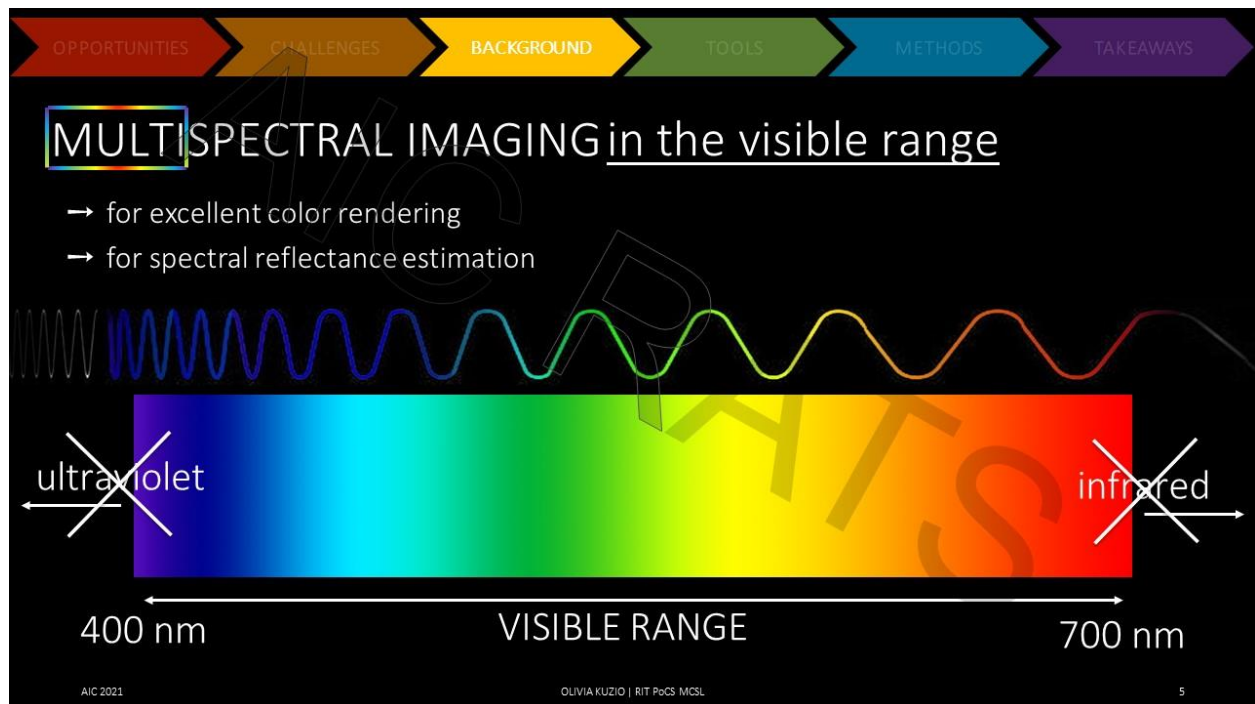
AIC 2021 OLIVIA KUZIO | RIT PoCS MSL 4

So: why is multispectral imaging not a routine imaging technique outside of science labs?

- Perceived complexity limits accessibility
- Must be made more accessible to more people in terms of concept, practice, and cost-benefit

Our perspective: use a needs-based approach rather than a data-driven approach to make performing multispectral imaging more manageable

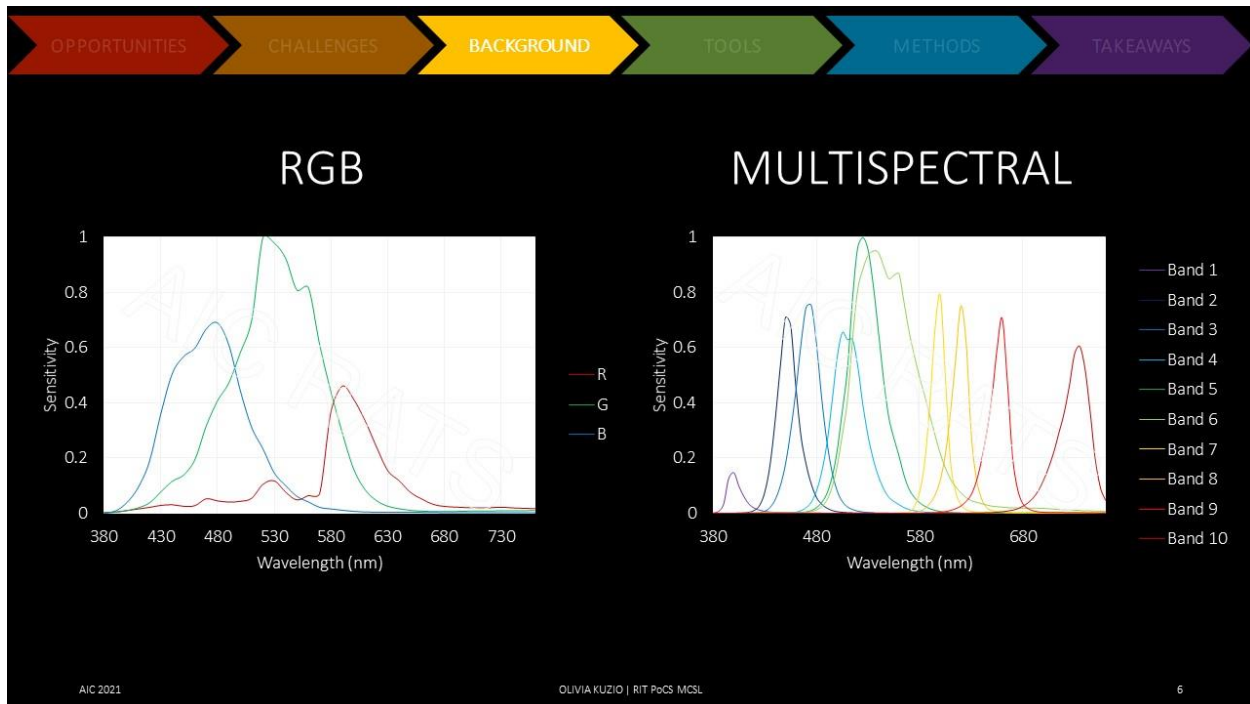
- Always ask: “How good is good enough?” and “What are the necessary efforts?” based on the purpose of the imaging to be done



Multispectral imaging in the context of this presentation: visible range (400 – 700 nm)

- Focus on excellent color rendering and spectral estimation capabilities based on visible range data only

Note: the prefix “multi-” is used throughout to describe the number of bands our spectral imaging system has (6 – 10)

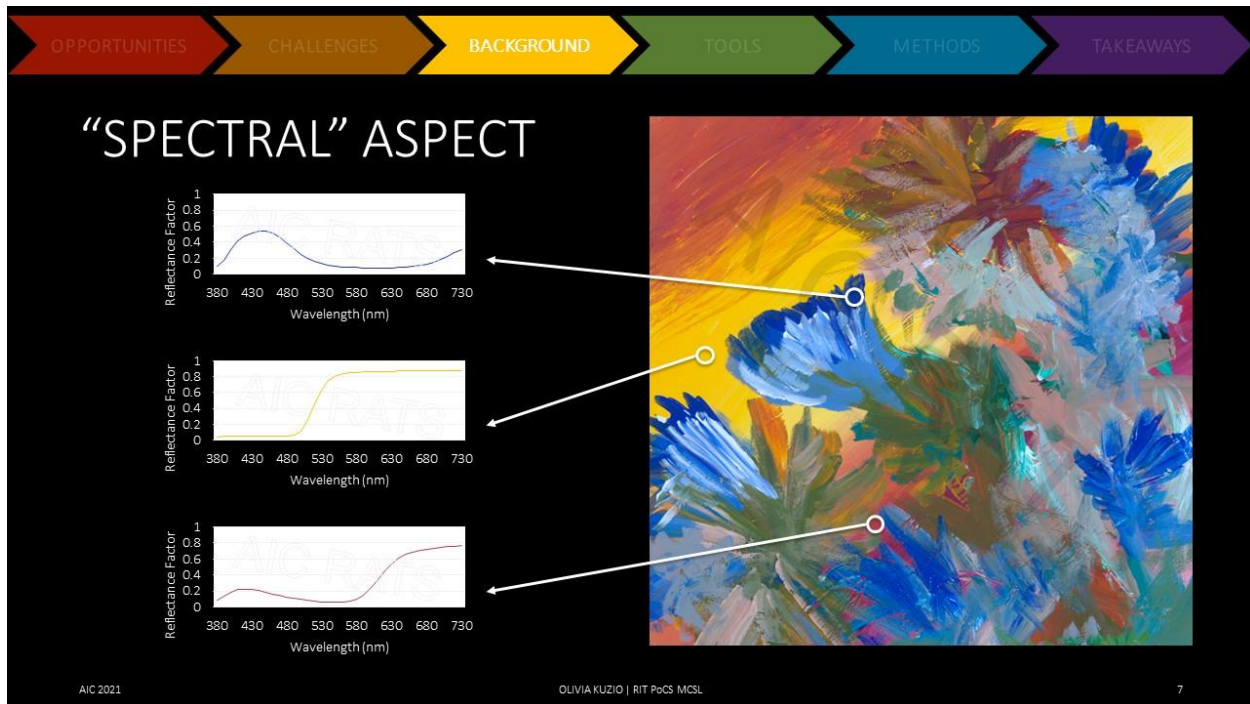


Graphical comparison of familiar RGB color imaging vs. arbitrary multispectral imaging

Left: 3-band sensitivity of an RGB camera

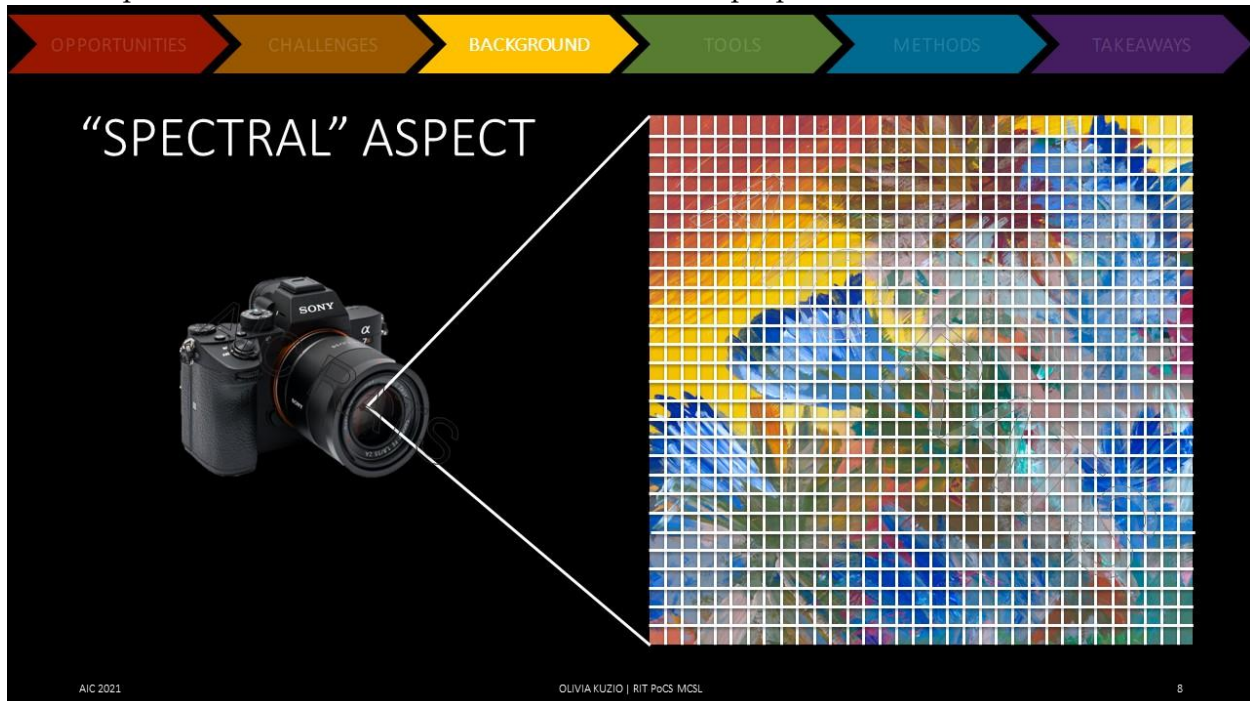
Right: same kind of information for one of our multispectral imaging strategies - in this case, a mode with 10-bands

- More, narrower bands with respect to RGB
- Sampling the spectral range with more bands provides information that can be transformed into both a spectral reflectance “data cube” and a color-managed RGB image

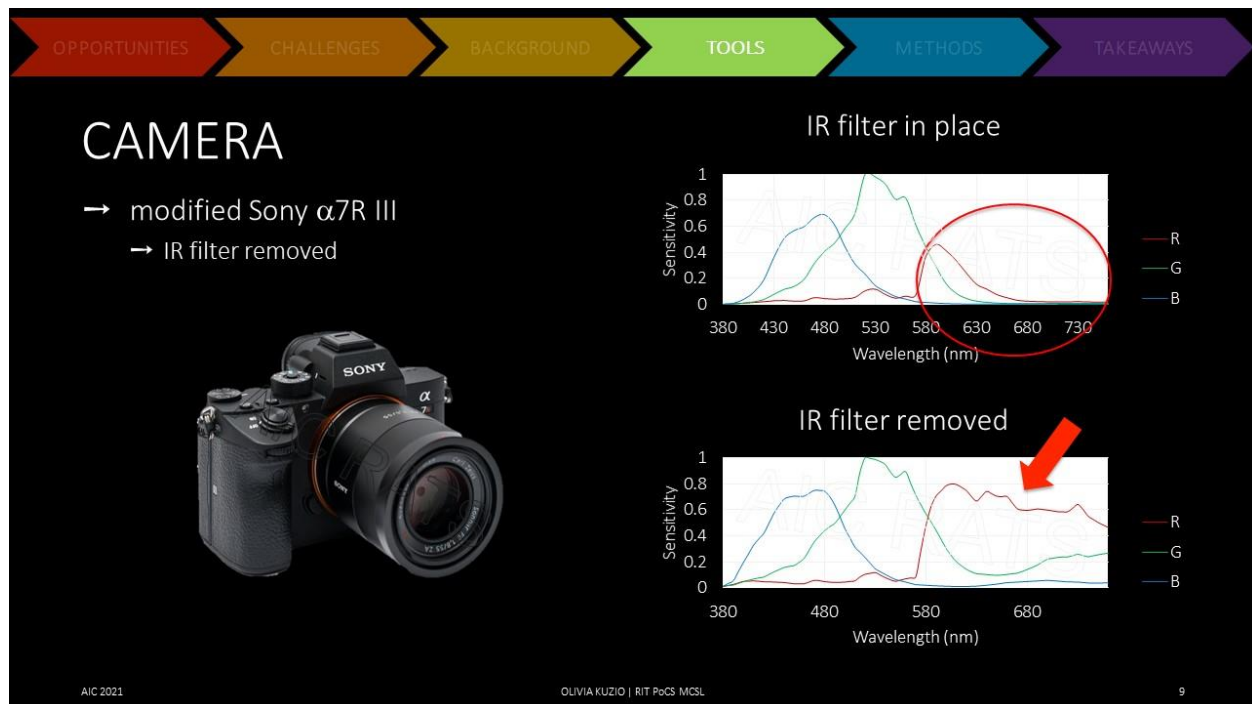


Most well-known feature of spectral imaging: spectral images = spectral reflectance estimation

- Spectral reflectance = both color and material properties

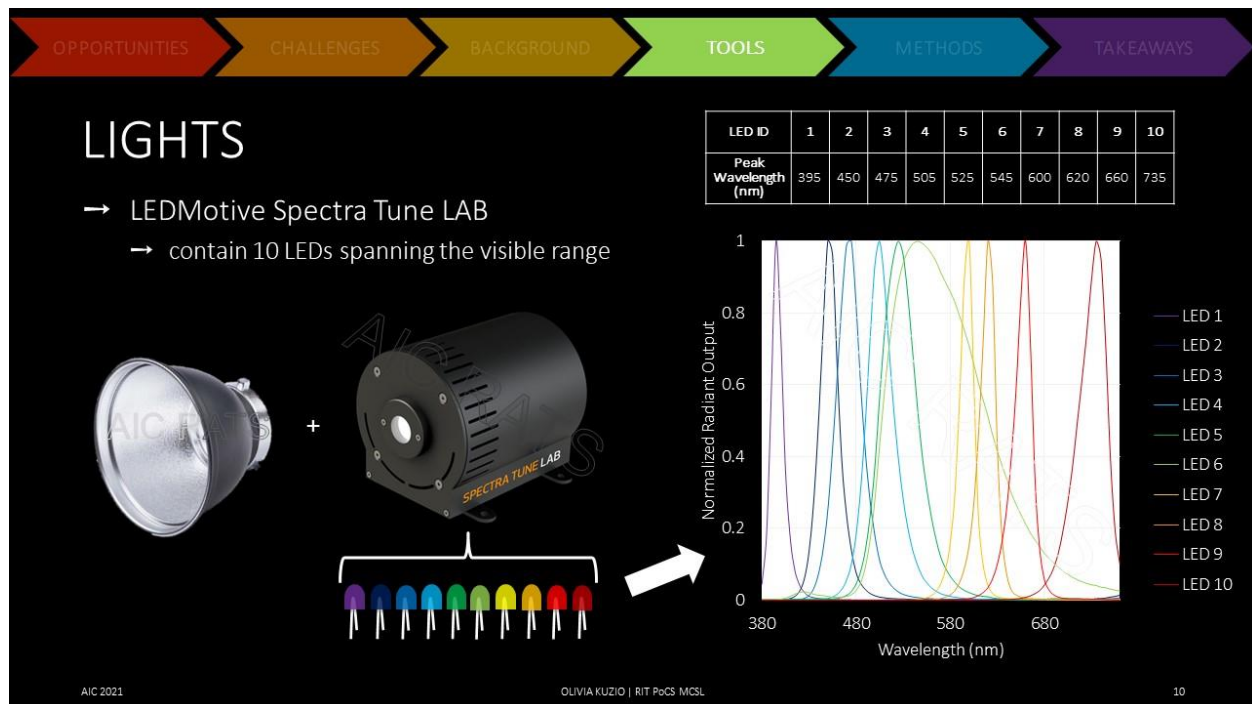


Spectrophotometer: reflectance at a single point vs. spectral imaging: reflectance at every pixel of the image



A more accessible multispectral imaging strategy should use more familiar tools

- Our system utilizes a commercially available RGB DSLR: a modified Sony $\alpha 7R$ III
 - Common modification: internal IR filter removal, extending the camera's red band sensitivity to longer wavelengths

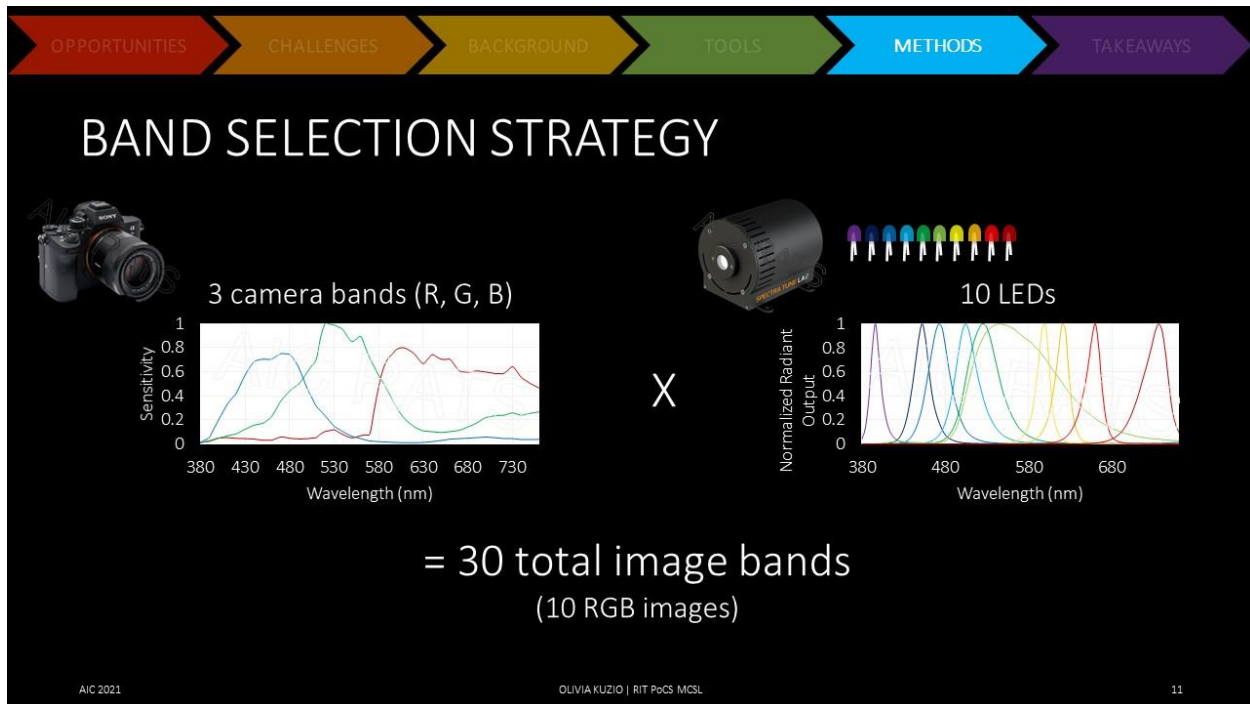


LED-based method utilizes illumination by light fixtures containing LEDs with narrowband characteristics

- Each light contains 10 distinct LEDs that emit light within specific bands of wavelengths (see plot)

Form factor of lights

- Small
- Internal integrating sphere for light uniformity
- External reflector
- Bottom line: they look and feel like typical studio strobes, improving their user-friendliness



Paired together, these two tools enable the collection of more spectral bands than are necessary for this needs-based approach

- Camera: 3 bands (RGB)
- LEDs: 10 bands
- Camera x LEDs = ability to capture 30 total bands, if capturing 1 RGB image per LED

A method of selecting relevant data from the over-sampled data is necessary

OPPORTUNITIES CHALLENGES BACKGROUND TOOLS METHODS TAKEAWAYS

BAND SELECTION STRATEGY

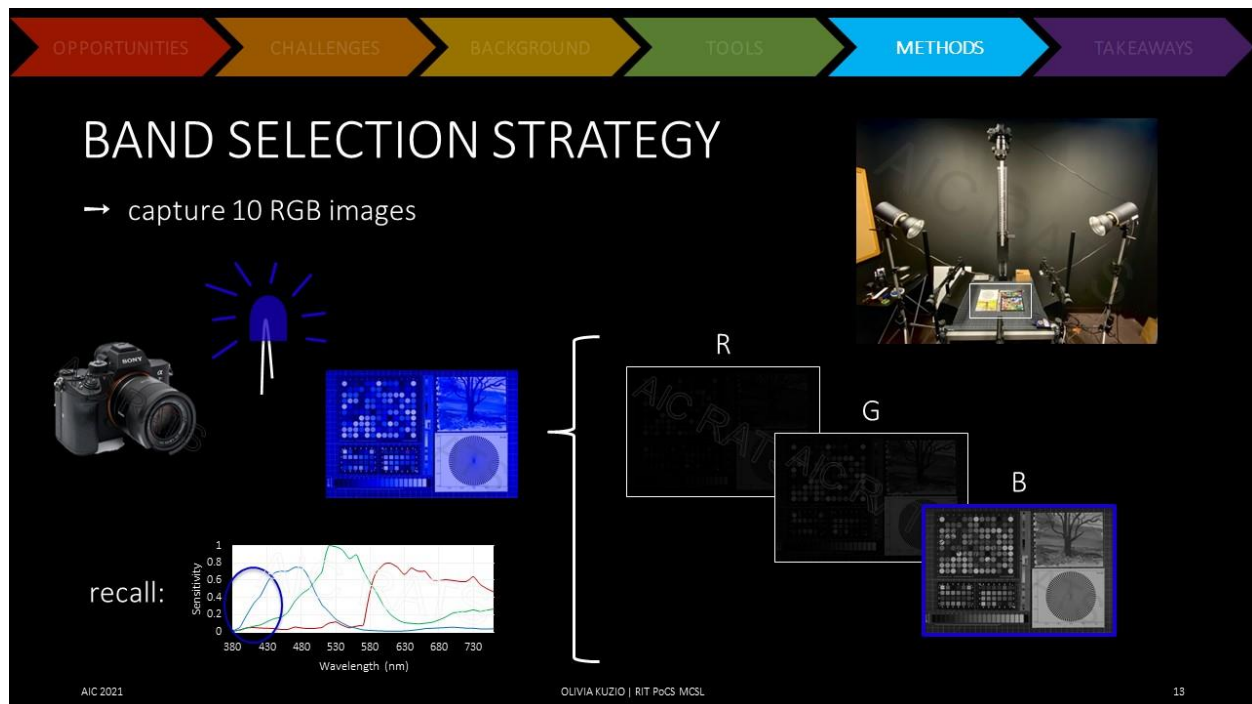
→ capture 10 RGB images



AIC 2021 OLIVIA KUZIO | RIT PoCS MSL 12

Visualization of the set of 10 RGB images (30 total “spectral” bands), where 1 image is captured per LED

- Each image is a regular RGB color image
- Not every band of every image contains useful information




E.g. consider an image captured under illumination by one of the blue LEDs

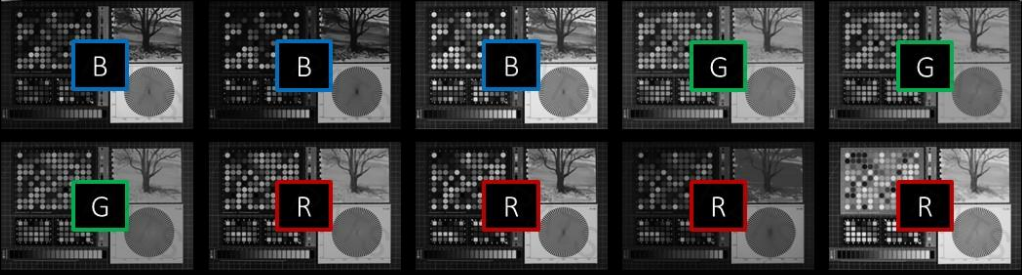
- Only the blue camera band has high sensitivity to these wavelengths; red and green bands are not sensitive to these wavelengths, and so do not contain much signal
- Therefore, disregard red and green bands; only retain the blue band for inclusion in the multispectral band set

OPPORTUNITIES
CHALLENGES
BACKGROUND
TOOLS
METHODS
TAKEAWAYS

BAND SELECTION STRATEGY

- capture 10 RGB images
- choose the R, G, or B band from each image that contains the most signal

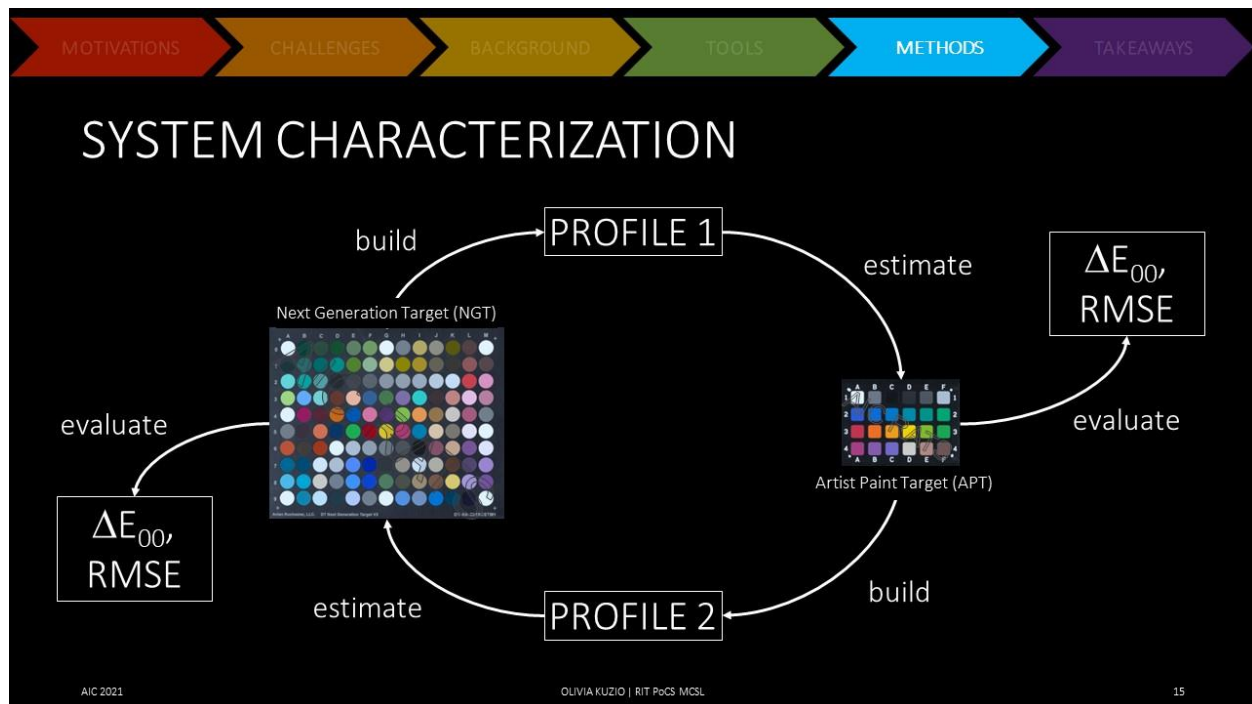




AIC 2021
OLIVIA KUZIO | RIT PoCS MSL
14

Band with highest signal matches visual appearance of the RGB image, i.e. the images that look blue contain the most signal in the blue channel, etc.

10 chosen bands = 10-band mode multispectral image set



Characterize the multispectral imaging system as operated in this 10-band mode

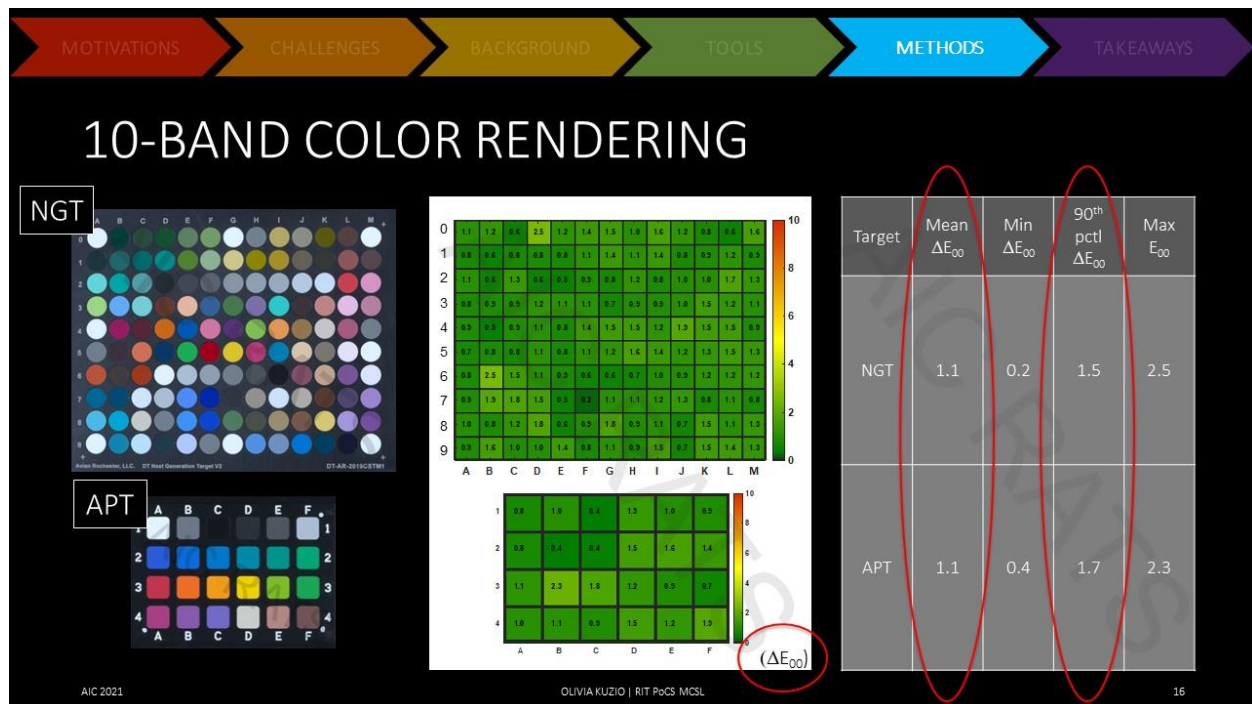
- Remember the goal: a simplified multispectral imaging method that provide great color rendering and spectral reflectance estimation capabilities

Characterization method: cross-profiling using two color targets

- For each target, build a profile to calculate its color and spectral reflectance information
- Use these profiles to estimate the color and spectral reflectance of the opposite target
- Evaluate the performance of the 10-band mode by calculating difference metrics (ΔE_{00} and RMSE) between the estimated values and the measured values

Why these particular targets?

- Large gamut of colors and spectral reflectance variety to test over
 - Next Generation Target contains a specific subset of “heritage colors”
 - Artist Paint Target contains real paints to serve as a model system for cultural heritage materials




Resulting color accuracy evaluation for 10-band mode

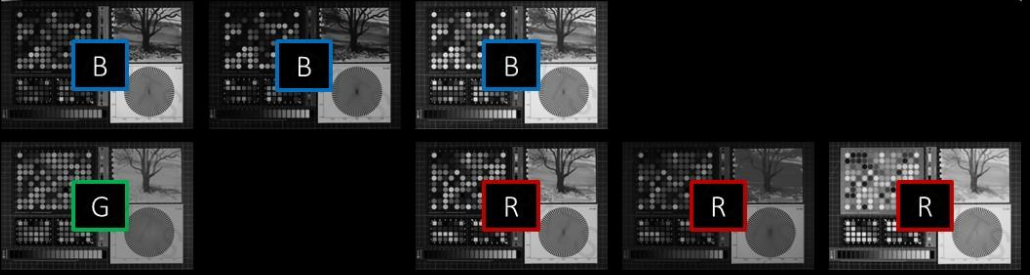
- Middle: heat maps that provide both a quantitative and qualitative measure of color accuracy
 - Quantitatively: number in each square = ΔE_{00} color difference between measured color and the color reproduced by the 10-band multispectral imaging method
 - Qualitatively: heat map encoding ranges from dark green for small color differences to red for large color differences (mostly green = good)
- Right: statistics summarizing ΔE_{00} values
 - Typically reported: mean
 - In this case, 1.1 ΔE_{00} for both targets
 - Also worth considering: 90th percentile
 - In this case, 90% of the patches are reproduced with an error of 1.5 and 1.7 ΔE_{00} or less, respectively

MOTIVATIONS
CHALLENGES
BACKGROUND
TOOLS
METHODS
TAKEAWAYS

BAND REDUCTION

- systematically exclude single, pairs, and groups of bands when profiling
- re-evaluate color & spectral estimation performance based on each reduced input set





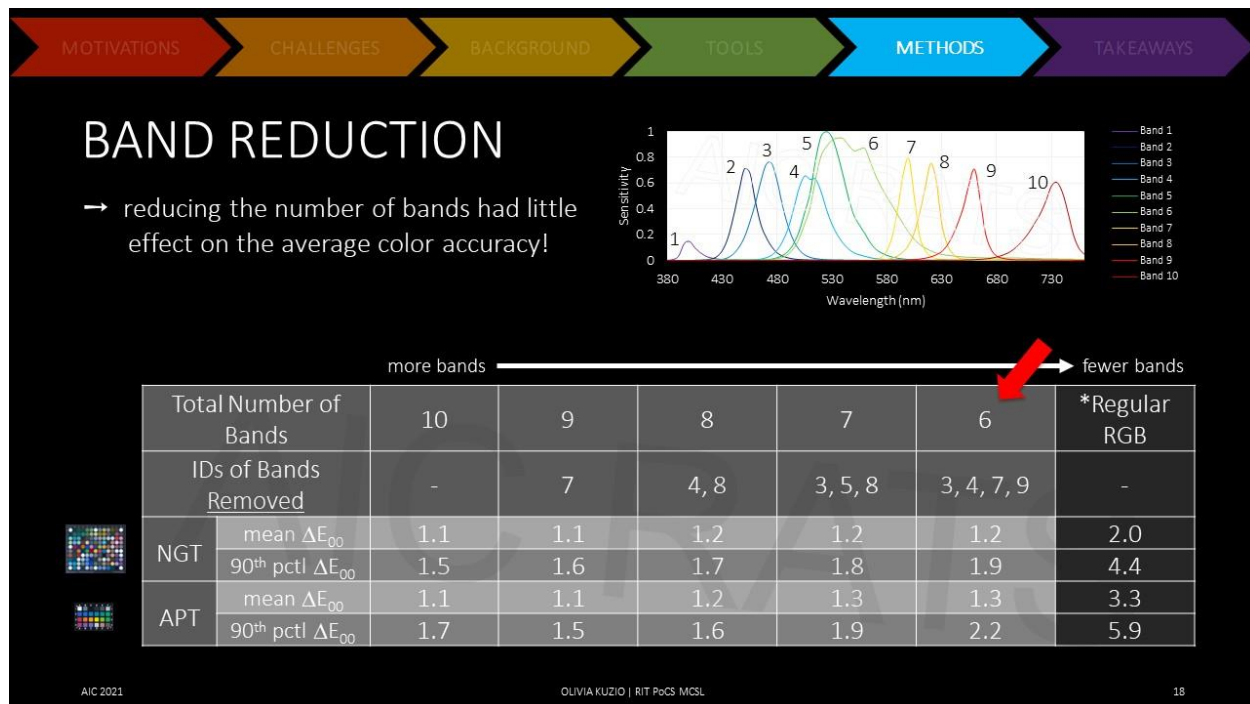
AIC 2021
OLIVIA KUZIO | RIT PoCS MSL
17

Is it necessary to use 10 bands, corresponding to one from each of the 10 LEDs, to obtain color accuracy as good as that communicated on the previous slide?

- If not, how few bands are needed to still achieve a highly accurate color rendering?

Experiment:

- Systematically remove more and more spectral bands from the original set of 10
- Then quantify how reducing the number of spectral bands affects the color accuracy evaluation



Summary of spectral band reduction experiment

- Given a target total number of bands, we determined which from the overall set of 10 could be removed to attain the best color accuracy possible for that number of bands

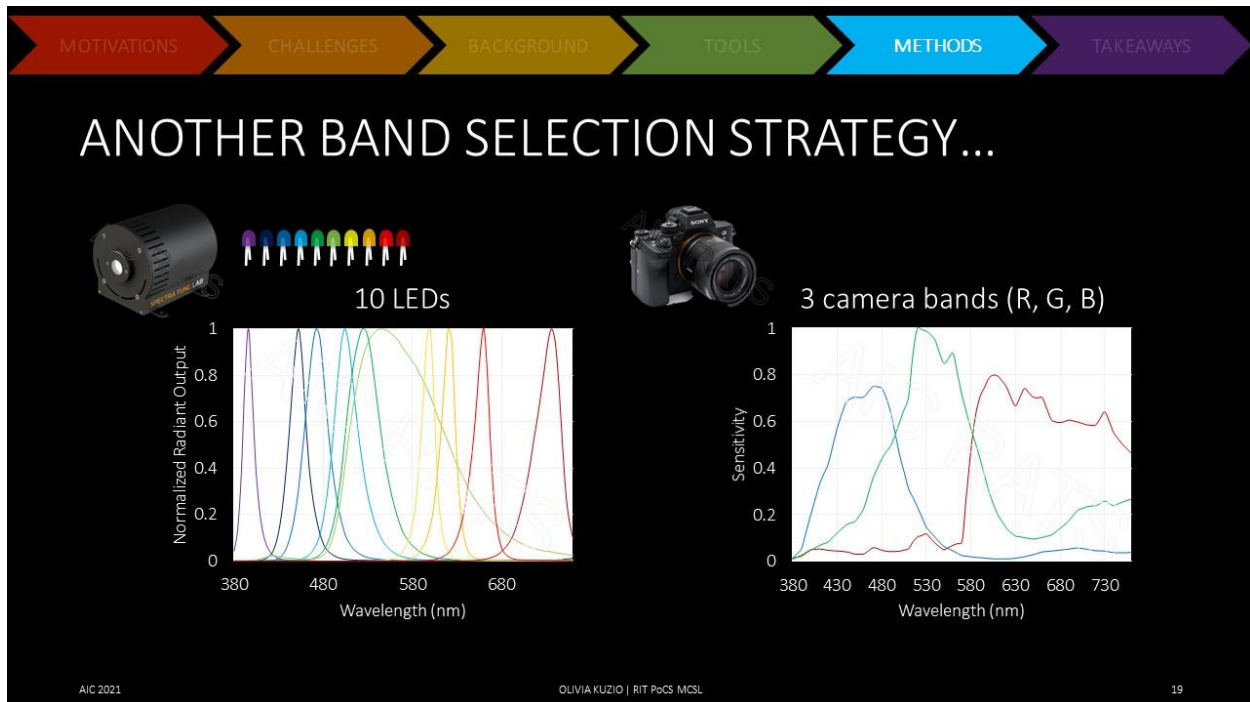
Overall takeaway: reducing the number of bands had little effect on the average color accuracy

- Read this from the table by moving from more channels on the left to fewer on the right; observe that the mean ΔE_{00} value does not significantly increase for either target as more bands are removed
- 90th percentile values do increase slightly
 - This indicates that there are some outlier color patches that are difficult to reproduce accurately with less spectral coverage

Note that reduction to a set of 6 spectral bands maintains high color rendering accuracy

Note that the final column reports results for regular RGB imaging of the same targets

- Observe the improvement that multispectral imaging affords over RGB imaging
- Note also that the perceptible limit for color differences in digital images is $\sim 2 \Delta E_{00}$
 - Compare this threshold to the values in the table
 - Multispectral imaging falls below this limit for all but one reported ΔE_{00} value
 - RGB imaging falls at or above this limit



- Thus far the “spectral” nature of the imaging system was defined with respect to the 10-band LEDs

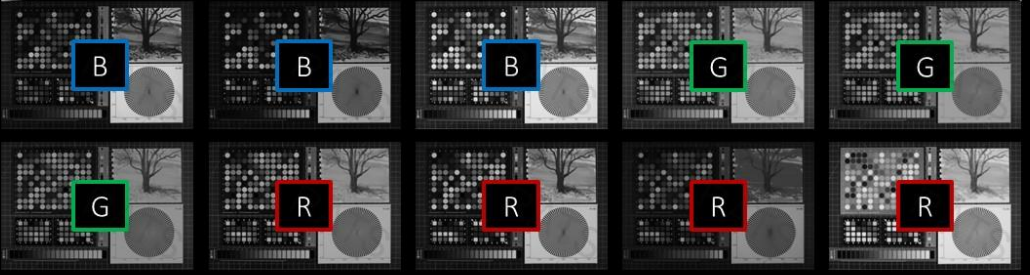

However, there are ways of leveraging the 3-band nature of the RGB camera in the system and using this to our advantage

- This was inspired by the observation from the band reduction experiment that images rendered from as few as 6 bands maintain a mean color accuracy equivalent to the 10-band mode

MOTIVATIONS CHALLENGES BACKGROUND TOOLS METHODS TAKEAWAYS

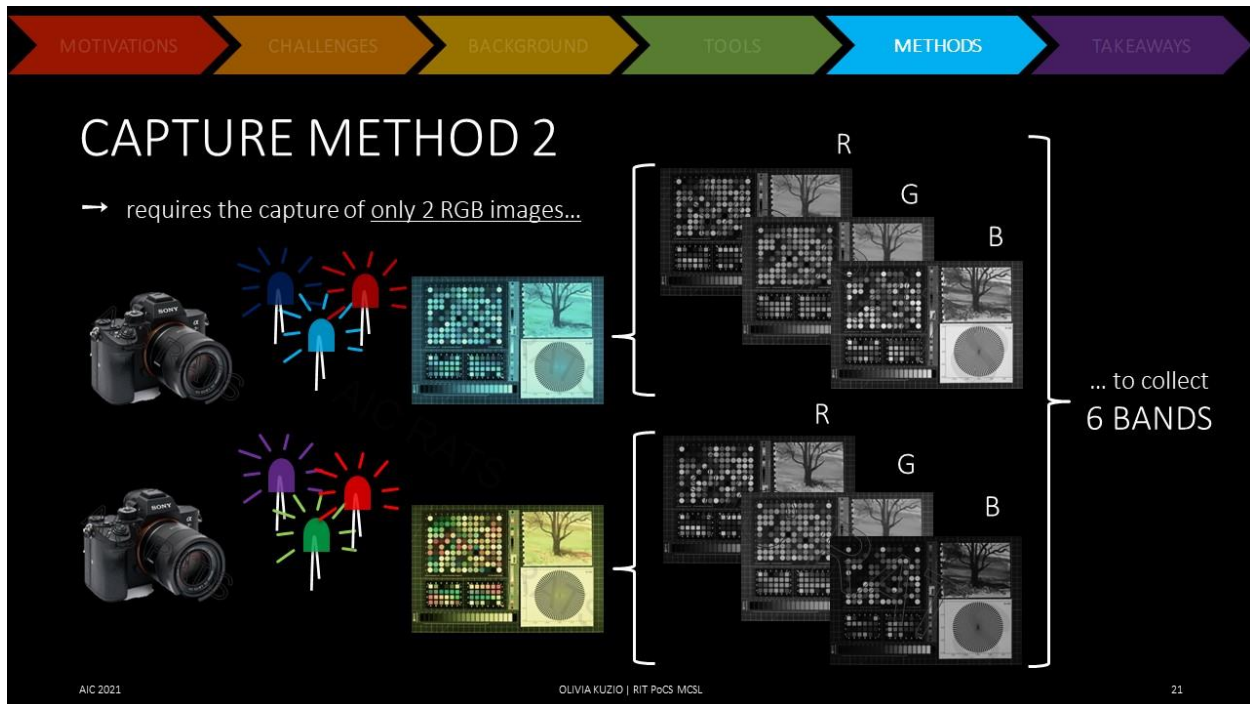
CAPTURE METHOD 1

- 10 spectral bands
- requires the capture of 10 RGB images



AIC 2021 OLIVIA KUZIO | RIT PoCS MSL 20

In the capture method previously discussed, 10 RGB images were captured, and from each image, only the band with the highest signal was included in the multispectral band set

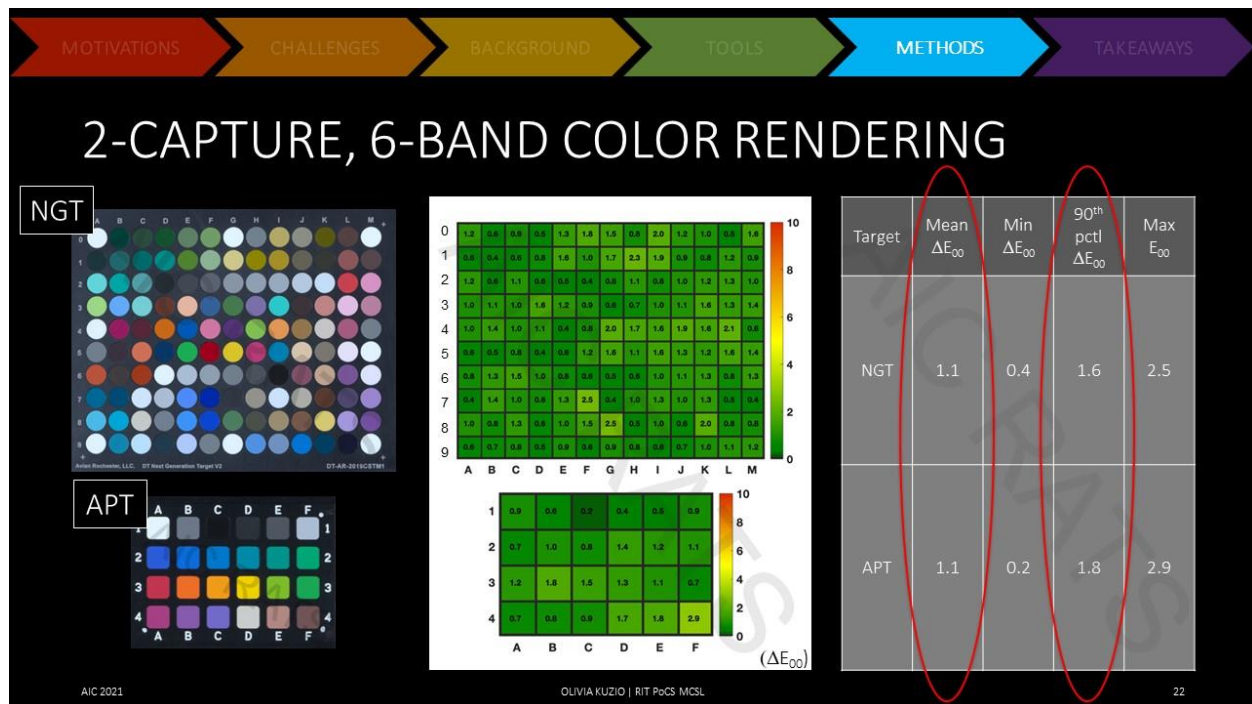


In a different capture strategy, combinations of the LEDs were optimized to get useful information in the R, G, and B camera bands of every image

Implication: only 2 images are required to collect 6 useful, signal-containing multispectral bands

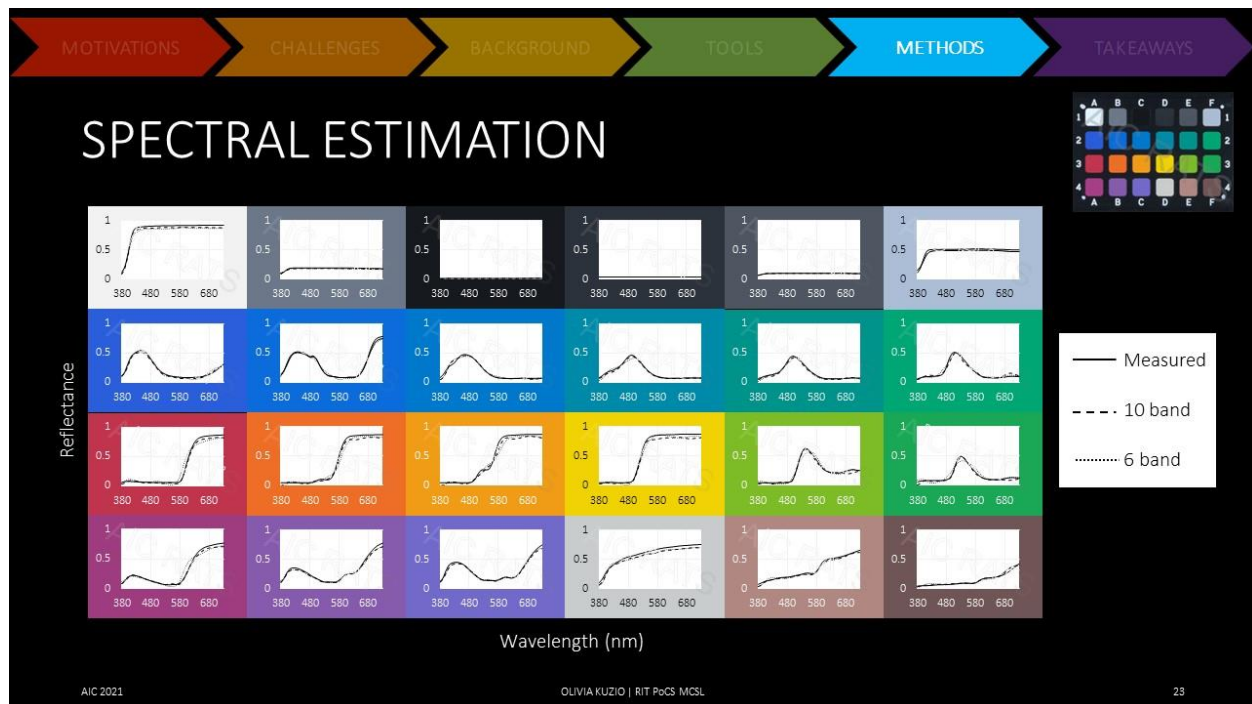
- More efficient than throwing away two-thirds of the captured data, like in the previous strategy

Recall: based on the band reduction experiment. a system having as few as 6 spectral bands proved reasonable for producing color accurate images



Resulting color accuracy evaluation for 6-band mode

- Simpler capture strategy, yet little change in color accuracy with respect to the 10-band mode, as expected
- Heat maps: still mostly green
- ΔE_{00} statistics: nearly equivalent to 10-band mode



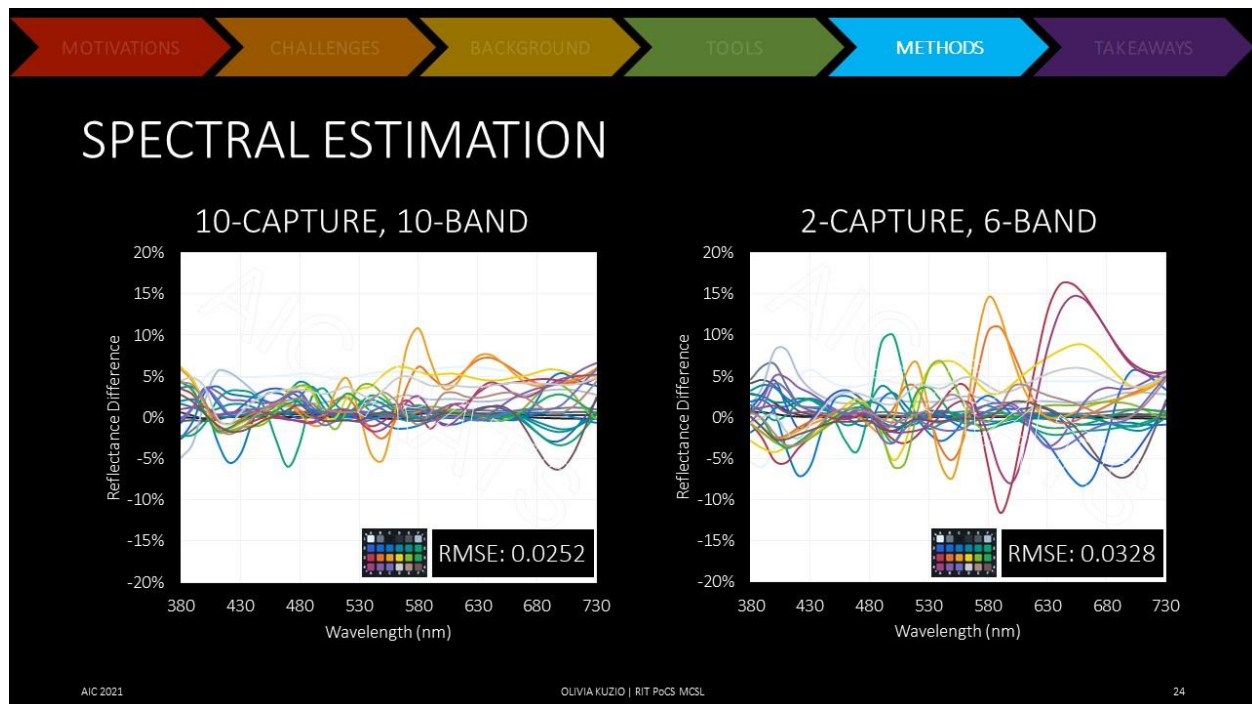
Spectral reflectance estimation capabilities of 10-band and 6-band modes

In each plot: spectral reflectance for the corresponding patch in the Artist Paint Target (color-coded)

- Solid line: measured spectral reflectance
- Dashed line: spectral reflectance estimated from 10-band mode
- Dotted line: spectral reflectance estimated from 6-band mode

Visual assessment: both estimated curves match the measured curve well for most patches

- Reflectance properties of many artists' materials do not have sharp features in the visible range; therefore, a system based as few as 6 bands can be sufficient for estimating such smooth curve shapes

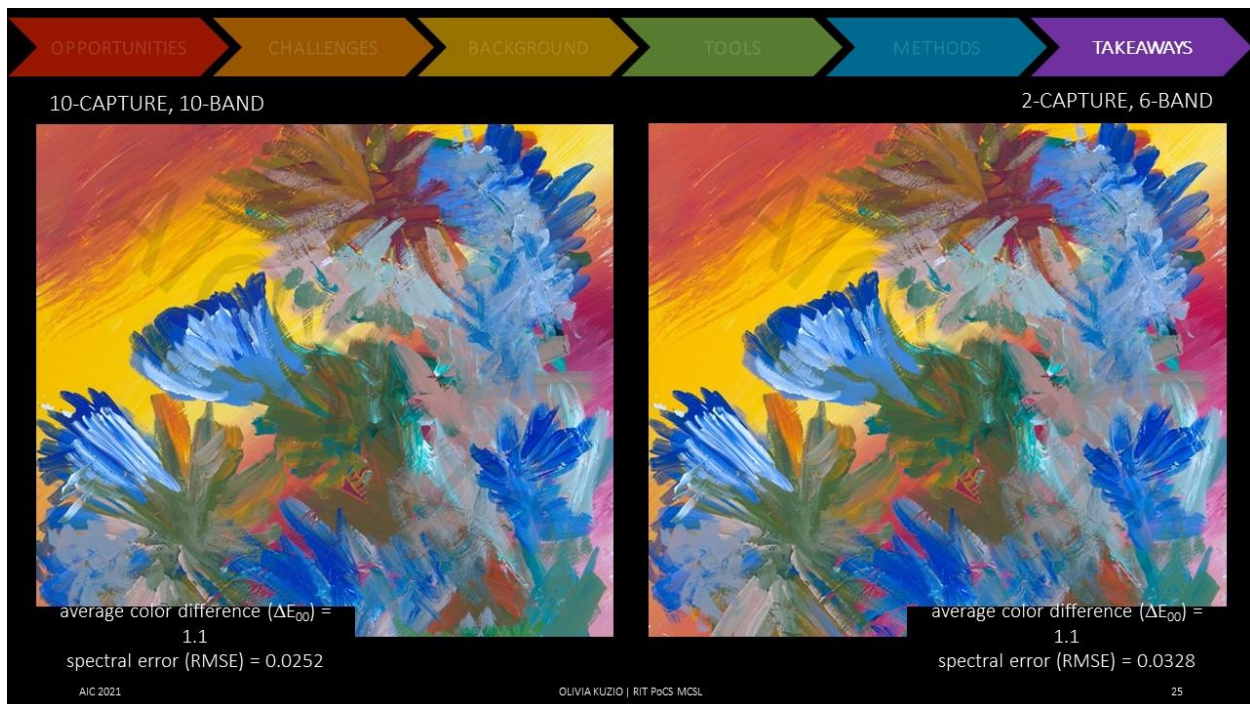


A closer look at the spectral reflectance estimation capabilities of 10-band and 6-band modes using spectral difference plots

- These plots illustrate the differences between the estimated reflectance spectra for the 10-band and 6-band modes with respect to the measured reflectance spectra
 - A perfect spectral reflectance match would be a flat line at zero percent reflectance difference
 - Any deviation from zero indicates spectral estimation error, and the further from zero, the more discrepancy between the measured and the estimated spectrum

Takeaways:

- 1) 10-band mode slightly outperforms the 6-band mode. It has no spectral deviations of more than ~10% (note y-axis range of -20% to +20% difference)
- 2) 6-band mode still performs well: maximum spectral difference for some pink and orange patches is ~15%



An illustration of differences between 10-band, 10 capture vs. 6-band, 2-capture modes using images of a real painting

Recall: average color difference is the same for both modes ($\Delta E_{00} = 1.1$)

- So, on average, the overall color rendering will be similar
- However, there are slight differences in the color rendering, particularly for the highly chromatic reds and oranges (recall from previous slide)

Also recall: the spectral error metric of RMSE is slightly different for the two approaches (0.0252 for 10-band mode vs. 0.0328 for 6-band mode)

- The 10-band spectral reflectance data cube will, on average, slightly better describe the material properties of the paints

The question: is the color difference noticeable if you were not told it exists? Does the spectral estimation error preclude material classification studies?

The bottom line: do differences/errors of this level matter?

- Application/imaging intent dependent
- Consider: how many spectral bands need to be captured to meet a certain threshold of goodness?

WHAT DO YOU NEED?

HOW GOOD IS GOOD ENOUGH?

WHAT ARE THE NECESSARY EFFORTS?

CONSIDERATIONS...

- desired output
- color image
 - color rendering accuracy
- spectral reflectance
 - spectral estimation accuracy
- efficiency
- expense

AIC 2021 OLIVIA KUZIO | RIT PDCS MSSL 26

Emphasis on this needs-based approach

- What is needed?
- What is the purpose of the imaging?
- What is the threshold of goodness that need to be met?
- How many bands are needed to capture data that will meet that threshold?
- Consider tradeoffs between complexity, efficiency, etc.

Moving forward: continued emphasis on simplifying thinking about and practicing spectral imaging toward democratizing the technique for broader use



Optical 3D Scanning System to Enable 3D Viewing, Sharing and Printing of Artworks

Yi Yang, Xingyu Zhou, Darlene In, Xingchang Xiong, Kunze Yang, Xing Chen, Heather McCune Bruhn, Xuan Liu

Original Abstract

Optical coherence tomography (OCT) is a non-invasive imaging method that can be used to study the surface features and subsurface structures of delicate cultural heritage objects. However, one of the limiting factors that is preventing OCT for broader applications in art conservation is the system's small field-of-view (FOV) (Song, Xu, and Wang 2016). This limits the OCT system's ability to cover a mesoscale or macroscopic region of interest (ROI), such as a painting.

We present a hybrid scanning platform combined with effective algorithm to achieve macroscopic OCT (macro-OCT) imaging. With this new system, we present a proof of concept spectral 3D reconstruction of objects such as an impressionist style painting. We first acquire enface images from each OCT scan and digitally stitch these images together to form a large image of the painting. This enables the system to achieve high resolution OCT imaging with increased FOV to generate high definition 3D surface model. We then demonstrates the potential applications of the OCT data by rendering 3D volumetric data into standard virtual reality (VR), augmented reality (AR), and 3D printing formats. Using the 3D data acquired by the macro-OCT system, the team converted it into standard 3D files which can be used for online viewing, VR and AR. The team demonstrated these concepts through viewing the model from a webpage and a cellphone using AR. Finally, the team 3D printed a 1:1 sample 3D model.

This type of digital copy could serve as a backup method to capture the best possible details of art works to hedge against the worst-case scenario, such as war, terrorism, natural disaster, heist, and other catastrophes. The 3D surface model of paintings also can be used in classes to enhance art viewing experiences, especially for online courses. Collaborators will be able to rotate, zoom in and out to view details of art works such as brushstrokes and learn about various painting styles. 3D printed painting samples can be used to assist visually impaired users to experience various painting techniques, such as Van Gogh's brushstrokes and Pointillism demonstrated by Seurat's works. Furthermore, surface model of ancient coins or metallic objects can be 3D printed to give visually impaired visitors touch experience. Finally, the OCT provides a minimally invasive method to generate the cross-sectional information of paintings, which can be used for art conservation work.

Reference:

Song, Shaozhen, Jingjiang Xu, and Ruikang K Wang. 2016. "Long-Range and Wide Field of View Optical Coherence Tomography for in Vivo 3D Imaging of Large Volume Object Based on Akinetic Programmable Swept Source." *Biomed. Opt. Express* 7 (11): 4734–48.
<https://doi.org/10.1364/BOE.7.004734>.

Titian's *Rape of Europa*: Artist's Pigments and Changes Revealed through Macro-XRF Mapping

Jessica Chloros^{1*} and Dr. Aaron Shugar², with Gianfranco Pocobene¹, Dr. Bruce Kaiser, Richard Newman³, and Courtney Books⁴

¹Isabella Stewart Gardner Museum, 25 Evans Way, Boston, MA 02115

²Buffalo State College, Garman Art Conservation Department, Rockwell Hall 230, 1300 Elmwood Ave, Buffalo NY 14222

³Museum of Fine Arts, 465 Huntington Avenue, Boston, MA 02115

⁴Saint Louis Art Museum, One Fine Arts Drive, Forest Park, St. Louis, MO 63110

*Corresponding Author: Jessica Chloros, jchloros@isgm.org

Extended Abstract

Titian's *Rape of Europa* (1562, 180 x 205 cm), is one of six pictures the artist painted for King Philip II of Spain between 1551 and 1562. The paintings are large-scale mythological scenes inspired by Ovid's epic poem 'Metamorphoses'. Titian called the paintings 'Poesie' as he considered them to be visual manifestations of poetry. Over the centuries, the works were dispersed throughout Europe and America; *Rape of Europa* entered the Gardner Museum collection in 1896. The painting, along with its companion paintings from the commission will be reunited for the first time since 1704 for a major travelling exhibition (London, Madrid and Boston, March 2020 – January 2022). The exhibition prompted both an in-depth technical study and extensive treatment of the painting.

Rape of Europa was the last painting executed by Titian for the Poesie commission and the technical study provided the opportunity to gather valuable information about the artist's painting techniques from his late period. A full complement of imaging and analytical techniques was employed for the investigation. High resolution imaging was carried out in visible, ultra-violet (UV) and infra-red wavelengths and x-radiographs taken in 1979 were digitized and stitched together, allowing for a detailed examination of the painting's structure and condition. These combined imaging techniques revealed that the painting is in an excellent state of preservation, no major changes were made to the composition other than the position of the bull's tail and putti figures in the sky, there was very little restoration other than along the edges and down the center seam where the two canvases were joined and there was a uniform natural resin varnish.

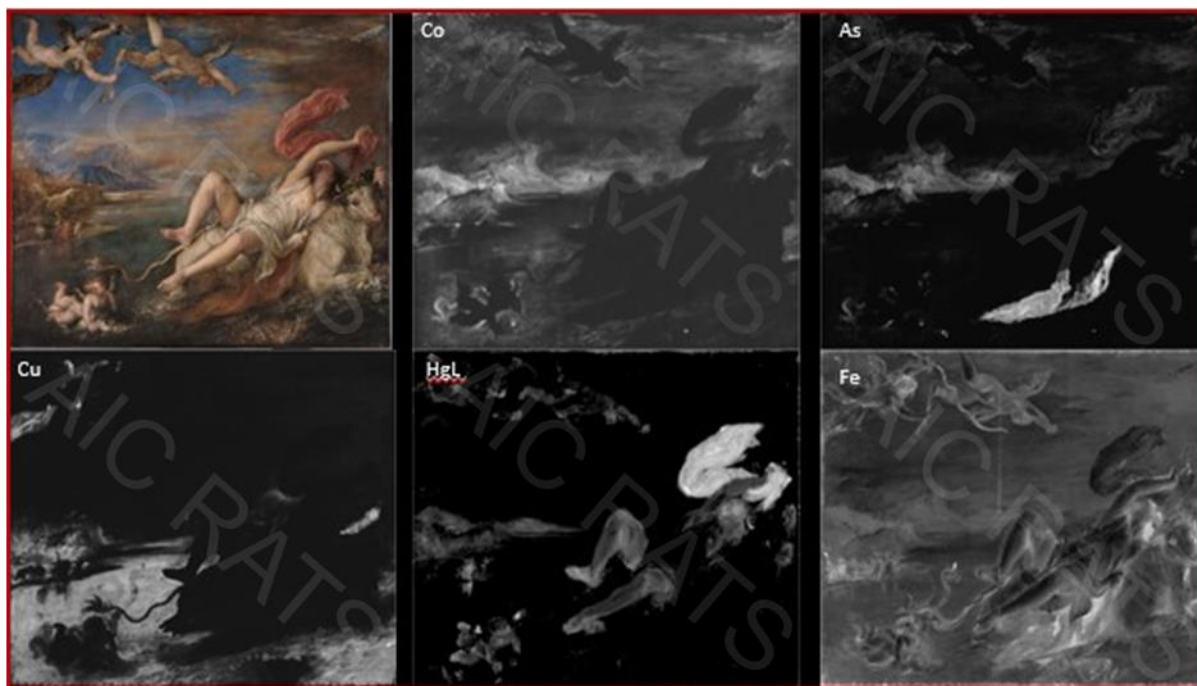
The extent to which certain pigments were used by Titian and their change over time called for elemental analysis of the entire painting using X-ray fluorescence mapping (sometimes termed MA-XRF). Without access to a large-scale, expensive scanning system the scale of the painting created logistical problems implementing accurate scanning of the surface. A novel approach was devised to analyze the elemental composition of pigments.

The painting was hung on a French cleat system that allowed it to be moved level and smoothly left to right for scanning each horizontal row. A Bruker 5i handheld XRF unit was then attached to a DeWitt 400E gantry to scan the entire surface gridded into forty sections. As each row was completed, the painting was shifted to the next cleat on the wall to scan the next row. This set up ensured proper alignment and registration throughout the process. The scanning took three conservators two and an half weeks to complete as each 30 x 40 cm gridded section took roughly three hours to scan.



It is also important to note that structural work was completed on the painting prior to XRF scanning. The painting was previously attached to a wood strainer (not original) that was in poor condition and did not allow for tensioning of the canvas. As a result the painting hung somewhat loosely, creating surface undulations, which can cause variation in the collected photon intensities during XRF scanning. The variation in photon intensities causes variable intensities in the resulting map and the effects are compounded when multiple maps are stitched together. The structural work entailed reinforcing the canvas edges with strips of new linen canvas to enable re-stretching and proper tensioning of the painting. A new stretcher was fabricated and modified to incorporate light-weight panel inserts which provide a continuous rigid support for the painting. A loose lining canvas composed of Belgian linen was then stretched over the panel insert stretcher followed by re-stretching of Rape of Europa onto its new stretcher support. The analysis of the 40 separate stitched together XRF maps taken on the new planar surface produced over 250,000 spectra resulting in 18 separate elemental maps. The maps provided details of alterations made to the composition by the artist and confirmed extensive smalt degradation, particularly in the right half of the sky. In addition to smalt, other pigments inferred from the analysis include: ultramarine, azurite, vermillion, iron earth pigments,

red lake pigment, orpiment/realgar, lead-tin yellow, verdigris/copper resinate and lead white.



The XRF maps also enabled strategic targeting of sampling for cross-sectional analysis, with multiple questions often answered with one sample, thereby reducing the number of samples taken. The cross-section samples were also submitted for elemental analysis by scanning electron microscopy with electron dispersive spectroscopy (SEM-EDS) using a JEOL JSM-6460LV scanning electron microscope with an Oxford Instruments X-Max^N energy-dispersive X-ray spectrometer and 80 mm² detector. The results of the technical study not only produced rich information about Titian's paint materials but also informed the approach taken with cleaning and restoration.

Research and Technical Studies
Specialty Group and the Society of the
Preservation of Natural History
Collections Presentations

Comparative Analysis of Consolidants Used to Treat Paper Shale Fossils

Catherine G. Cooper^{1*}, Conni J. O'Connor²

¹National Center for Preservation Technology and Training (NCPTT), National Parks Service, Natchitoches, LA 71457

²Florissant Fossil Beds National Monument, National Parks Service, Florissant, CO 80816

*Corresponding Author: Catherine G. Cooper, Catherine.Cooper@nps.gov

Extended Abstract

Florissant Fossil Beds National Monument (FLFO) houses an important collection of fossils that are known and studied world-wide (Meyer 2003). The collections include paper shale specimens, primarily consisting of insect and plant fossils, that are particularly fragile due to their lamellar structure and composition and sensitivity to humidity (Reinthal 2015). Condition assessments of paper shale fossils in the FLFO collections indicate that they are in danger of delamination, flaking, cracking, and breaking, which can cause loss of material and data, and may limit access to specimens for physical study and exhibition to prevent further damage (Shelton et al. 2015). The fossils are contained in individual layers within these lamellar structures, so loss of a single layer can mean loss of that fossil entirely. Various consolidants have been used to stabilize these samples in the past, but studies on their effects on the samples have been limited (Senge and Voellinger 2019).

In this study, we compare how five different consolidants applied to paper shale fossils from Florissant Fossil Beds National Monument age when exposed to accelerated weathering. The consolidants chosen included three reaction adhesives: two name-brand versions of ethyl-cyanoacrylate super glue (Aron Alpha 241F and PaleoBond 40), and medical grade butyl-octyl cyanoacrylate blend (GluStitch GluSeal), and two poly vinyl butyral solution adhesives: Butvar B-76 and Butvar B-98 mixed at 5% w/v in ethanol. Due to the unique nature of these specimens, any change in physical properties of the surface can be considered a failure. Failures ranked from most severe to least: failure of consolidant bonds, flaking and loss of material, change in color of sample, change in gloss of sample.

Each consolidant was used to treat five samples, and there were five untreated samples prepared as controls, for a total of thirty samples used in this experiment. Sample treatment included flooding the surface of the sample with the chosen consolidant and adhering an untreated paper shale chip to the upper left corner of the sample's surface. This allowed for examining weathering of the consolidant as well as any change in its adhesion over the course of the experiment.

Color, gloss, surface roughness, and FTIR data were collected before and after treatment and then after each 200-hour accelerated weathering cycle. The samples were

exposed to a total of 800 hours of accelerated weathering under artificial light in a QUV weatherometer following ASTM D904 (ASTM 2013). This was used as the first experimental phase to examine how the consolidants themselves age under worst case scenario conditions. All consolidants maintained adhesive bonds, but a few samples exhibited signs of impending delamination.

Results from this experiment indicate that the two Butvars cause the least overall change in appearance when compared to the control samples. Butvar B-98 evidenced the least overall color change over the course of the experiment, closely followed by Butvar B-76 (fig. 1). Gloss and surface roughness measurements were interpreted together because surface roughness can impact gloss readings. The ethyl cyanoacrylates show the least amount of overall change in gloss from before treatment, through treatment and accelerated light aging. The ethyl and butyl-octyl cyanoacrylates also showed the greatest change in surface roughness, and examination of the surfaces under magnification show beading of the cyanoacrylates on the surface (fig 2.). These beads can scatter the light used in the glossmeter, impacting the data. The Butvars did not alter the surface roughness of the samples appreciably.

The next experiment in this project will focus on examining how paper shale fossils treated with these same five consolidants age when exposed to cycling temperature and relative humidity similar to exhibit displays and collection storage conditions at Florissant Fossil Beds National Monument.

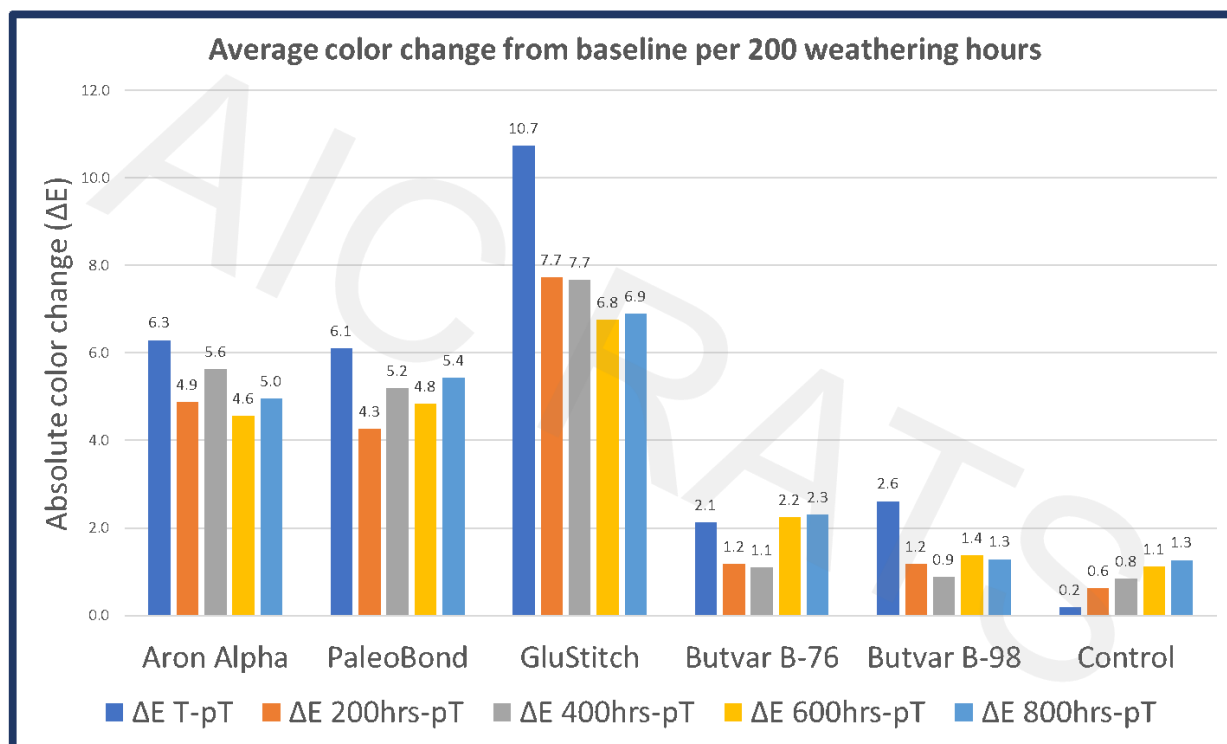


Figure 1: Bar graph showing the average absolute change in color for samples treated with each consolidant compared to the pre-treatment baseline color measurements. Note the

largest color change occurred between treatment (T) and pre-treatment (pT) for most treated samples.

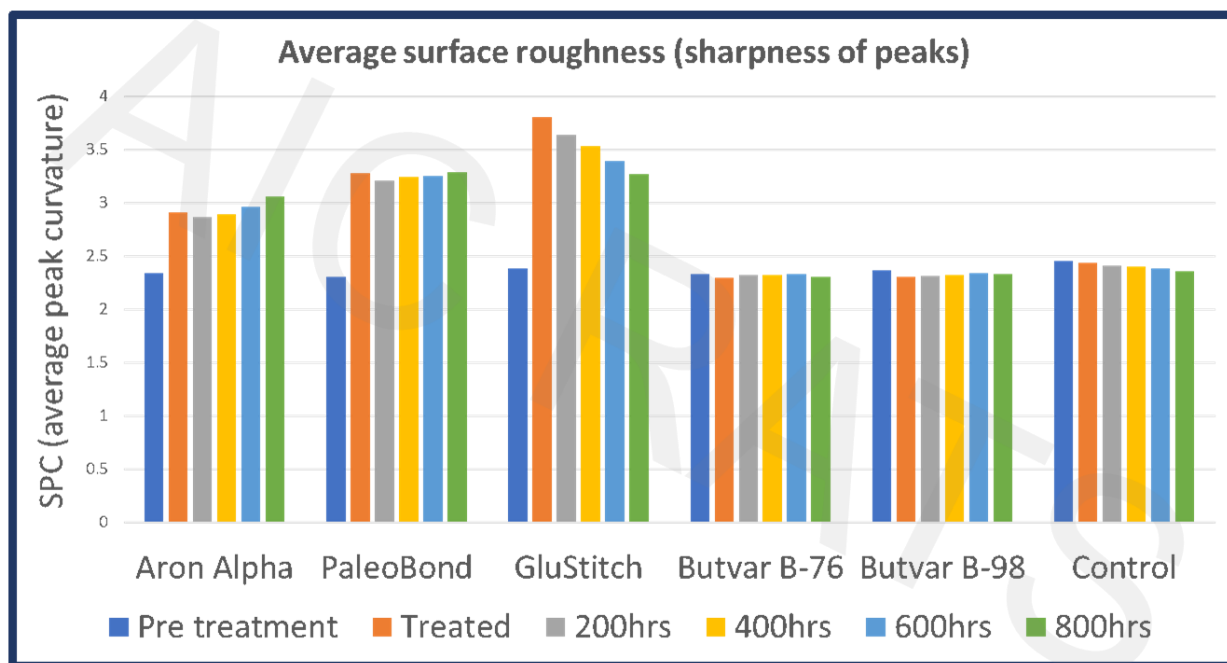


Figure 2: Average surface roughness measurements (SPC) for samples treated with each consolidant measured at each stage of pre-treatment, treatment, and 200-hour weathering increments. Note the spike in surface roughness measurements from pre-treatment to treatment in the samples treated with cyanoacrylates.

References:

ASTM (American Society for Testing and Materials). 2013. Standard Practice for Exposure of Adhesive Specimens to Artificial Light. ASTM D904-99 (2013). Philadelphia: ASTM.

Meyer, Herbert W. 2003. *The Fossils of Florissant*. Washington and London: Smithsonian Institution.

Reinthal, Elizabeth. 2015. *Reinthal Final Report* [Unpublished]. Paleontological Resource Program Records (FLFO 9771), Florissant Fossil Beds National Monument. Florissant, CO.

Shelton, Sally Y, Mariah G. Slovacek, Heather Falkner, and Elizabeth Reinthal. 2015. *Handbook for the Care and Conservation of Paper Shale Fossils* [Unpublished]. Paleontological Resource Program Records (FLFO 9771), Florissant Fossil Beds National Monument. Florissant, CO.

Senge, Dana, and Theresa Voellinger. 2019. Florissant Fossil Beds National Monument: Collections Condition Survey. Intermountain Region Museum Services Program Conservation Laboratory. Tucson, AZ. Paleontological Resource Program Records (FLFO 9771), Florissant Fossil Beds National Monument. Florissant, CO.

Reconstructing Asia's Ancient Ivory Trade: PCR and NGS Analysis of Elephant Tusk Sections from the Field Museum's Java Sea Shipwreck Collection

Lisa C. Niziolek^{1*}, Stephanie E. Hornbeck¹, Claire Scott^{1,2}, Gary M. Feinman¹, Felix Grewe¹, and Cynthia R. Wagner²

¹ Field Museum of Natural History, 1400 S. Lake Shore Drive, Chicago, IL, 60605

² Department of Biological Sciences, University of Maryland, Baltimore County, Baltimore, MD 21250

* Corresponding author: Lisa Niziolek, lniziolek@fieldmuseum.org, (312) 665-7426

Extended Abstract

In 1999, the Field Museum, Chicago, acquired 7,500 items from the archaeological remnants of a maritime trading vessel—now known as the Java Sea Shipwreck (JSW)—that sank in the Java Sea in Indonesia in the late 12th century (Niziolek et al. 2018). Although Chinese ceramics and iron comprised much of the cargo, also found were hundreds of fine-paste *kendis* (handless, spouted water vessels); resin used in incense, sealants, and adhesives; sections of raw elephant ivory for medicinal and decorative applications; and storage jars that might have held spices, tea, fish sauce, and other comestibles (Mathers and Flecker 1997). Much of our team's early research focused on examining and sourcing porcellanous materials from the shipwreck (Niziolek 2015, 2017, 2018; Niziolek et al. 2015; Xu et al. 2019a; Xu et al. 2019b; Xu et al. 2020), but over the past several years we have been investigating other parts of the cargo, including the resin (Lambert et al. 2017) and ivory, that provide evidence of ancient large-scale socioeconomic networks that linked societies from Japan to the African continent.

Based on historical accounts such as Song dynasty official Zhao Rugua's 13th-century description of Chinese and Arab trade in China (*Zhufan Zhi [Record of Foreign Peoples]*), elephant tusks originated from several countries in Asia and Africa (Zhao 2012 [1911]). Ivory from Middle Eastern markets, which came from African elephants, was thought to be of higher quality than ivory from Asian elephants. Hunters reportedly brought the tusks they had procured to Merbat (Oman), and then the materials were transshipped to Southeast Asia. According to Zhao, tusks imported from the Middle East had a clear white color with delicate streaks whereas tusks from other places were smaller and had a reddish tint. The larger tusks of African elephants with their extensive dentine regions have been historically prized by ivory-carvers. Researchers initially thought the ivory from the JSW may have originated from elephants in Southeast Asia (Mathers and Flecker 1997:1; Miksic 1997:29); the tusk sections found at the JSW site probably passed through Palembang on

Sumatra, but based on their size, our team hypothesized they were from African, not Asian, species.

A total of 16 elephant tusk sections were recovered at the JSW site (Mathers and Flecker 1997) (Figure 1); 12 are in the Field Museum's Anthropology collection. The tusk segments are in raw form; they were not worked or carved into objects. They have extensive structural damage, with heavily abraded exterior surfaces and numerous complete breaks, deep cracks, and holes from mollusks (Figure 2); however, a diagnostic visual identifier of elephant ivory was detectable—a cross-hatch, or overlapping spiral pattern, evident in the dentine of the tusk in the cross-section cut, sometimes called “Schreger lines,” after Bernhard Gottlob Schreger who first noted their diagnostic significance in 1800. This intersecting arc pattern, visible to the naked eye or under low magnification, is present only on mammoth and elephant ivory. Acute arc angles on mammoth ivory distinguish it from elephant ivory, which has obtuse arc angles. Based on the Schreger lines present in the ivory from the JSW, we know that these tusks are from elephants. Schreger lines, however, cannot be used to differentiate between African and Asian species. In fact, no non-destructive techniques can be used to definitively distinguish between African and Asian elephant species. (See Hornbeck 2016.)



Figure 1. Two elephant tusks shortly after their 1996 recovery from the 12th-century Java Sea Shipwreck underwater archaeological site. Note the presence of circular, white, biological marine organisms on the surface. © Field Museum, courtesy Pacific Sea Resources.

Fortunately, small amounts of cellular material can be extracted from tusks, which allows DNA to be isolated and molecularly analyzed in order to differentiate among the three known living elephant species (e.g., Ishida et al. 2013; Wozney and Wilson 2012), providing crucial information for reconstructing ancient ivory trade routes (e.g., Gao and Clark 2014; Lane 2015; Niziolek and Respass 2017; Respass and Niziolek 2016; Tripathi and Godfrey 2007). Although they share the taxonomic family Elephantidae, African elephants, *Loxodonta africana* (savanna/bush) and *Loxodonta cyclotis* (forest), and Asian elephants, *Elephas maximus*, are different species. After consultation in 2017 with ivory specialist Terry Drayman-Weisser, Conservator Emerita at The Walters Art Museum in Baltimore,

MD, in 2018, Field Museum researchers collaborated with Wagner and Scott at University of Maryland, Baltimore County, Hornbeck and Niziolek removed samples from three tusks. Wagner and Scott isolated DNA from three tusks from the JSW collection for a Polymerase Chain Reaction (PCR) of a short mitochondrial marker region known to differ between African and Asian elephants (see Table 1) (see Kitpipit et al. 2017). By Sanger sequencing the three SNPs (single nucleotide polymorphisms) contained within the PCR-amplified region, two ivory samples from the Java Sea Shipwreck were identified as African elephant.



Figure 2. A 2019 photograph of elephant tusk section from an African bush/savanna elephant found at the 12th-century Java Sea Shipwreck underwater archaeological site. The evident, extensive post-recovery structural damage may pertain to drying after recovery from a water-logged environment. Length: 59 cm; width: 17 cm; height: 17 cm. © Field Museum, catalog number 351825.

In 2019, we aimed to assemble and annotate regions of the mitochondrial genome of the ivory by next-generation sequencing (NGS). Complete mitochondrial genome assemblies would allow us to clearly distinguish the Asian from the African elephant by 847 SNPs and learn additional information about the elephants whose tusks we analyzed (Brandt et al. 2012). As a summer intern in the Field Museum's Grainger Bioinformatics Center, Scott used powdered samples from six tusk sections to conduct NGS (Tables 1 and 2). NGS was not as successful as anticipated. We could not sequence the elephant mitogenomes using NGS because larger amounts of contaminated DNA (mostly from bacteria and biological marine organisms [see Figure 1] that attacked the ivory and other materials that lay submerged in seawater for eight centuries) were competing with lower amounts of elephant DNA.

Despite these challenges, Scott and Grewe were still able to get important results using PCR by performing Sanger sequencing on an amplified portion of the mitochondrial genome. This approach successfully sequenced mitogenome regions of interest, which contain some distinct SNPs. Overall, we were able to determine that six tusk samples came from African elephants, and we can tentatively say that three of these tusks are from African bush/savanna elephants (*Loxodonta africana*). After Scott's analysis, Grewe could identify mitogenome reads in one of the NGS ivory samples and confirmed that the ivory sample was indeed from an African bush/savanna elephant (*Loxodonta africana*). (See Table 2.)

The DNA analysis that our team conducted on the elephant tusk pieces found at the wreck site has provided important evidence of the large scale of pre-modern trading networks and the diversity of products and communities involved. Through this collaborative, interdisciplinary research project, we determined which method was most effective for working with this highly degraded material, allowing for identification of the origin of several of the ivory pieces. As demonstrated by the data from the JSW and exemplified by the ivory research, long-distance, “global” exchange, profit, high-intensity production for exchange were all as much a part of the pre-modern, pre-Columbian world as they are part of contemporary economic activities.

Table 1. Elephant tusk sections from the Java Sea Shipwreck collection sampled for DNA analysis.

Field Museum Cat. No.	Sample Prep Method	Sample Weight (g) (combined)
351336 (2 samples)	Powdered	0.54
351367 (1 sample)	Powdered	0.43
351368 ^a (3 samples)	Cleaned fragment	0.54
351368 (2 samples)	Powdered	0.47
351369 (2 samples)	Powdered	0.46
351370 (2 samples)	Powdered	0.55
351371 (2 samples)	Powdered	0.54
351372 (2 samples)	Powdered	0.46
351373 ^a (1 sample)	Cleaned fragment	0.62
351539 (2 samples)	Powdered	0.46
351540 (2 samples)	Powdered	0.42
351825 ^a (3 samples)	Powdered	0.58

^a Part of the initial 2018 DNA analysis conducted by Scott and Wagner at University of Maryland, Baltimore County

Table 2. Results from DNA analysis of elephant tusk samples from the Java Sea Shipwreck collection.

Field Museum Cat. No.	Analysis Method(s)	Genus or Species	Common Name
351336	NGS ^b , PCR/Sanger	<i>Loxodonta</i>	African elephant
351368 ^a	PCR/Sanger	n/a	n/a
351371	NGS ^b , PCR/Sanger	<i>Loxodonta</i>	African elephant
351372	NGS/PCR/Sanger	<i>Loxodonta africana</i>	African bush/savanna elephant
351373 ^a	NGS ^b , PCR/Sanger	<i>Loxodonta africana</i>	African bush/savanna elephant
351540	NGS ^b , PCR/Sanger	<i>Loxodonta africana</i>	African bush/savanna elephant
351825 ^a	NGS ^b , PCR/Sanger	<i>Loxodonta africana</i>	African bush/savanna elephant

^a Part of initial 2018 analysis conducted at University of Maryland, Baltimore County.

^b NGS unsuccessful.

Acknowledgements

Support for this project came from the Commander Gilbert E. and Katharine Phelps Boone family fund, the Andrew W. Mellon Foundation, and the Grainger Bioinformatics Center. We are also grateful for the assistance of Terry Drayman-Weisser, Conservator Emerita at The Walters Art Museum; Jamie Kelly, Field Museum Head of Anthropology Collections; longtime Field Museum volunteer Peter Gayford; our colleagues in the Mammals Department at the Field Museum (especially Negaunee Curator of Mammals Lawrence Heaney and Negaunee Collection Manager of Mammals Adam Ferguson); and Field Museum Data Analysts Yukun Sun and Brian Ho.

References Cited

- Brandt, A.L., Ishida, Y., Georgiadis, N.J., and Roca, A.L. (2012), Forest elephant mitochondrial genomes reveal that elephantid diversification in Africa tracked climate transitions. *Molecular Ecology*, 21:1175–1189. DOI: 10.1111/j.1365-294X.2012.05461.x
- Gao, Y., and Clark, S.G., (2014), Elephant ivory trade in China: Trends and drivers. *Biological Conservation*, 180:23–30.
- Hornbeck, S.E., (2016), Elephant ivory: An overview of changes to its stringent regulation and considerations for its identification. *Objects Specialty Group Postprints*, Volume Twenty-two, Hamilton, E., and Dodson, K., (eds.), pp. 101–122. Washington, DC: The American Institute for Conservation of Historic & Artistic Works.
- Ishida, Y., Georgiadis, N.J., Hondo, T., and Roca, A.L. (2013), Triangulating the provenance of African elephants using mitochondrial DNA. *Evolutionary Applications*, 6:253–265. DOI: 10.1111/j.1752-4571.2012.00286.x
- Kitpipit, T., Thongjued, K., Penchart, K., Ouithavon, K., and Chotigeatin, W., (2017), Mini-SNaPshot multiplex assays authenticate elephant ivory and simultaneously identify the species origin. *Forensic Science International: Genetics*, 27:106–115.
- Lambert, J.B., Levy, A.J., Niziolek, L.C., Feinman, G.M., Gayford, P.J., Santiago-Blay, J.A., and Wu, Y., 2017, The resinous cargo of the Java Sea Wreck. *Archaeometry* 59(5):949–964. DOI: 10.1111/arc.12279
- Lane, P.J., (2015), Introduction: archaeological ivories in a global perspective. *World Archaeology* (Archaeological Ivories), 47(3):317–332. DOI: 10.1080/00438243.2015.1046252
- Mathers, W.M., and Flecker, M. (eds.), 1997, *Archaeological Recovery of the Java Sea Wreck*. Annapolis: Pacific Sea Resources.
- Miksic, J. (1997), Historical background. In: Mathers, W.M., Flecker, M. (eds.), *Archaeological Recovery of the Java Sea Wreck*, pp. 5–33. Annapolis: Pacific Sea Resources.
- Niziolek, L.C., (2015), A compositional study of a selection of Song dynasty Chinese ceramics from the Java Sea Shipwreck: results from LA-ICP-MS analysis. *Journal of Indo-Pacific Archaeology, Special Issue: Papers from the Conference Recent Advances in the Archaeology of East and Southeast Asia* 35:48–66.

Niziolek, L.C., (2017), Jingdezhen ceramics at sea during the Song Dynasty: evidence from the Java Sea Shipwreck. In 海上丝绸之路：陶瓷之路 (Maritime Silk Road: Ceramic Road), Guo, J. (ed.), *Proceedings of the Maritime Silk Road—Ceramic Road International Seminar on Jingdezhen Ceramics and Strategy of “One Belt, One Road,”* pp. 327–346. Beijing: China Social Sciences Press.

Niziolek, L.C., (2018), Portable X-Ray fluorescence analysis of ceramic covered boxes from the 12th/13th-century Java Sea Shipwreck: a preliminary investigation. *Journal of Archaeological Science: Reports* 21:679–701. DOI: 10.1016/j.jasrep.2018.08.029

Niziolek, L.C., Feinman, G.M., Kimura, J., Respass, A., and Zhang, L (2018), Revisiting the date of the Java Sea Shipwreck from Indonesia. *Journal of Archaeological Science: Reports* 19 (June):781–790. DOI: 10.1016/j.jasrep.2018.04.002

Niziolek, L.C., and Respass, A., (2017), Globalization in Southeast Asia’s Early Age of Commerce: evidence from the 13th-century Java Sea Shipwreck. In *The Routledge Handbook of Archaeology and Globalization*, Hodos, T. (ed.), pp. 789–807. United Kingdom: Routledge.

Niziolek, L.C., Xu, W., and Feinman, G.M., (2015), Chinese ceramics from the Java Sea Shipwreck of the Song Dynasty. *Bulletin of Chinese Ceramic Art and Archaeology* 6 (December): 37–41 (in Chinese).

Respass, A., and Niziolek, L.C., (2016), Exchanges and transformations in gendered medicine on the Maritime Silk Road: evidence from the thirteenth-century Java Sea Wreck. In *Histories of Medicine in the Indian Ocean World, Vol. 1, The Medieval and Early Modern Period*, Winterbottom, A., and Tesfaye, F., (eds.), pp. 81–113. Hampshire, England: Palgrave Macmillan.

Tripathi, S., and Godfrey, I., (2007), Studies on elephant tusks and hippopotamus teeth collected from the early 17th century Portuguese shipwreck off Goa, west coast of India: Evidence of maritime trade between Goa, Portugal and African countries. *Current Science*, 92(3):332–339.

Wozney, K.M., and Wilson, P.J., (2012), Real-time PCR detection and quantification of elephantid DNA: Species identification for highly processed samples associated with the ivory trade. *Forensic Science International*, 219:106–112.

Xu, W., Niziolek, L.C., and Feinman, G.M., (2019a), Zhaowahai Chenchuan Chushui qingbaici chandi yanjiu: bianxieshi XRF chengfen fenxi 爪哇海沉船出水青白瓷产地研究：便携式XRF成分分析 [Sourcing qingbai porcelains from the Java Sea Shipwreck: compositional analysis using portable XRF]. *Zhishang Kaogu* (in Chinese).
<https://mp.weixin.qq.com/s/efQHkGYPkEZxgJCDB3Ukyg>

Xu, W., Niziolek, L.C., and Feinman, G.M., (2019b), Sourcing qingbai porcelains from the Java Sea Shipwreck: Compositional analysis using portable XRF. *Journal of Archaeological Science* 103:57–71. DOI: 10.1016/j.jas.2018.12.010

Xu, W., Niziolek, L.C., Feinman, G.M., and Kelly, J., (2020), Yi wares from the Java Sea Shipwreck. In *Minqing Yiyao Kaogu Diaocha Fajue Baogao [Report of archaeological surveys and excavations of the Minqing Yi kilns]*, Fujian Museum (ed.), 304–308. Fuzhou: Haixia Chubanshe (in Chinese).

Zhao, R. c. 1200, (trans. 2012 [1911]), *Chau Jukua his work on the Chinese and Arab trade in the twelfth, and thirteenth centuries, entitled Chu-Fan-Chi*. W.W. Rockhill (trans.). Hong Kong: Forgotten Books.

Put the Lime in the Coconut; An Investigation of the Mechanical and Aging Properties of Coconut Shell and Recommendations for Compatible Conservation Materials

Elena Bowen

Original Abstract

Coconut shell is a material that has been used in cultural heritage across the continents and has been linked with human migration and colonization for thousands of years. Though ubiquitous, as a material coconut shell lacks the extensive conservation research done on similar cellulosic materials such as wood. Coconut shell objects are housed and displayed in museums across the globe, without knowledge of the effects of humidity, temperature, or lighting and no information about coconut shell morphology for identification and responsiveness to conservation treatment. This study attempts to address all of these gaps by conducting aging, humidity, and adhesive tests on coconut shell samples as well as examination of coconut shell cross-sections under magnification. The ultimate goal of this work is to provide suggestions for best practices for coconut shell objects in museum collections and inspire future research into coconut shell as a material.

Thin sectioning of a coconut bowl was done in two directions following the procedures used for wood sampling and imaged under magnification. A literature search and analysis of the samples using portable Fourier-transform infrared (FTIR) spectroscopy provided the basis for compositional comparison of coconut shell and wood. As has been shown with the extensive research done on wood, the microstructure of a material can help to predict its behavior when exposed to non-ideal conditions. With wood, the directionality of its cell structure indicates that it responds anisotropically to environmental changes. This allows us to predict the direction of cracking. There is no such information about coconut shell. By comparing the microstructure and composition of coconut shell with that of wood, I hope to reveal more information about its aging characteristics and responsiveness to environmental factors. For environmental testing, coconut shell samples were subjected to fluctuating humidity conditions, light chamber aging, and Oddy testing. The final round of testing consisted of broken coconut shell slivers adhered with either Paraloid B-72 or Jade R and subjected to stress testing.

From this research, I hope to begin to show how coconut shell objects can be cared for in museum collections and where future research might fill in the gaps to better understand and care for this material. Environmental guidelines for the display and storage of coconut shell including humidity and temperature guidelines, appropriate light levels, and storage

guidelines based on interactions with specific materials have been developed from test results. From my investigations, I will propose ways to monitor and identify light fading and propose future areas of study. From adhesive testing and surveying of institutions around the globe, I will also provide recommendations for compatible adhesives and treatment methods.

Mineral Transformations on Pyrite: Microscopic to Macroscopic Perspectives

Chris Tacker

Original Abstract

“Pyrite disease” is usually approached as a problem in oxygenated water of variable pH, but in collections, it is a problem of abundant oxygen and variable humidity. This talk reviews the current scientific literature to create a cohesive view of the chemical reactions. This microscopic view provides a context in which to examine macroscopic ways to thwart the reactions.

The pyrite surface (Fe_2S_2) is rapidly attacked by electron acceptors (oxygen and water) to oxidize iron atoms, and the electrons, water and/or oxidants rearrange to oxidize the sulfur next. Pyrite is a semiconductor, so mobile electrons on the surface and in the crystalline body of the pyrite move to sustain these reactions, dependent on the conductivity of the pyrite. Eventually melanterite ($\text{Fe}_2\text{SO}_4 \cdot 7\text{H}_2\text{O}$) forms, grows and continues to scavenge water, transferring part of it to the pyrite surface and creating a damp micro-environment. Once melanterite forms, a positive feedback loop is possible: water diffuses to the pyrite surface, and oxidation of Fe^{2+} in melanterite to Fe^{3+} produces another electron acceptor for further oxidation. Deliquescence of melanterite in its own puddle produces acidity, greatly boosted by small amounts of Fe^{3+} . Acidity begins to be generated in the high ionic strength liquid through oxidation and dissolution of the Fe^{3+} sulfate minerals.

The scientific literature provides some surprises. Grain size dependence of the reaction is a result of the large surface area with rapid surficial electron transport, the “proximity effect.” Oxygen and water attack the pyrite surface in seconds to minutes, and the surface develops its own film of water. The efflorescent minerals also develop a film of water, apparently a feature common to iron sulfate minerals. This film of water is highly resistant to removal at lower humidity, so oxidation reactions proceed under low-humidity storage, bolstered by oxygen availability. Efflorescent mineral products depend on the previous efflorescent minerals, suggesting that the process is controlled by kinetics, not equilibrium.

In this context, control of “pyrite disease” requires control of electron mobility, which is unlikely once the reactions have begun. Stopping oxidation/hydration requires removal of surficial water, and storage under anoxic, dry conditions.

These results apply to the system Fe-H-S-O in humid air. Reaction between pyrite and clay minerals short-circuits the reactions described above. Instead of melanterite, deliquescent halotrichite ($\text{Fe}_2\text{Al}_2(\text{SO}_4)_4 \cdot 22\text{H}_2\text{O}$), and alkali-bearing jarosite, form in addition to the regular suite of iron sulfate minerals. The clay serves as a source/sink for the cations as well as electrons and water. Preliminary results for controlled humidity experiments between pyrite and reference clays will be presented.

Long term storage requires a degree of prediction. The reactivity of pyrite is determined by conductivity of electrons, so a database of pyrite conductivity is highly desirable. Long term storage is then dependent upon low-oxygen environments as well as low-to-no humidity environments.

Early Plastics, Taxidermy, and Conservation at the Field Museum

Daniel Kaping

Original Abstract

The deterioration of early plastics is a challenge for conservators and taxidermists alike, especially when considering the care of aged semi-synthetic models. This study explores pathways for the immediate and future care of degraded cellulose nitrate and cellulose acetate natural history models created by Leon Walters, with a primary goal of extending their function as educational tools. The significance of these models to the history of taxidermy is also recognized, contextualized through a short overview of innovations at the Field Museum of Natural History. A brief look at the production history of cellulose ester plastics, their chemistry, and their stability issues is likewise included in order to better understand the breakdown of these materials over the last century. A discussion of methods to retain structural integrity follows, showcasing recent triage stabilization treatments of mammalian and herpetological models. Lastly, future display improvements are considered with an eye towards affordability and sustainability.

Research and Technical Studies Specialty Group Presentations: Case Studies

The Development and Application of Instrumental Methods for the Identification of Materials and Processes used in the Manufacture of Orotone Photographs

Ivanny Jacome Ottati, Claire Kenny, Tami Lasseter Clare

Original Abstract

Distinguished by their characteristic brilliancy, orotones (also called Curt-tones, goldtones, or Doretypes) were popular from the late 19th century through the 1940s. Orotone photographs are positive images on glass with a gold-colored metallic coating or backed with a reflective material. The coating consisted of a metallic powder dispersed in a liquid carrier, and it was applied to the emulsion after development. Contemporary sources describe the use of a “banana liquid or oil” in the manufacture of the metallic coating. Although the materials and process used in the production of orotones have been previously documented, there is limited published scientific research on the subject. Extant technical studies on 20th century orotones, published by Siegfried Rempel in 1986 and Richard Stenman in 2011, are somewhat limited in scope but lay an appropriate foundation for broader study. This study focused on expanding the work of Rempel and Stenman by using different instrumental techniques to analyze a wider scope of photographs. Twelve orotones, four hand-colored orotones, and two silvertones produced by 10 known artists and 2 unknown artists were analyzed. This sample set included orotones by Edward S. Curtis, who along his brother Asahel Curtis and other American Pacific Northwest photographers, was a notable practitioner of the process. The photographs, dating from the early-mid 20th century, were from the University of Washington Libraries’ collection, and one of the orotones was from the Portland Art Museum.

X-ray Fluorescence (XRF) spectroscopy, Fourier Transform-Infrared (FT-IR) spectroscopy, Raman spectroscopy, Scanning Electron Microscopy in tandem with Energy Dispersive X-ray Spectroscopy (SEM/EDS), and Pyrolysis coupled to Gas Chromatography Mass Spectrometry (Py-GC/MS) were used to identify the materials and pigments used in the production of these photographic types. The analysis revealed that copper and zinc alloys were used in the backing of all the orotones; no gold was identified. Collodion was detected in an orotone sample with a proteinaceous emulsion, indicating that it was a component of the banana liquid. The proteinaceous emulsion in one of the orotones was identified as gelatin. Vermilion and Prussian blue pigments were used in hand-colored orotones, and aluminum was identified as the metallic pigment in the backing of silvertones. Ongoing research aims to identify other components of the banana liquid by Py-GC/MS, including the use of amyl acetate and other materials for the purpose of understanding occasionally observed embrittlement and delamination condition issues.

These results and continued research will increase the body of knowledge on orotones and silvertones and aid in the long-term preservation of these historical photographs.

A Low-Cost, Open Source Micro-fading Tester: Construction, Characterization, and Use

JP Brown, Jacob Thomas

Original Abstract

Micro-fade testing provides a semi-quantitative method of predicting the fading rate of light-fugitive colored materials due to light exposure (Whitmore, Pan, and Bailey 1999) -- essentially, an Oddy test for museum lighting. However, the equipment is expensive for most conservation laboratory budgets (USD 25-35k), and there is no modern standard open-source software for acquisition and analysis of the results. The currently available free software (Getty Spectral Viewer v.2) is unsatisfactory in that it does not provide real-time data acquisition which makes it hard to monitor the test for excessive damage, and because it does not provide color shift analysis in terms of CIEDE2000.

In this paper we present a complete retro-reflective MFT instrument due to Thomas that can be built from standard ThorLabs optical components in an afternoon, and is hardware agnostic in its choice of light source and spectrometer. The system uses a revision of Getty Spectral Viewer which provides real-time color shift monitoring as CIEDE2000 during data acquisition which is due to Brown (in conjunction with Vincent L Beltran at the Getty Conservation Institute). The purchase cost of the complete system is ca. USD 8k including a spectrometer, light source, equipment for characterizing the MFT spot, focusing rails, and specialist tools for the assembly.

The main advantages of the system are low build cost and simple data acquisition and analysis. The principal disadvantage is manual focusing, which is similar to most of the more expensive builds except the Instytut Fotonowy system (Fotonowy 2020) and the instrument assembled by Prof. Haida Liang at Nottingham University (Liang et al. 2011). The most controversial design decision is probably the use of a variable power LED light source (delivering 2.85 mW as tuned) in place of the more usual xenon lamp.

We discuss the effect of our design decisions in both hardware and software, what we learned while refining the build, and present an analysis of the repeatability of measurements on different substrates using an example instrument which was recently built at the Field Museum. In particular, we compare the use of the instrument on smooth graphic substrates to its use on rougher social history surfaces, and provide an appreciation of the effects of the LED light source compared to a xenon source.

Annotated Slides

A low-cost, open source micro-fading tester: construction, characterization, and use.

2021 AIC/SPNHC Joint Virtual Annual Meeting
Research and Technical Studies Session, May 26, 2021

JP Brown

Field Museum, 1400 S Lake Shore Drive, Chicago, IL, USA
jpbrown@fieldmuseum.org

Jacob L Thomas

Jacob Thomas MFT consultancy, Gamla Björlandavägen 164, Göteborg 41728 Sweden
jacoblthomas@gmail.com

Micro-fade testing provides a semi-quantitative method of predicting the fading rate of light-fugitive colored materials due to light exposure (Whitmore, Pan, and Bailey 1999) -- essentially, an Oddy test for museum lighting. However, the equipment is expensive for most conservation laboratory budgets (USD 25-35k), and there is no modern standard open-source software for acquisition and analysis of the results. The currently available free software (Getty Spectral Viewer v.2) is unsatisfactory in that it does not provide real-time data acquisition which makes it hard to monitor the test for excessive damage, and does not provide color shift analysis in terms of CIEDE2000.

ABSTRACT

In this paper we present a complete retro-reflective MFT instrument due to Thomas that can be built from standard ThorLabs optical components in an afternoon, and is hardware agnostic in its choice of light source and spectrometer. The system uses a revision of Getty Spectral Viewer which provides real-time color shift monitoring as CIEDE2000 during data acquisition which is due to Brown (in conjunction with Vincent L Beltran at the Getty Conservation Institute). The purchase cost of the complete system is ca. USD 8k including a spectrometer, light source, equipment for characterizing the MFT spot, focusing rails, and specialist tools for the assembly.

The main advantages of the system are low build cost and simple data acquisition and analysis. The principal disadvantage is manual focusing, which is similar to most of the more expensive builds except the Instytut Fotonowy system (Fotonowy 2020) and the instrument assembled by Prof. Haida Liang at Nottingham University (Liang et al. 2011).

The most controversial design decision is probably the use of a variable power LED light source (delivering 2.85 mW as tuned) in place of the more usual xenon lamp.

We discuss the effect of our design decisions in both hardware and software, what we learned while refining the build, and present an analysis of the repeatability of measurements on different substrates using an example instrument which was recently built at the Field Museum.



Good evening, I am Dr. Jacob Thomas, (JACOBLTHOMAS@GMAIL.COM). I have been prototyping and building MFT since 2007, when at the TATE as a PhD student on the anoxia and MFT project I began to covet my neighbor's instrument. As planned, I was to be the anoxia guy bagging paper, ageing it and smelling the results and Andrew Lerwill was to be the MFT guy building a cool instrument and fading holes in paper. Don't get me wrong, as an analytical chemist I do like headspace GC-MS, but MFT really appealed to me because it allowed for operando type experiments. I really wanted to do real materials, real conditions and real time experiments and the MFT hinted at those possibilities. My first instrument, which I will not discuss today was a MFT built into a temperature and atmosphere-controlled cell so that I could rapidly cycle between simulated cold dark storage and display environments and perform, at times, multiply conjugated experiments to detect color change, measure water loss and VOC formation. What that instrument taught me is that to do a good MFT measurement requires control of many parameters, and the list gets longer depending on how stringent is your "good enough" threshold. At some point you must declare an instrument fit or unfit for purpose, I have a drawer full of the latter and have (co) developed a few of the former.

But let's begin at the beginning.

0-45° MFT

An update to the classic MFT design first built by the Paul Whitmore lab. Now at the Yale Institute for the Preservation of Cultural Heritage



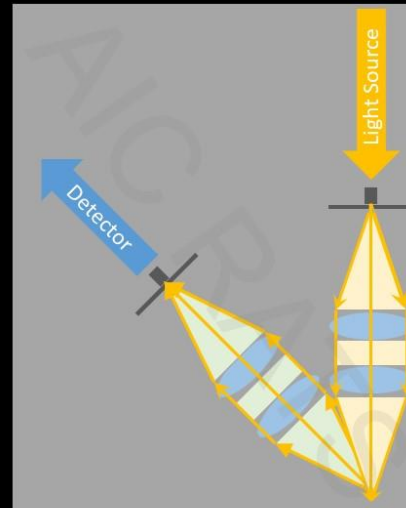
This is a classic MFT design: 2 probes, separate illumination and collection optics arranged in a 0-45 geometry. Connections are made to a light source and a spectrometer via SMA terminated fiber optics. Any, fiber coupled source can be used, but the historically Xe lamps have been used. Currently efforts are being made to shift from Xenon lamps to LED lamps for MFT measurements.



The automated MFT from Fotonow, full disclosure, I helped develop this instrument and I am a distributor for its sale, JACOB.THOMAS@FOTONOWY.PL. I will not speak about this instrument here except to say that it is also a 0-45 design and works in the same way, to a greater or lesser extent, as the original MFT, but with some significant improvements in usability. I spun the idea for this instrument off from my post doc at Jagiellonian University, it is a good example of setting the threshold for 'good enough' at an extremely high level. Moreover, we at Fotonowny are always inching that threshold up as we learn more about what the conservation community needs. You can ask me questions over email if you like.

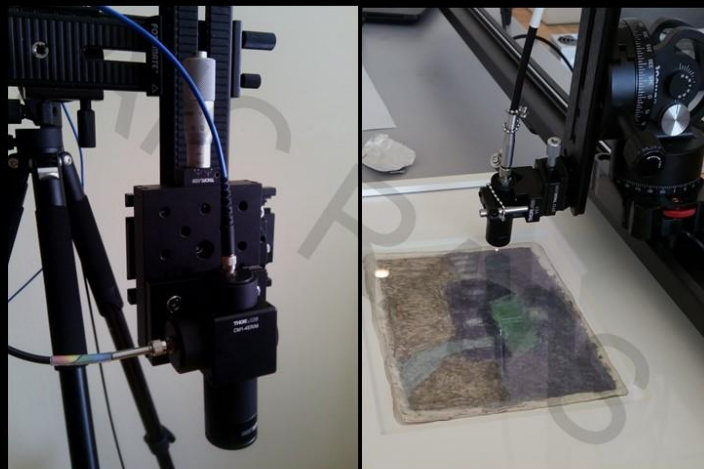
0-45° MFT

The operating principle is the same in both cases. Light is directed onto the object surface with a set of optics and the diffuse reflected light is collected with another.



Fibers are connected with SMA adapters to the probe head. In the probe head, one convex lens 'looks back' at the fiber end. The end of the fiber is positioned at the BFL of the lens, and the numerical aperture (NA) of the lens should be \geq to the NA of fiber to collect all the light and avoid over filling the lens. A second convex lens 'looks forward' to the object surface. Between the lenses the light is collimated, that is the light rays are parallel. At the focus point the surface is at the FFL of the front lens. Both probes must be aligned and confocal. This can be a challenge particularly if your instrument is moved from site to site.

Retro reflective MFT



There are 4 retro reflective MFT designs. I will discuss the two that I have contributed to but there are also the GCI Ball lens contact MFT and the MoMA bare fibre nearly contact MFT.

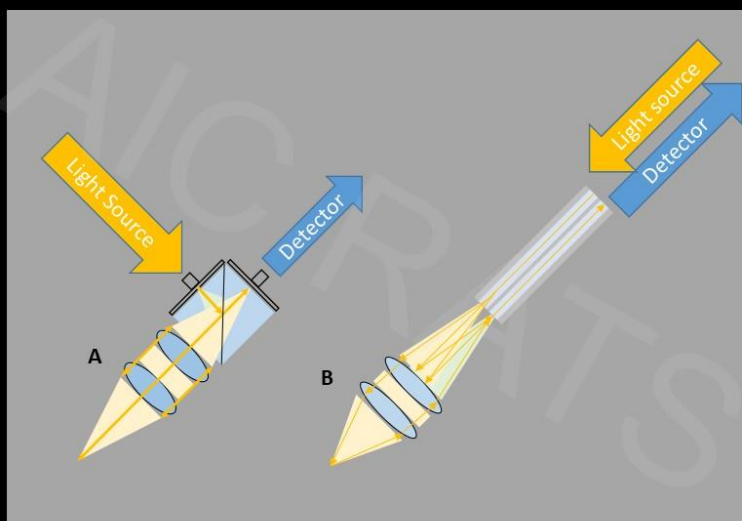
A: In a beam splitting-retro reflective MFT (BS-RR MFT), fibres are connected with SAM adapters to the probe head. One lens 'looks back' at the fibre end. As with the 0-45 MFT, the NA of the lens should be \geq or 0 to the NA of fibre to collect all of the light. The end of the fibre is positioned at the BFL of the lens. A second lens 'looks forward' to the object surface. Between the lenses the light is collimated, that is the light is parallel. In the beam splitting RR MFT a 90:10 (R:T or T:R) splitting cube is placed in the beam path. This allows a single probe for both light delivery and collection, and also functions to reduce the intensity of the light being sent to the spectrometer. This design is stable, robust, and no re-alignment of the beam paths is required because they are fixed. Also note that the forward lens can be exchanged to change the spot size (and power density) like changing objectives on a compound microscope or prime lenses on a camera.

B: In a bifurcated fibre-retro reflective MFT (BF-RR MFT), a bifurcated fibre, arranged as either 2 cores or 6 and 1 cores or other multicore combinations deliver the light and collect the light using the same simple 2 lens system which is identical to a one of the lens systems from a 0-45 MFT described above. This design is simple and can be made ultra-compact for hard-to-reach places.

Retro reflective MFT

A: Beam splitting RR-MFT

B: Bifurcated probe RR-MFT



These designs grew from my work at Jagiellonian University and the National Museum in Krakow. I first built a classic 0-45 MFT based on a Whitmore design then began to explore ways to make it different and on occasion better by expanding upon Lerwill's Tate MFTs.

I used an iterative prototyping approach to reduce complexity, increase robustness, improve usability, eliminate sources of error, and most importantly eliminate the need to realign the optics after each time I moved the instruments. Both RR designs have fixed illumination and collection paths. Once built, they do not need to be realigned. But more on these issues in the next few slides.

Why RR MFT?

- Open source parts lists
- Probe alignment
- Focusing
- Robustness during transport

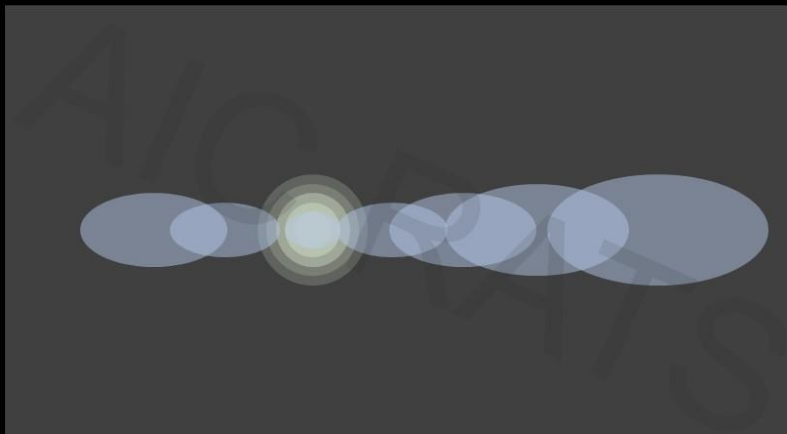
Item	Image	Part Name
1		BS-RR MFT Probe (Lot#) (0.01 Kips)
2		M26L02-1 (Lot#) (0.01 Kips)
3		M26L02-1 (Lot#) (0.01 Kips)
4		B01-1 (Lot#) (0.01 Kips)
5		B02E-8060-1 (Lot#) (0.01 Kips)
6		B02E-8060-1 (Lot#) (0.01 Kips)
7		B01CP2-1 (Lot#) (0.01 Kips)
8		B01L03-1 (Lot#) (0.01 Kips)
9		B01L10-1 (Lot#) (0.01 Kips)
10		B01SMA-1 (Lot#) (0.01 Kips)
11		B01W02-1 (Lot#) (0.01 Kips)
12		PT-1 (Lot#) (0.01 Kips)
13		AC264-050-A-M-1 (Lot#) (0.01 Kips)
14		AC264-050-A-1 (Lot#) (0.01 Kips)
15		AC264-050-A-M-1 (Lot#) (0.01 Kips)
16		AC264-076-A-M-1 (Lot#) (0.01 Kips)
17		B02E-1 (Lot#) (0.01 Kips)
18		CAPNS-1 (Lot#) (0.01 Kips)
19		COM1-4ER-1 (Lot#) (0.01 Kips)
20		PM18-401-1 (Lot#) (0.01 Kips)
21		C3186CU-1 (Lot#) (0.01 Kips)
22		B01RR-P10-1 (Lot#) (0.01 Kips)
23		M07L02-1 (Lot#) (0.01 Kips)

The first issue I encountered was finding a publicly available, up to date parts list for either the Whitmore or the Lerwill MFT, I found this very frustrating, and so now I curate parts lists for my RR MFT designs which I make freely available to all persons who ask. This includes the parts and tools you need to build and characterize your own MFT. If you can build it yourself, here is the list for the BS-RR MFT probe, but you can drop me an email at JACOB.LTHOMAS@GMAIL.COM if you want the parts list which you can use to create a shopping cart with all that you need to build a MFT probe as well as recommendations for spectrometers, light sources and positioning systems.

Probe alignment: I found that my manual 0-45 MFT probes would come out of alignment during transport and would require re-alignment and recharacterization (degree of overlap, concentricity of the spots, illuminated area, luminometric calibration) which could take significant time away from measurements on site and would need to be repeated once I returned to the lab. This issue almost made me throw in the towel on many occasions.

Focusing 0-45 MFT

The collection optic is at 45° to the surface, and so is an oval that translates across the object surface during focusing. The focus point is when the spots have minimum area and area aligned resulting in maximum signal to the detector.



Focusing was also an issue with the 0-45 particularly for paper objects with floating mounts that were stored in solander boxes up to the time for measurement. We found that our 0-45 MFT was particularly suited for measuring micrometer scale paper deformation, because any movement on the Z axis by the paper due to humidity/water content changes during a measurement resulted in the loss of concentricity of the spots and an apparent color change orders of magnitude higher than reality, not to mention near heart attacks on a few occasions.

We did experiment with different fiber combinations and settled upon having an observation spot smaller than the irradiated area to allow for some microscale paper deformation without resulting in a loss of data. But that is really a story for another day.

Focusing a retro reflective MFT

The collection optic is the same as the illumination optic, and so focusing is a matter of minimizing spot size. Both optics are always aligned.



The RR MFT does away with this. As long as your cube is orthogonal to the incident light from the illumination fiber, and beam paths through the cube are the same length the irradiation and observation fibers are aligned. And you can use either apparent spot size or spectrometer load level to find the focus point. Much simpler, much more robust and in my opinion easier to focus.

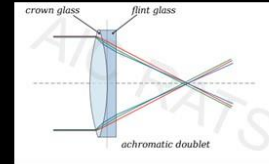
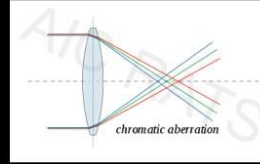
The nuts and bolts of an MFT

Things to consider when adapting a design

- Lenses
- Fibre optics
- Light sources
- Spectrometers

Optical path considerations

- Chromatic aberrations
 - Resolved by using achromatic lenses achromatic doublets or triplets
- Beam spreading at the beam splitter
 - The light projected onto the beam splitting cube spreads on the surface requiring a repositioning of the rear lens away from the ideal working distance.
- Lens focal lengths, numerical aperture and positioning
 - Conjugate ratios and impact on magnification



When building an MFT, you need to build a system(s) to collect light from a fiber, to focus it onto an object, to collect it from the surface and refocus it onto a fiber and deliver that light to the detector.

In the simplest system, a single Steinheil achromatic triplet lens can be used to collect the light from a fiber and focus it onto an object with a 1:1 conjugate ratio while simultaneously correcting for all primary chromatic aberrations. This would work very well with a BF-RR-MFT. Note that this does not correct for other lens aberrations.

One can also use a pair of convex lenses, and if at least one is an achromatic doublet then you can also correct for chromatic aberrations. One could also use an aspheric lens to correct for spherical aberrations, and if your budget stretches that far, an aspherised achromatic lens. This system allows you to have different conjugate ratios between the lenses, and thus change the spot size because you are effectively projecting an image of the fiber end onto the object and the magnification of the image is dependent on the conjugate ratio.

You can of course make more complicated lens systems, but the goal of this exercise was to make the MFT as simple as possible.

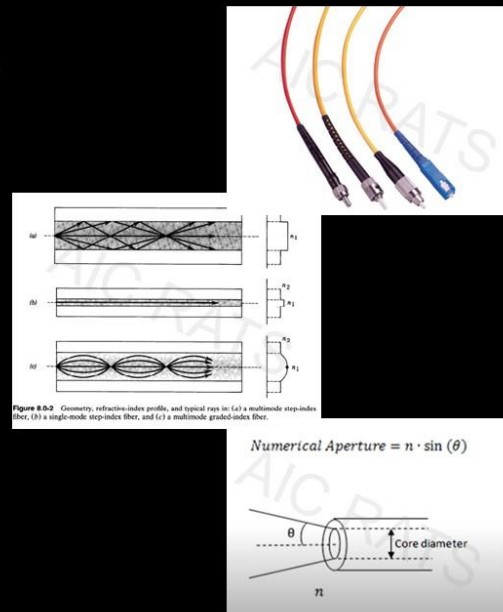
When choosing lenses, aside from focal length and diameter, you would like to have a match between the NA between the lenses and the fibers. You will either underfill or overfill the lens by the ratio of the NA of the lens-fiber system. Generally underfilling is a smaller problem than overfilling for our applications, so a larger NA on the lens is better, but there are also geometric considerations, and sometimes, the ideal situation is not possible. This is particularly true with the BS-RR MFT which has a constraint of the dimensions of the beam splitting cube. When I built my MFT, achromatic lenses were not available in the

diameter, focal length and antireflective coating that I needed to work with the cube so I compromised on focal length which means that I have a smaller NA than I would like.

In retrospect I could use collimating lenses before the cube and then a single focusing lens after the cube, but that is a new design, and I really am trying to limit my generation of new MFT prototypes.

Fibres, things to consider

- Connectors
- Single mode or multimode
 - Step index or graded index
- Hydroxyl content
 - Low OH for 400 to 2500 nm
 - High OH for 250 to 1200 nm
- Solarisation resistant
 - Required for UV applications and Xe lamps
- Armour cladding
 - Added protection
- Diameter and numerical aperture
 - Impacts how much light can be coupled into the fibre, the spot size and spectral power density



Connectors

SMA — due to its stainless-steel structure and low-precision threaded fiber locking mechanism, this connector is used mainly in applications requiring the coupling of high-power laser beams into large-core multimode fibers. Typical applications include laser beam delivery systems in medical, bio-medical, and industrial applications. The typical insertion loss of an SMA connector is greater than 1 dB.

ST — the ST connector is used extensively both in the field and in indoor fiber optic LAN applications. Its high-precision, ceramic ferrule allows its use with both multimode and single-mode fibers. The bayonet style, keyed coupling mechanism featuring push and turn locking of the connector, prevents over tightening and damaging of the fiber end. The insertion loss of the ST connector is less than 0.5 dB, with typical values of 0.3 dB being routinely achieved.

FC — the FC has become the connector of choice for single-mode fibers and is mainly used in fiber-optic instruments, SM fiber optic components, and in high-speed fiber optic communication links. This high-precision, ceramic ferrule connector is equipped with an anti-rotation key, reducing fiber endface damage and rotational alignment sensitivity of the fiber. The key is also used for repeatable alignment of fibers in the optimal, minimal-loss

position. Multimode versions of this connector are also available. The typical insertion loss of the FC connector is around 0.3 dB.

SC — the SC connector is becoming increasingly popular in single-mode fiber optic telecom and analog CATV, field deployed links. The high-precision, ceramic ferrule construction is optimal for aligning single-mode optical fibers.

The standard connector for almost every research grade spectrometer and source is SMA. There are many good reasons to spend extra money to have FC-PC connectors for your system.

Single or multi-mode

Single mode-small core step indexed fibers

Multimode, by definition have larger cores and the light guided by the fiber has access to the higher modes.

Graded indexed fibers reduce modal dispersion relative to step indexed mm fibers.

Because we are working with broad band (white) light that is not coherent, we will almost invariably use multimode fibers and these will almost always be step index fibers.

Diameter and NA

More light can be coupled into larger diameter fibers. Likewise, fibers with larger NA (bigger acceptance angles) are easier to couple to divergent sources. Square law applies. Also note that though large NA fibers can couple more light the large NA means that they spread that light out into a larger cone at the other end, and this means that they can over fill lenses and waste all that hard sought-after light. In the end, you might get more light onto the surface of the object with that 550 μm , 0.22 NA fiber than the 600 μm 0.39 NA fiber.

Other stuff

If you are going to use a Xe source, or any UV containing source you need to use a high OH (high hydroxyl content in the fiber core) fiber, and preferably one that is solarisation resistant.

Note that light sources, particularly Xe sources, get hot, and you might burn your fiber, consider a hot mirror between the source and the fiber.

You can have the fiber ends coated with an anti-reflection (AR) coating, this will reduce coupling losses, but I do not think that this is applicable for our application.

If weight is not a consideration, think about armor cladding for your fibers. This will help prevent broken fibers.

Light sources

Xe or LED?

- Xe is the standard source for solar simulation across many fields, but this is changing with more and more LED based AAA solar simulators entering the market
- LED sources are less expensive to purchase, less expensive to operate, they are robust, do not require filtering to remove UV and/or IR, intensity is easily modulated with driving current without changing the spectral power distribution, however...

Other sources

- Halogen, why not if you are using tungsten halogen sources in your museum?
- Violet pumped LED sources, Sora white LEDs use a violet emitter to pump the phosphors. This gives superior colour rendering, but all that high energy light is worrying... There are not many good options for fibre coupled violet pumped white LED sources, just this from Prizmatix, <https://www.prizmatix.com/FC/FC-BBW-LED.htm>
- LED light engines: see below

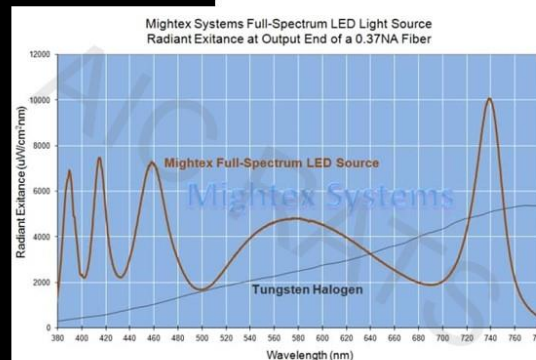
LED and great but,

Not all LED sources are created equal.

You need an actively cooled source, or you risk thermal drift resulting in a spectral shift with time. Color temperature is not a good predictor of the spectral power distribution of a LED, except in the broadest of terms. CRI of LED emitters can be abysmal, though they are improving. There is a huge, and unhelpful, variance between LED emitters between batches and even within a single batch, on occasion.

LED light engines

- LED light engines use multiple, independently controllable LED emitters coupled into a single fibre output.
- The resulting spectral power distribution can be shaped to simulate different light sources, e.g. different colour temperatures of LED, violet pumped LED, tungsten halogen sources, Xe sources, UV filtered indoor daylight. It is like having many sources in one small box (plus the LED controller).
- But it is not as bright as a Xe source. However, I think that this is feature.



Here is a link to the Mightex full spectrum source. I am not a distributor and I am not affiliated with Mightex in anyway, but I really like their source. I use it with all of my MFT and I highly recommend it for MFT and FORS applications.
<https://www.mightexsystems.com/product/full-spectrum-led-light-sources-for-spectrometers/>. I use the FSS-0380-0780-000-SLC-MA04-MU configuration with the dual manual and computer controlled 4-channel driver.

Spectrometers, which to choose

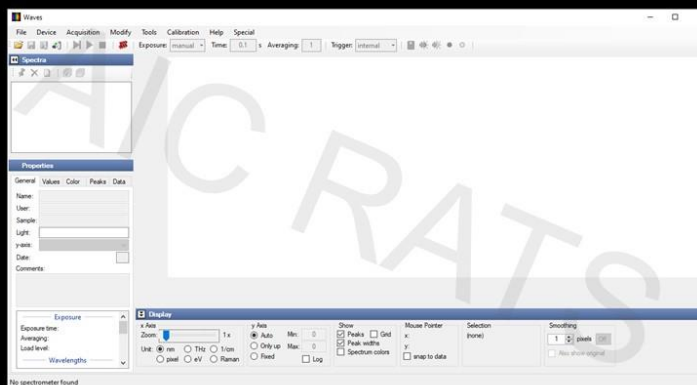
- Spectral resolution
- Range
- Dynamic range
- Integration time
- Spectral noise and stray light
- Sensitivity
- Data transfer rates
- Software and ease of use
- Price
- Not relevant, you need 10 nm resolution, if that, for colour measurement, important if you want spectra.
- Range is important. You need 380 to 780 nm.
- Will you use this for high and low intensity work?
- Will you need ND filters to attenuate the light?
- Important, but not a deal breaker in this application.
- Again, important but not a deal breaker for this application
- Speed here is key if you want to transfer data to your computer every second or faster
- Software is in the top 2 most important features. If it is not easy to use, it won't be used.
- Price is key. You can spend as much as you like on a spectrometer.

This is where 'good enough' comes into play. How will you use your MFT? To compare to BWS? To measure color? To what accuracy? To do spectroscopy? In the visible range? Beyond? Mechanism elucidation? Pigment/dye ID? All of the specs are important for some applications, but the biggest factor, after cost, for our applications is software and ease of use. If you are familiar with a spectrometer and its software already, then your choice is made. But if you are new to this issue, then the spectrometer with the easiest software to learn and use will be your best choice.

My choice, the Qmini Wide-Vis

Features

- Wavelengths range from 225–1000 nm
 - This covers the full range of the Mightex source as well as what you would expect from a hotmirror filtered Xe or halogen source.
- Spectral sensitivity is optimized at 500 nm.
- Spectral resolution from 1.5 nm
- Miniature size (half a deck of cards)
- Powerful on-board electronics with processing and evaluation
- Free, easy to use, but still powerful software
- CHEAP
 - I mean really cheap.



Here is a link to the spectrometer at Broadcom,
<https://www.broadcom.com/products/optical-sensors/spectrometers/spectrometers-qmini/afbr-s20m2wv>. From here you can find a distributor or buy it on Mouser. Again, I am in no way affiliated with Broadcom, I just really like this spectrometer and have been using it or its predecessor since 2011 when I bought one with my pocket money as a not quite finished writing up PhD student. The software is, dare I say it, intuitive, and I have trained numerous conservators (and curators!) how to use the software with a MFT both in person and over ZOOM. It really is that easy to use. But the best part is that it is easy to apply a new radiometric calibration to the spectrometer taking into account the MFT probe head and measurement geometry.

Spot size and power characterisation

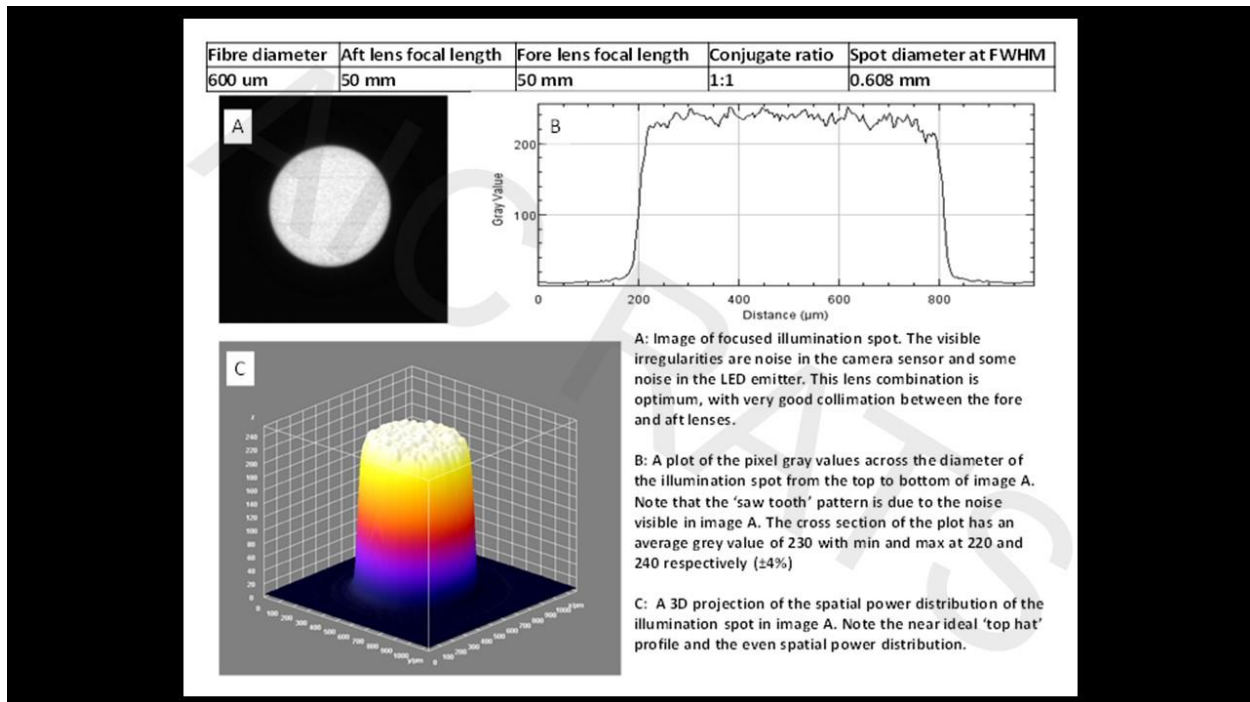
Fibre diameter	Aft lens focal length	Fore lens focal length	Conjugate ratio	Spot diameter at FWHM
600 μm	50 mm	50 mm	1:1	0.608 mm

Fibre diameter	Aft lens focal length	Fore lens focal length	Conjugate ratio	Spot diameter at FWHM
600 μm	50 mm	30 mm	1:0.6	0.360 mm

Fibre diameter	Aft lens focal length	Fore lens focal length	Conjugate ratio	Spot diameter at FWHM
600 μm	50 mm	75 mm	1:1.5	0.925 mm

LED lamp with all emitters at the maximum driving current	measured value	illuminance (lux)
	calculated value for 30 mm fore lens	2909
	calculated value for 50 mm fore lens	3.78 Mlux
	calculated value for 75 mm fore lens	1.33 Mlux
		0.575 Mlux

Ok so now you have built your MFT. You MUST characterize it. Measure the spot size, measure or calculate the illuminance and irradiance (yes both if you want to use UV or do wavelength dependent fading studies or even to publish your results in a non-conservation journal) at the measurement spot. Now you can report your color change in terms of dose in Mlux Hr or Joules (W s), rather than in terms of seconds of illumination and then relate this back to how much a blue woolen rag changed color in the same time. Really there is no excuse to not measure your spot size and illuminance at the measurement point at the very least. My parts list includes the tools to do this.



This is what you would like to see from your MFT characterization. Note that the sensor on my detector is not saturated. That flat top and near vertical sides are real. Be honest and use full width half maximum for your spot size.

Practicalities of measurements

- Shutter
 - TTL vs Aluminium foil
- White standards
 - Spectralon, compressed BaSO₄, Teflon tape wrapped 5-10 times around a popsicle stick
- Fuzzy surfaces
 - Where is the surface to focus upon?
- Measuring through glass
 - Working distance is key here
- Angle of incidence on the surface
 - 15 degrees off normal and JP's little foot
- 3D surfaces
 - Is there a significant impact on small differences in angle of incidence from my white reference surface and my object?

To shutter or not to shutter is a big question. Ideally you would have a TTL shutter inline with your source so that your spectrometer could control the light and turn it off automatically. These things are expensive (ca. 1000 USD) to add to an LED source after the fact. You can buy an LED controller with TTL function, but this is generally not a physical shutter, but rather a trigger to go from 0 to 100 really fast. This is not what we want for our measurements. We need a physical shutter to keep that LED emitter nice and hot and limit thermal drift and instability due to the driver over shooting and then correcting. Helpfully there is an inexpensive solution in a drawer in your kitchen, aluminum foil. A small slip of foil effectively blocks the beam and allows you to warm up the source while it is focused on your object.

White standards come in several varieties. Spectralon is by far the most common now, but compressed BaSO₄ was the standard for decades. However, in a pinch, a few wraps of Teflon plumber's tape, or relic wrap, around a popsicle stick will also serve as a relative white standard, and you get to have a treat as well. Sometimes it pays to forget key pieces of equipment at home.

Fuzzy surfaces, like that of a raspberry beret, you know the kind you find in a second-hand store, may the artist formerly known as Prince, in his benevolence forgive me, can be a challenge to focus upon since they have a poorly defined surface. I sometimes use a glass slide or cover slip to create a surface for measurements.

As suggested above you can use the RR MFT to measure through glass, just keep in mind your working distance. You might need to use the 75 mm lens (conjugate ratio of 1:1.5 and therefore a spot diameter of around 900 μm with a 600 μm diameter fiber) to be able to reach the object surface through the glazing. If the larger spot size is acceptable, then the reduced risk of damage during handling and dismounting is a great benefit, plus you can

measure in situ on the wall in a gallery with an audience of museum visitors. Love it or hate it, it is an outreach and awareness opportunity. Coordinate with the museum education people and guides, promote conservation and perhaps get some more funding for your section.

The most important part of the RR configuration, you do not need to, in fact you should not, measure at normal to the surface. You should be 10 to 15 degrees off normal to dump the specularly reflected light somewhere else and not back into your spectrometer. JP has designed a printable little foot for the BS-RR MFT. Ask him about it.

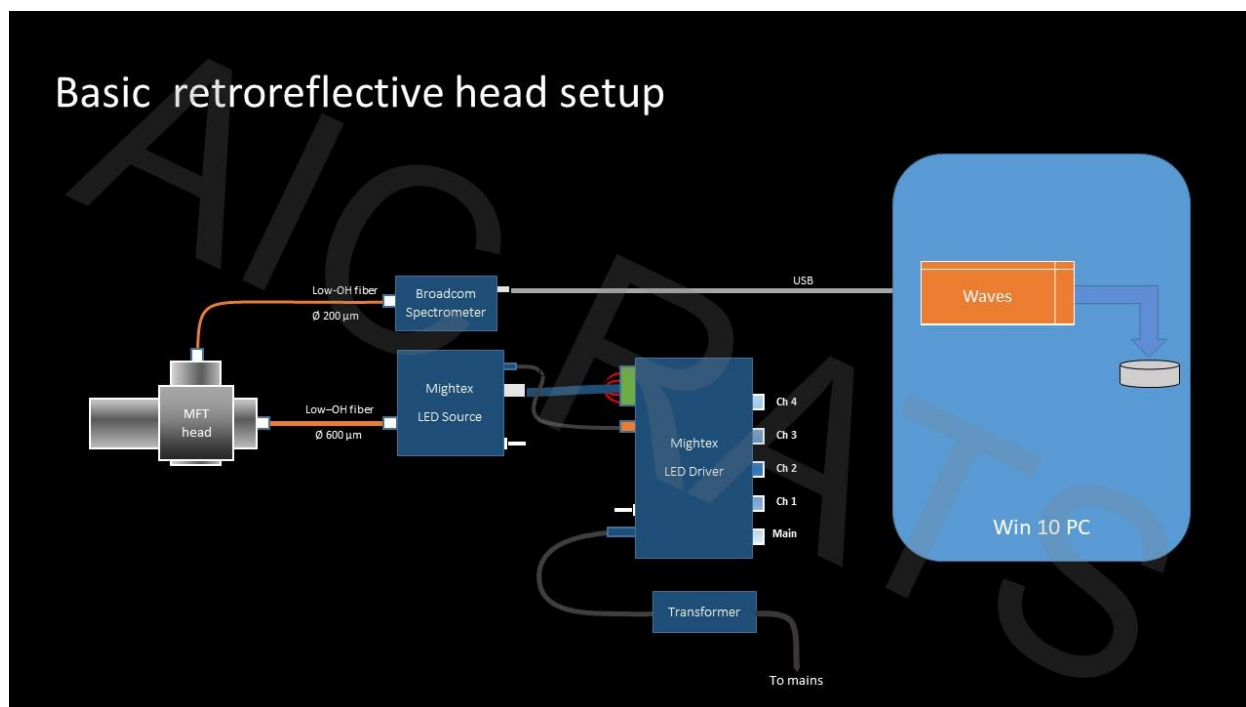
However, so while your white standard is flat and sits upon a table and it is easy to be 15 degrees off normal from its surface, 3D objects are less easy. Never fear, your white reference taken at 15 degrees seems to be valid for measurements taken at a range of angles, from about 10 ish to about 30 ish degrees, according to research by Betty Sacher at the UCL ISH, feel free to contact her. So like horseshoes, close counts with RR MFT.

Part 2: MFT Software Overview

JP Brown

Regenstein Conservator for Pacific Anthropology

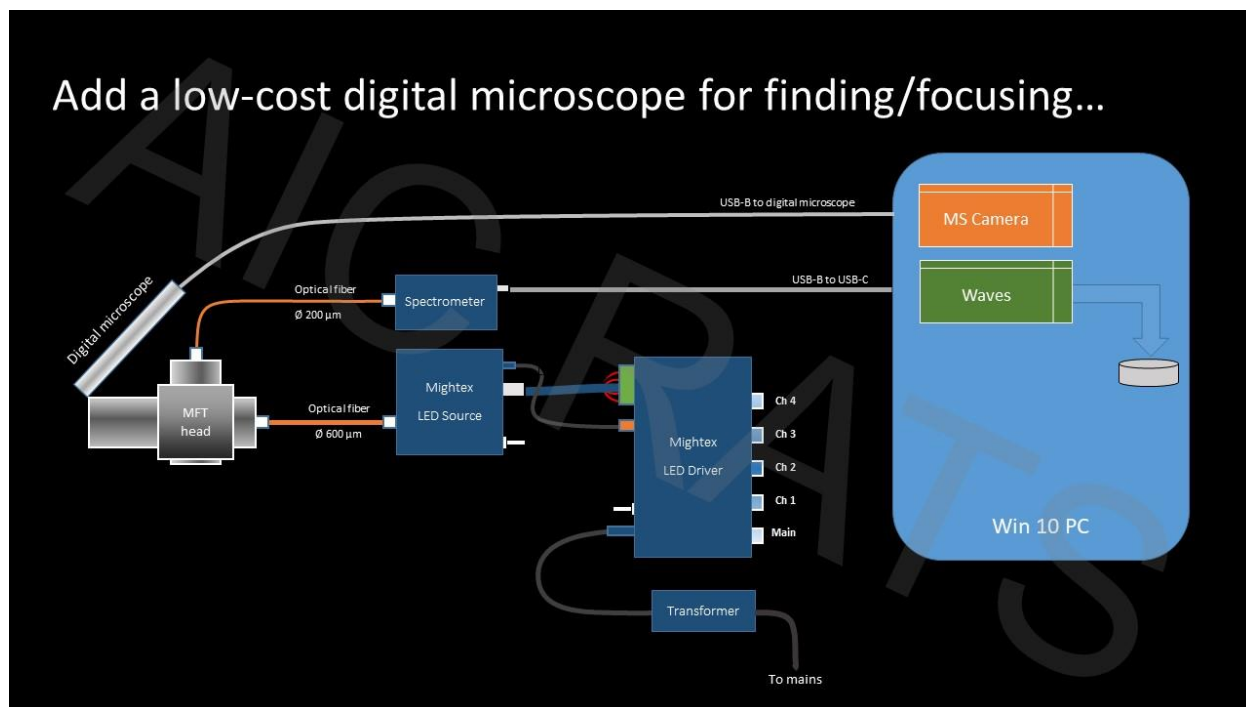
Basic retroreflective head setup



A basic MFT setup needs

- AMFT head
- Spectrometer (here we're using a Broadcom QMini Wide-VIS)
- Light source (here we're using a 4-channel LED source by Mightex).

Add a low-cost digital microscope for finding/focusing...



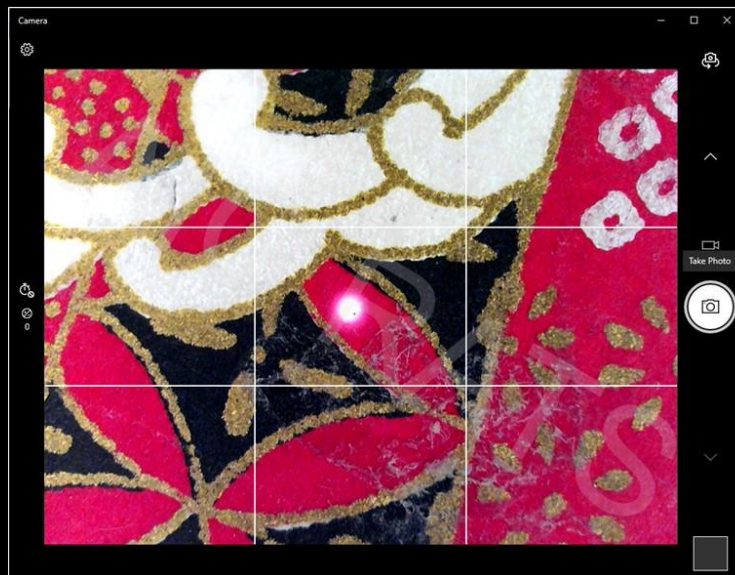
Add a 3D printed microscope holder and angle guide...



And a holder (CLICK) to secure it to the head – we 3D printed this holder.

And while we were printing things, we also printed a clip-on angle-guide to help us align the head repeatably.

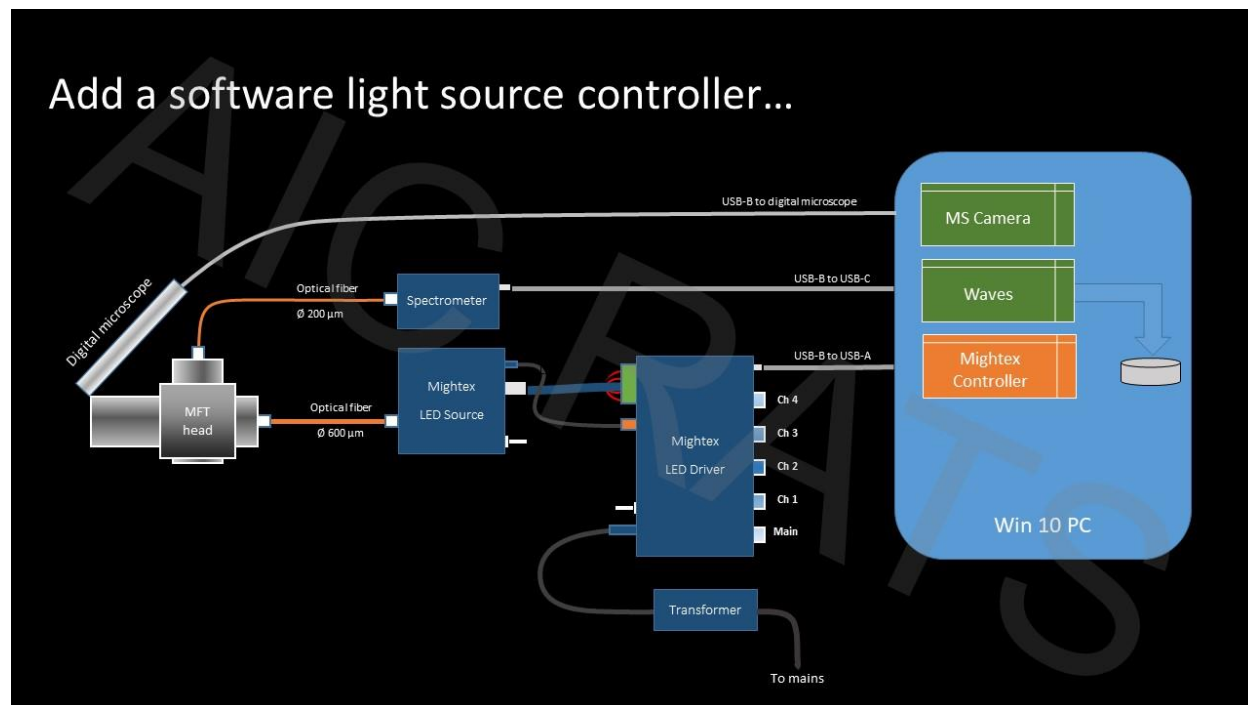
Use MS Camera (Win10) with microscope to locate spot...



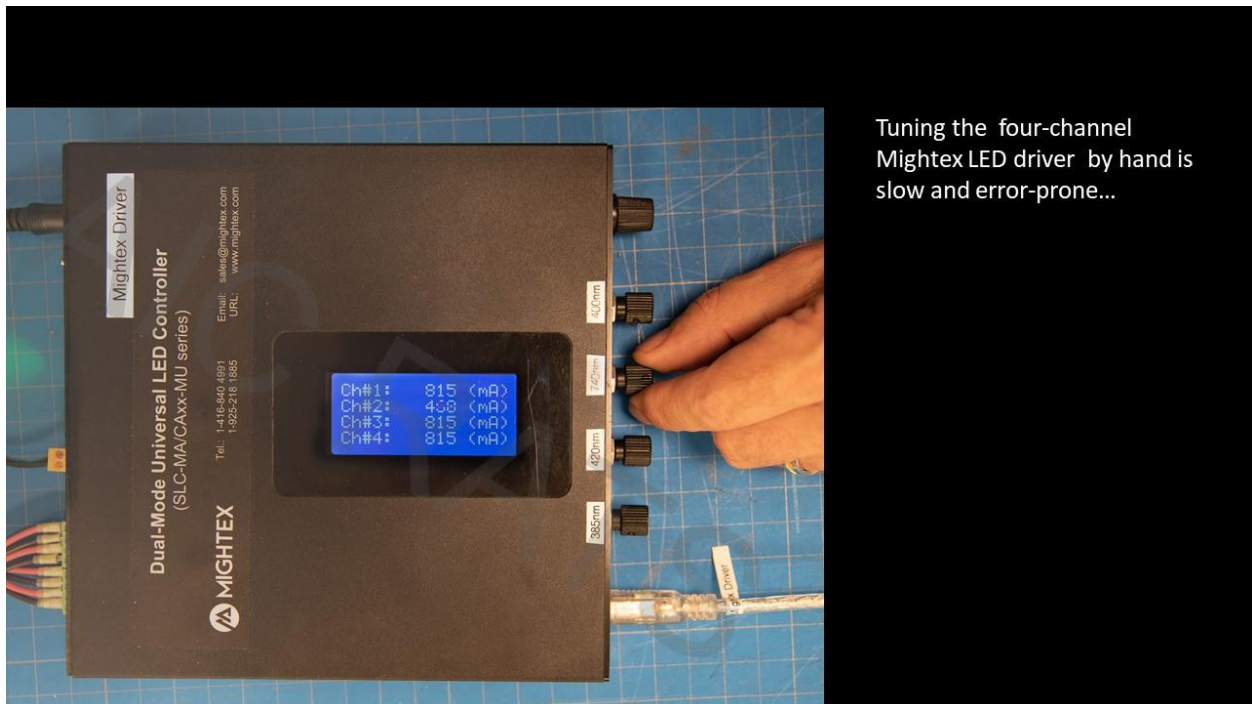
With the microscope, you can locate the MFT spot accurately on the object, and also get more repeatable focusing.

Microsoft Camera, which comes free with Windows 10, is perfect for this kind of live viewing...

Add a software light source controller...

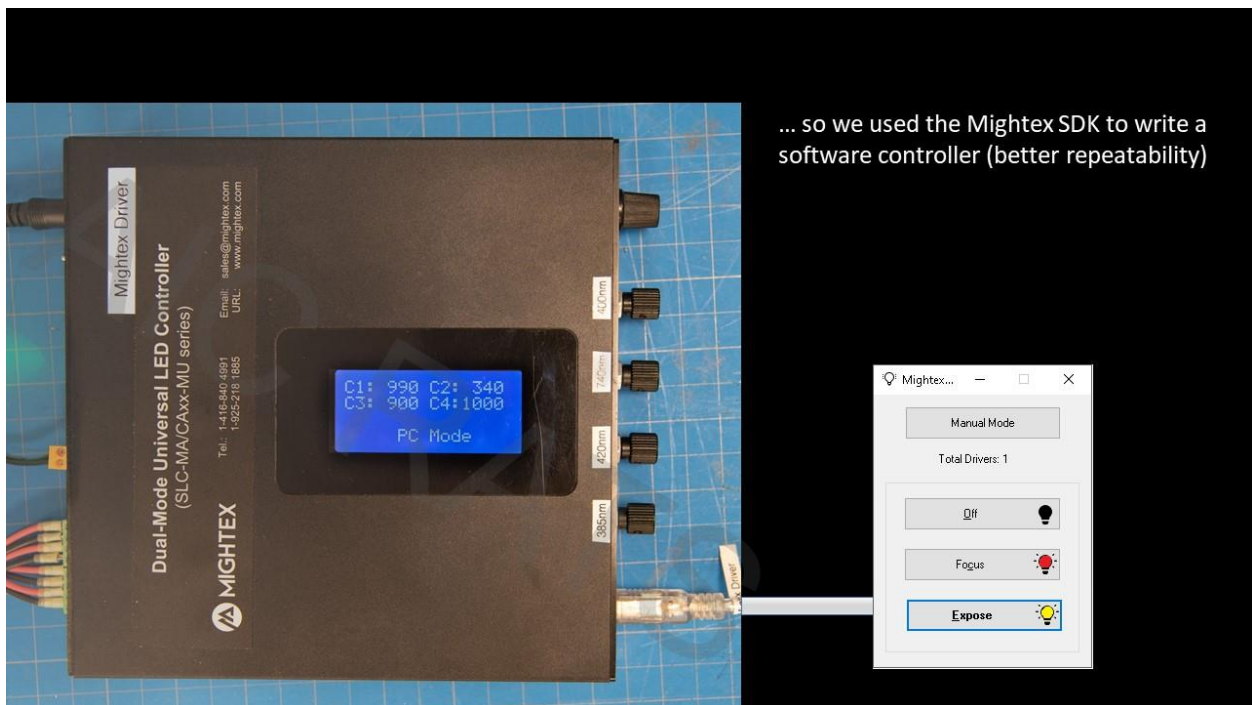


You can add a software light source controller...



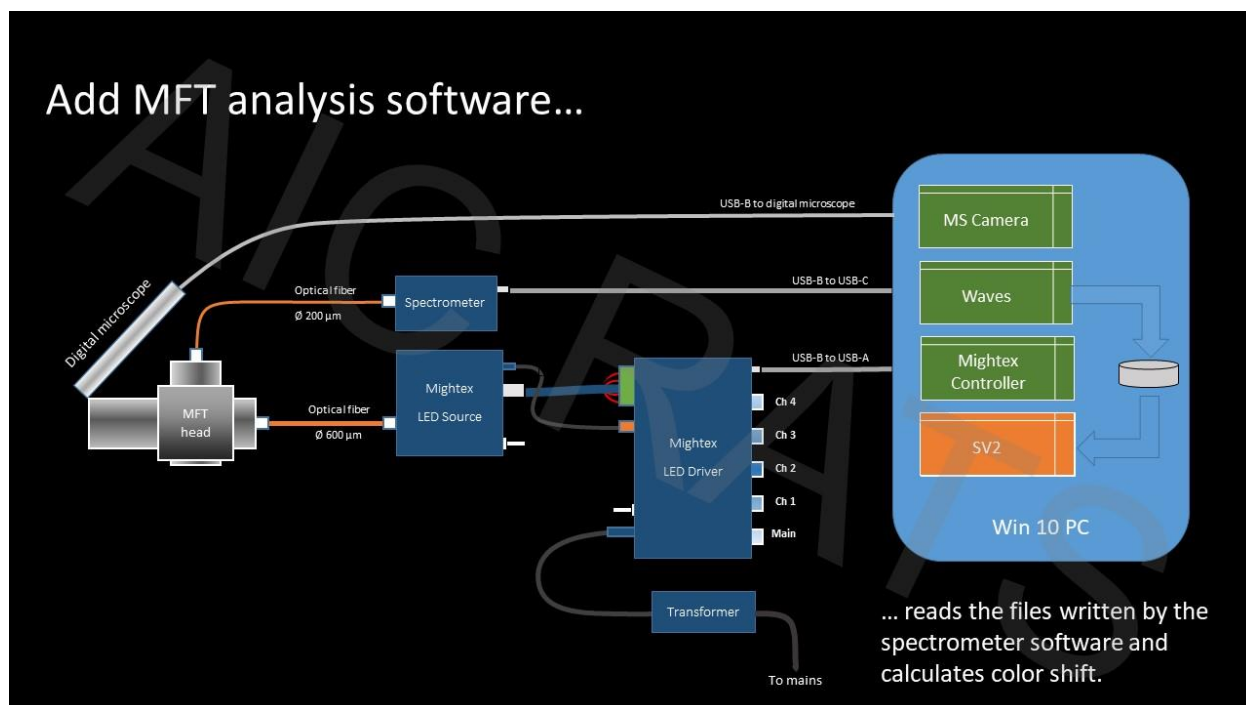
And then you're going to want to have control over the LED driver

- Now, you *can* set all four channels manually for focusing and exposure, but it's a real pain to get it right
- And since Mightex distributes a free software kit

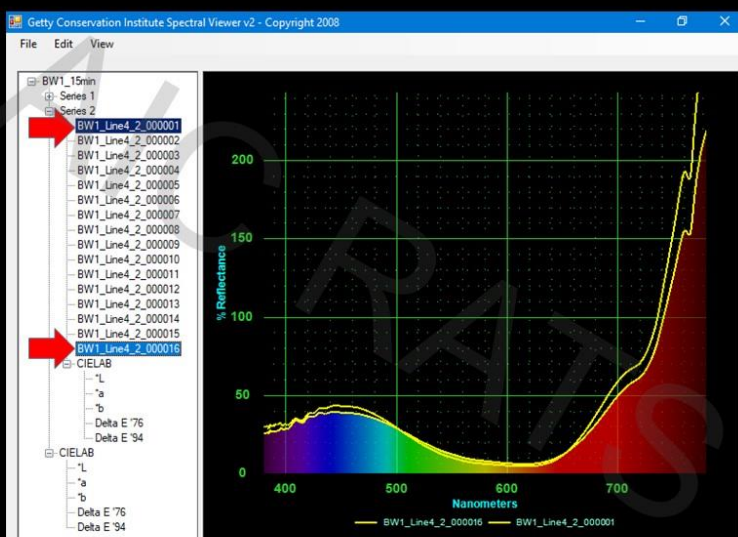


Or turn all the channels up to preset maxima when it's time for an exposure.

Add MFT analysis software...



Getty SpectralViewer v.2 (SV2) – spectral view



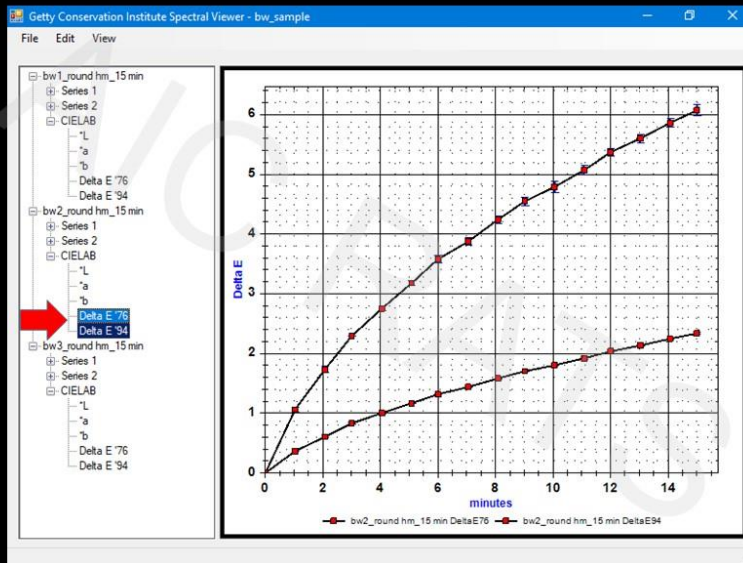
Imports and displays spectra

- CDI spectral file format only.

There's a lot to like about SV2 – it's simple to use and it does what it says on the box.

You can import spectral files written by Control Development spectrometers

Getty Spectral Viewer v.2 (SV2) – CIELAB view



Displays CIELAB values:

L^* , a^* , b^* , ΔE^*_{ab} , ΔE^*_{94}

- $L^*a^*b^*$ values are from values embedded in CDI spectral file header.
- ΔE^* values are calculated from the $L^*a^*b^*$ values embedded in the CDI spectral file header.
- Calculation of ΔE^*_{94} is incorrect.
 - The code reverses the reference and sample values in the calculation.

Notes on different ΔE^* values

ΔE^*_{ab}	<ul style="list-style-type: none"> - Sometimes referred to (incorrectly) in conservation literature as ΔE^*_{76}. - Value is the Euclidean distance between reference and sample color in the CIE $L^*a^*b^*$ color space. - Equation is commutative (you get the right value whether or not you mix up the reference and the sample). - Poor perceptual uniformity (the same ΔE^*_{ab} for two different reference colors <i>does not</i> imply the same degree of perceived color shift). - Tldr: Simple equation, but basically meaningless in terms of perceived color shift.
ΔE^*_{94}	<ul style="list-style-type: none"> - Calculation starts with Euclidean distance in the CIE $L^*a^*b^*$ space, which is then modified to improve perceptual uniformity. - Major improvement in perceptual uniformity over ΔE^*_{ab} except when comparing shifts in dark colors to shifts in light colors, or comparing blue colors to anything else. <ul style="list-style-type: none"> - (which is a bit of a problem if you are using shift in ISO Blue Wool fabrics as a standard). - Calculation is <i>not</i> commutative (you get incorrect values if you mix up the reference and the sample). - Tldr: somewhat more complex calculation, somewhat more meaningful comparisons of perceived color shift (except when comparing blues with other colors, or comparing colors which have noticeably different L^* values.)
ΔE^*_{00}	<ul style="list-style-type: none"> - Calculation starts with Euclidean distance in the CIE $L^*a^*b^*$ space, which is then <i>very heavily</i> modified to improve perceptual uniformity. - Equation is commutative, but calculation steps are complex and this is a difficult calculation to perform correctly. - Significant improvement over ΔE^*_{94} in terms of comparing perceived color shift between difference reference samples (especially w.r.t. comparing shifts in blues to shifts in other colors, or shifts in shifts in dark colors with shifts in light colors). - Tldr: Much more useful results than ΔE^*_{94} for MFT purposes. The calculation is complicated and easy to get wrong. Use a plug-in (e.g., ColorTools.xla) rather than hand-coding the calculation steps.

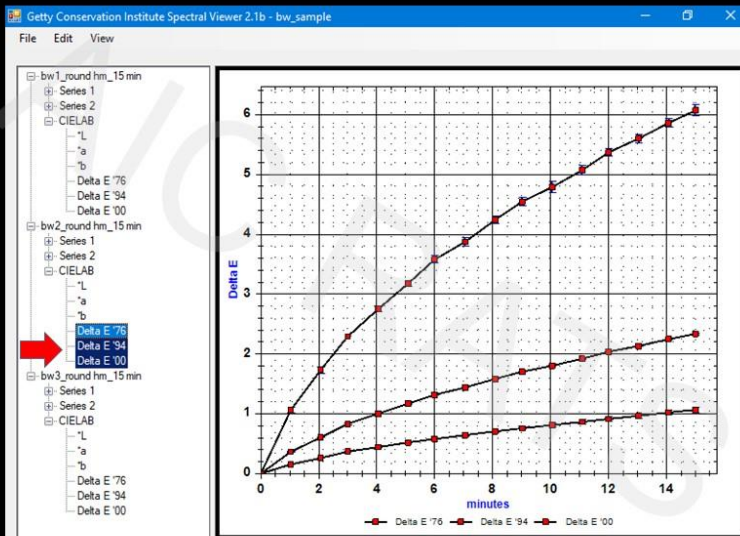
Major takeaways on different ΔE^* values

- The order that you plug the $L^*a^*b^*$ values into a ΔE^* equation can make a difference to the values you get from the calculation
 - the original (unexposed) color is the *reference* color,
 - the changed (exposed) color is the *sample* color.
- Always report *which* ΔE^* value you are using so that other users can assess your work
 - Values from the different ΔE^* calculations are not comparable.
 - Similar values of ΔE^*_{ab} for two different reference colors *does not* imply the same (or even similar) perceived color shift.
 - Similar values of ΔE^*_{96} for two different reference colors *may or may not* imply similar perceived color shifts.
- You should use ΔE^*_{00} for MFT work if you care about perceived color, otherwise use ΔR_{max} (Liang *et al*)

Notes on calculation of $L^*a^*b^*$ values

- $L^*a^*b^*$ values are calculated for a particular CIE Observer and CIE Standard Illuminant – it is important to report which Observer and Illuminant you use because it makes a difference to the values you get.
 - CIE Standard Illuminant D65 is commonly used (xenon sources are a reasonable approximation).
 - CIE 1931 2° Observer is commonly used, but may be less accurate (in terms of measuring perceived color shift) than the CIE 1964 10° Supplementary Observer.
- The calculation of $L^*a^*b^*$ is defined for spectral intensity sampled at 1, 5, 10, or 20 nm boundaries.
 - There is only a *very tiny* difference between the values calculated at 1 or 5 nm intervals (and, in fact, the result at 5 nm intervals is likely the more “accurate” value).
 - Values calculated by “continuous” equations are likely to be less accurate than the 1 or 5 nm data (although still likely to be more accurate than the uncertainty introduced by spectrometer wavelength-shift errors.)

Getty SpectralViewer v.2.1 (SV2.1)

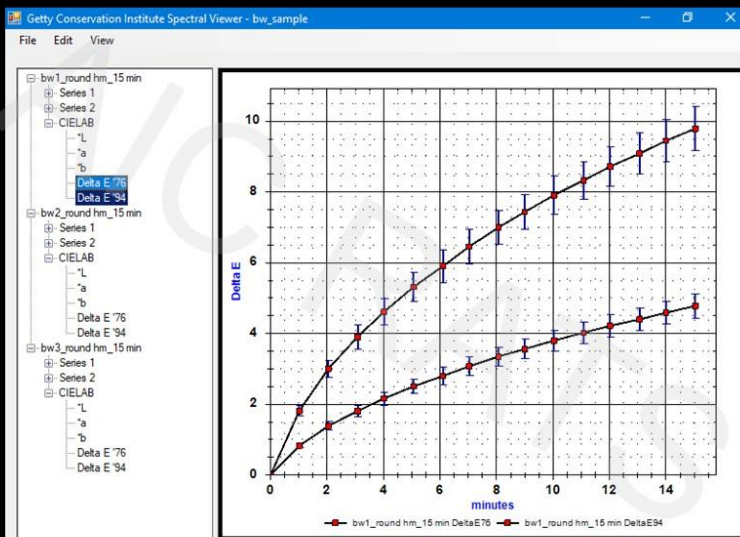


Displays CIELAB values:

L^* , a^* , b^* , ΔE^*_{ab} , ΔE^*_{94} and ΔE^*_{00}

- $L^*a^*b^*$ values are from the Ocean Optics spectral file header.
- ΔE^* values are calculated from the embedded $L^*a^*b^*$ values.
- ΔE^*_{00} calculation added.
- Error in ΔE^*_{94} calculation was corrected.

Remaining problems Getty Spectral Viewer v.2.1 (SV2.1)



- Requires CDI spectrometer file format.
 - Can't use other spectrometers.
- Error is displayed only in the y-axis
 - Uncertainty can also result from system delays in reading the spectrometer, so error in both axes makes more sense.
- Error is displayed as $\pm 0.5 \sigma_{\text{population}}$
 - $\pm 1 \sigma$ is more usual.
 - Given the small number of series, $\pm 1 \sigma_{\text{sample}}$ makes more sense.
- Analysis *after* all spectra are acquired.
 - Would be better to monitor the color shift in real time, so that you can stop test before damaging highly light-sensitive colors.
- User interface is a little dated
 - Hard to handle large data sets.
 - Hard to compare CIELAB from different surveys.
 - x-axis for CIELAB is always elapsed time.
 - No possibility of a^* vs. b^* plot, etc.
- Exporting data for use in other programs is hard.

SpectralViewer v.3 (SV3), currently in beta

v.3beta

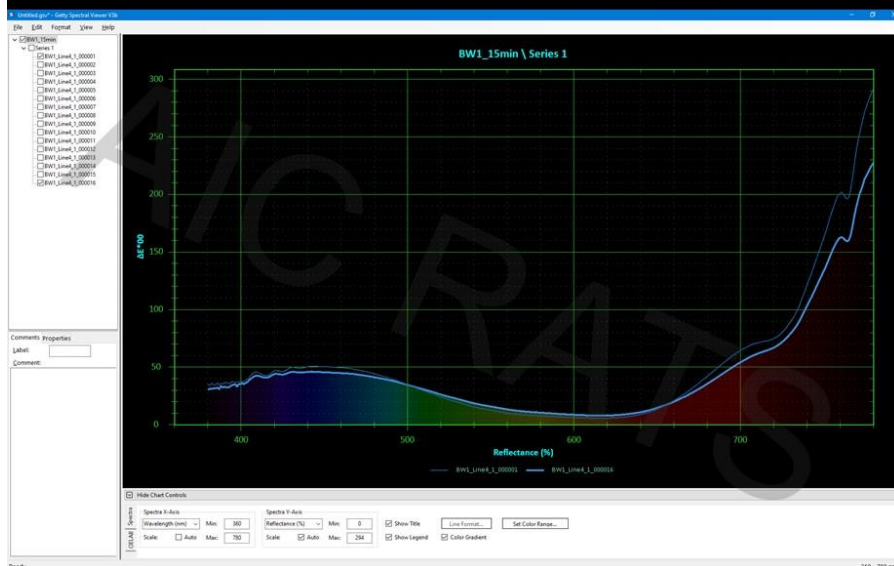


JP Brown,
David Carson

Spectral Viewer

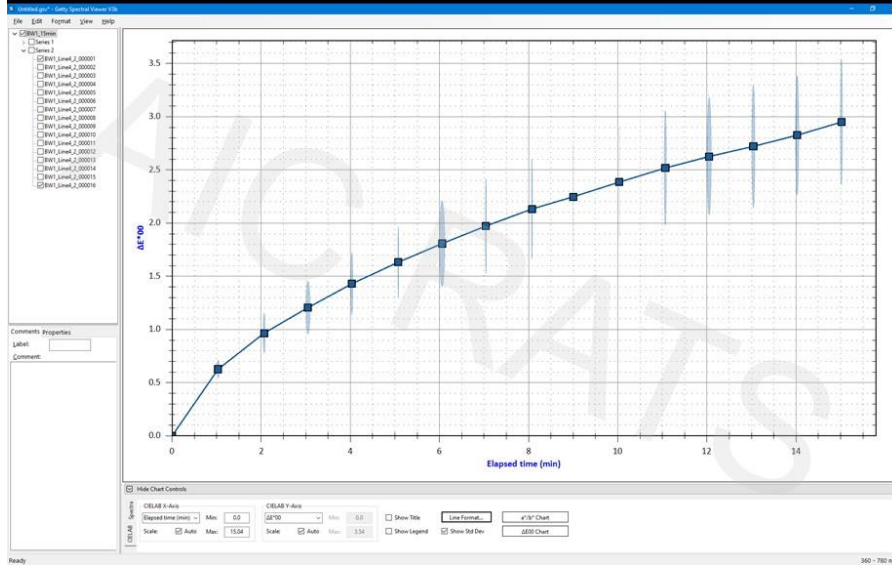
splash screen Image credit: <https://www.freeimageslive.co.uk/>

SpectralViewer v.3 (SV3) - spectral view

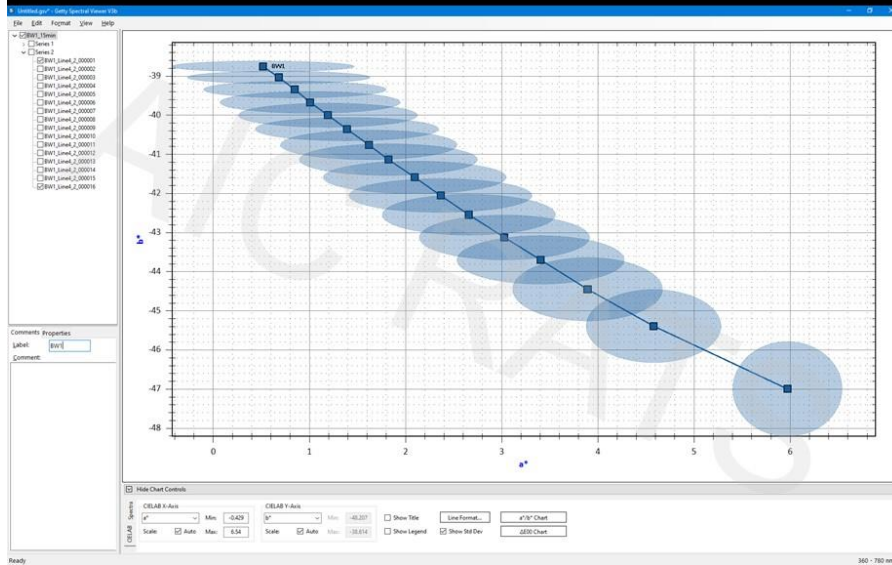


- Spectral file formats:
 - CDI
 - Ocean Optics
 - ASCII with header
 - Broadcom/RGB Photonics
 - uncompressed
- Automatic coloring of spectral lines
 - Line color is the color represented by the spectrum.
 - Optional feature to increase color difference.
- Automatic emphasis of last spectrum line.
 - Easier to understand the direction of color shift.

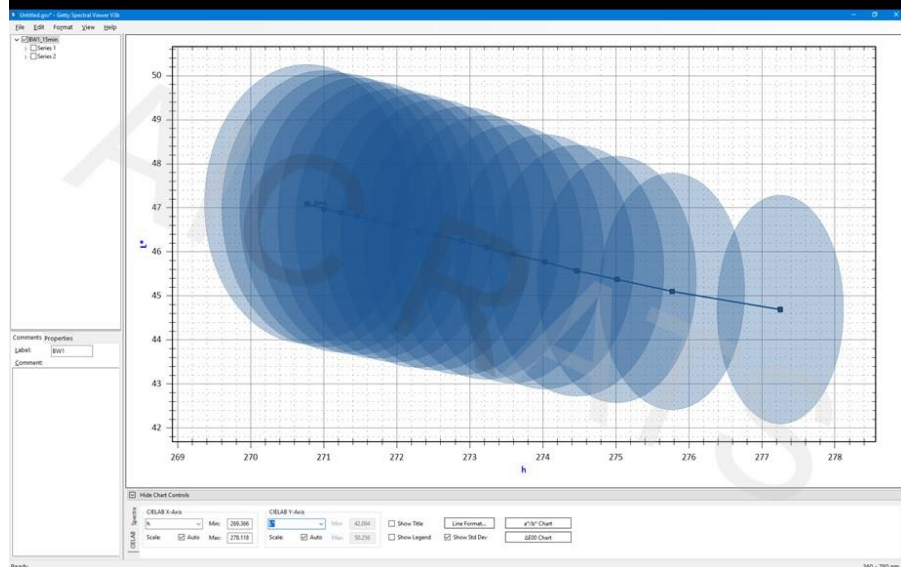
SpectralViewer v.3 (SV3) - CIELAB view



- Displays CIELAB values:
 - L^* , a^* , b^*
 - h , C^*
 - ΔE^*_{ab} , ΔE^*_{94} , ΔE^*_{00}
- X-axis can be any CIELAB variable (or elapsed time, or exposure)
- Y-axis can be any CIELAB variable
- Selection of axis variables is moved to a panel at the bottom of the screen.
 - Easier to navigate when there are lots of data.
- Error is displayed in both axes as a semi-transparent ellipse with major axes $\pm 1 \sigma_{\text{sample}}$

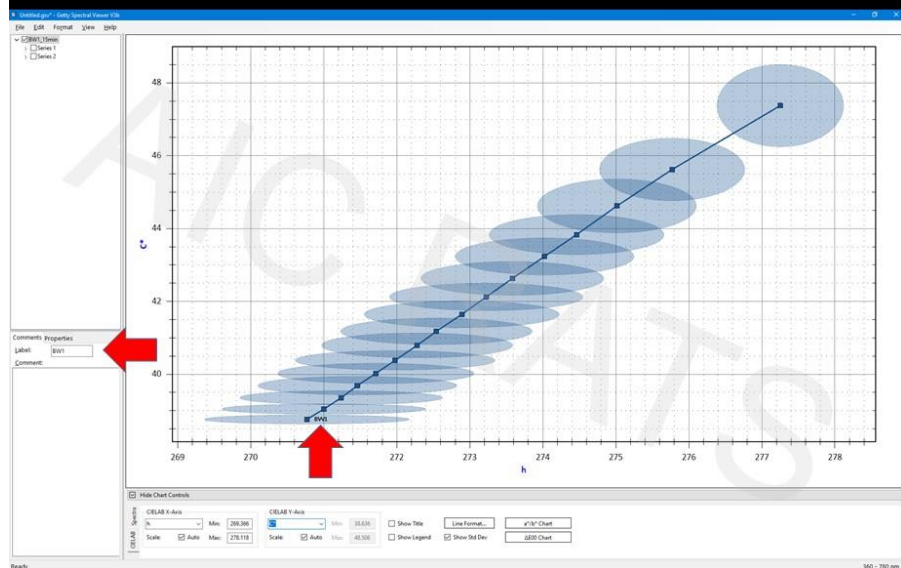
SpectralViewer v.3 (SV3) - a^*/b^* plot

- Having arbitrary assignment of CIELAB and ΔE^* values to x- and y- axes means that you can do an a^*/b^* plot (even though this is not actually very useful)...

SpectralViewer v.3 (SV3) - h/L^* plot

... Much more to the point, you can do an L^*/h (or L^*/C^*) plot.

SpectralViewer v.3 (SV3) - CIELAB line labels



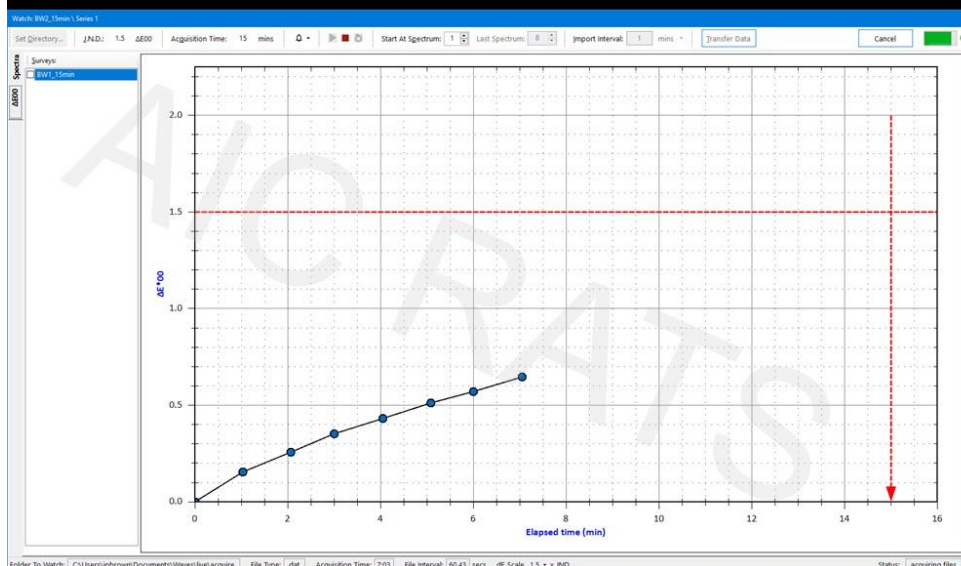
- Short text labels can be defined for each survey and series, and
 - By convention, the label display at the last point in the series or survey.
 - Positioning the label at the end helps to identify the direction of color shift.

SpectralViewer v.3 (SV3) - real-time acquisition



The "Watch" dialog allows you to review spectral files in real time as your spectrometer software writes them to disk.

SpectralViewer v.3 (SV3) - real-time acquisition



And watch how the resulting ΔE^*_{00} values change.

You can set the spectrum that you consider to be the reference color at any time during spectral acquisition.

- Makes the timing of unshuttering less stressful.

Limits on the acquisition time and the maximum allowable ΔE^*_{00} can be set (indicated on the chart by the dashed red lines).

- If the limits are exceeded, an audible alarm will sound.

And watch delta-E-2000 change in real time.

[beat]

You can set designated limits for

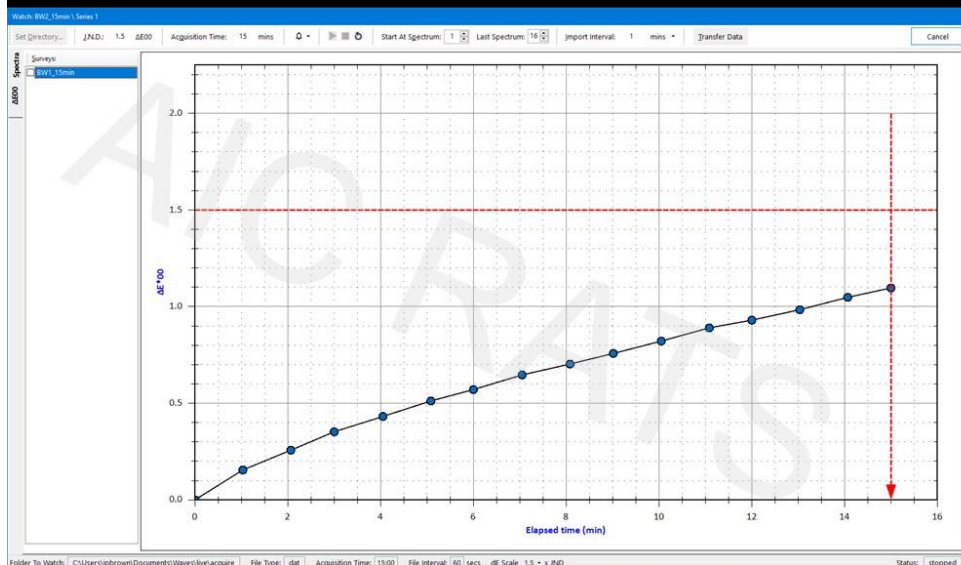
Delta-E (CLICK) and

The acquisition time (CLICK)

And there are audible and visual alarms (CLICK) if your values go out of range.

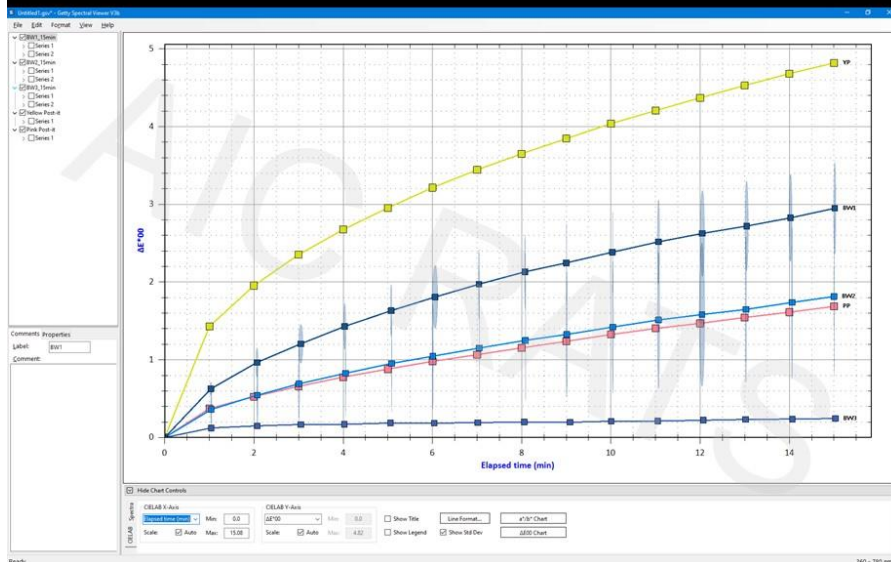
[beat]

Spectral Viewer v.3 (SV3) - real-time acquisition



After spectral acquisition is complete for a series, you can set the desired time interval between readings, and transfer the data to the main program.

SpectralViewer v.3 (SV3) - imported data



Multiple surveys for BW 1-3 reference values and the color shifts in off-brand Post-it notes.

Notes on elapsed time vs. exposure

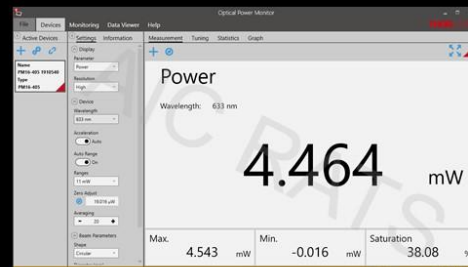
Elapsed Time

- Individual MFT users have reported results color change results in terms of elapsed time and color shift at an approximately constant exposure (xenon sources reduce measurably in intensity over their lifetime).
- To relate elapsed time to exposure, ISO Blue Wool standards have been exposed with the same setup at approximately the same time as the colors (same day) and the fading of the tested colors is related to the ISO Blue Scale.
- This approach makes it difficult to compare the change in different colors in detail when
 - samples are measured with the same setup on widely separated dates, or
 - samples are measured with different setups (e.g. two different MFT machines, or the same retroreflective machine with different forelenses).

Exposure

- Exposure can be calculated if one knows the length of time that the spot is illuminated, and the intensity of the MFT spot.
- The intensity can be calculated from the power of the incident light (say, spectral power in mW in the range 380-760 nm corrected to lumens) and the diameter of the focused MFT spot.
- Time is already being measured, the power can be characterized periodically with a spectral power meter, and the diameter of the MFT spot can be measured periodically by focusing the spot on a digital camera sensor and taking an image (assuming the pixel dimensions of the sensor are known).
- Once you know the light intensity and the time, you can report color change as a function of cumulative exposure and you more easily relate samples from widely separated dates, or samples from different MFT setups.

Measure power with Thorlabs optical power meter



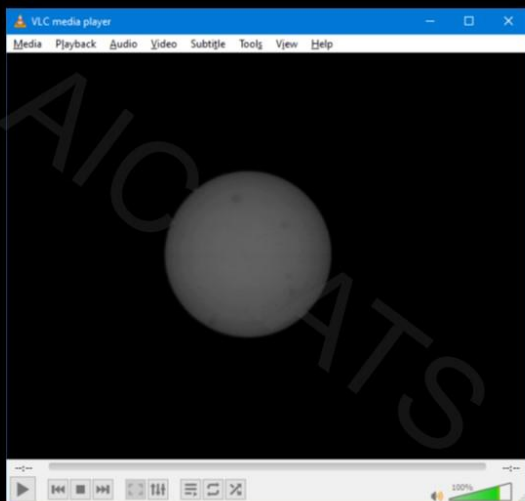
Focus the MFT spot on a hacked consumer web camera



- Removing the front cover, and then the lens assembly, of the Logitech C270 is easy.
- Once the sensor is exposed, focus the MFT on the sensor.

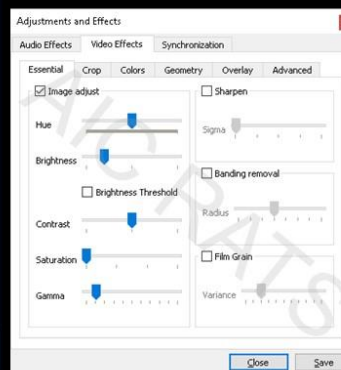
- turn down the light source power,
- (CLICK) focus the spot on the bare sensor,...

Take an image of the spot with VLC Media player

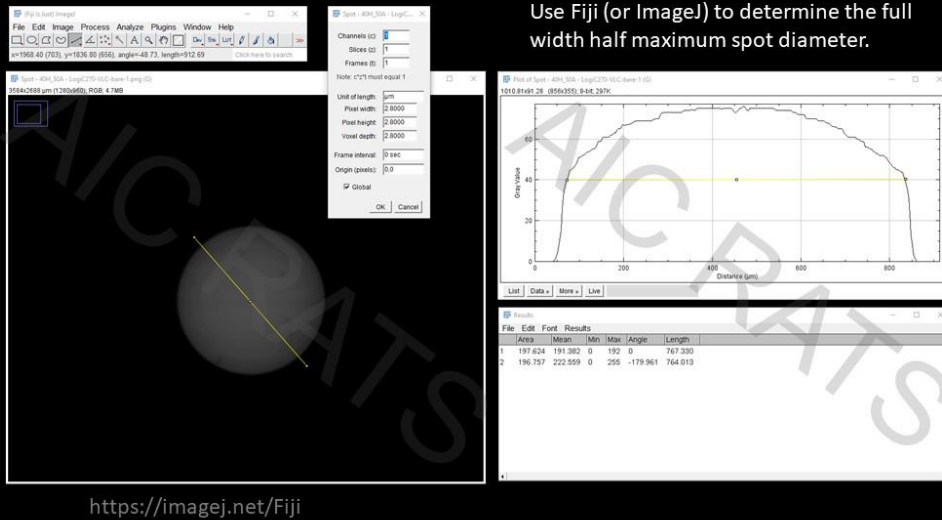


<https://www.videolan.org/vlc/>

Turn down light source (or add neutral density filter) and take pictures of focused spot with VLC Media Player (more controllable than MS camera, and gets all the sensor area as opposed to MS Camera's cropped view).



Measure the FWHM spot diameter from the image



SpectralViewer v.3 (SV3) - MFT Configuration

Add New MFT Configuration

MFT Configuration

Title: Retroreflective 50A/40H

Institution: The Field Museum

Spectrometer: Broadcom QMini WIDE-VIS

Light Source: Mightex LED { 990; 340; 900; 1000 } mA

Filters: -

Focusing method: Red spot minimization

Shutter: manual aluminium foil

Notes:

Spot Diameter: 0.673 mm

Luminous flux: 0.788 lumen

Beam Angle: 15 degrees from surface normal

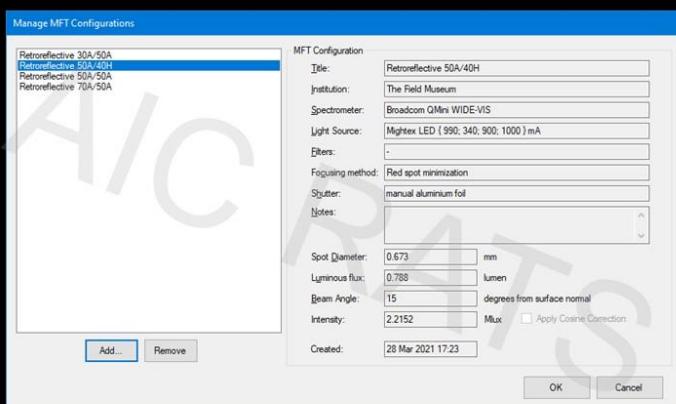
Intensity: 2.2552 Mlx ☐ Apply Cosine Correction

Created: 28 Mar 2021 17:23

OK Cancel

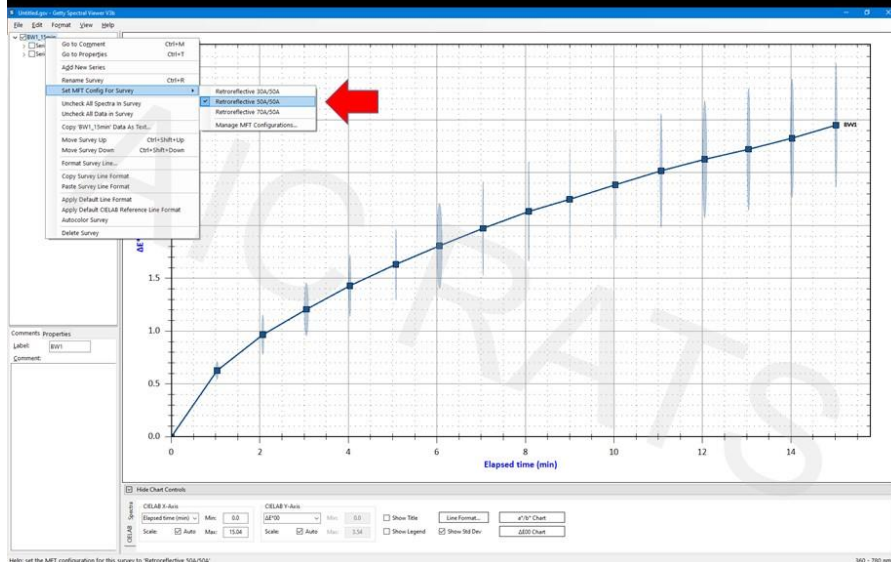
- GSV3 stores information about the MFT configuration used for each survey...
- ... along with information about the measured spot diameter, luminous flux, and the beam angle.
- These values can be used to calculate the intensity of the MFT spot in Mlx (with or without cosine correction).

SpectralViewer v.3 (SV3) - MFT Configuration



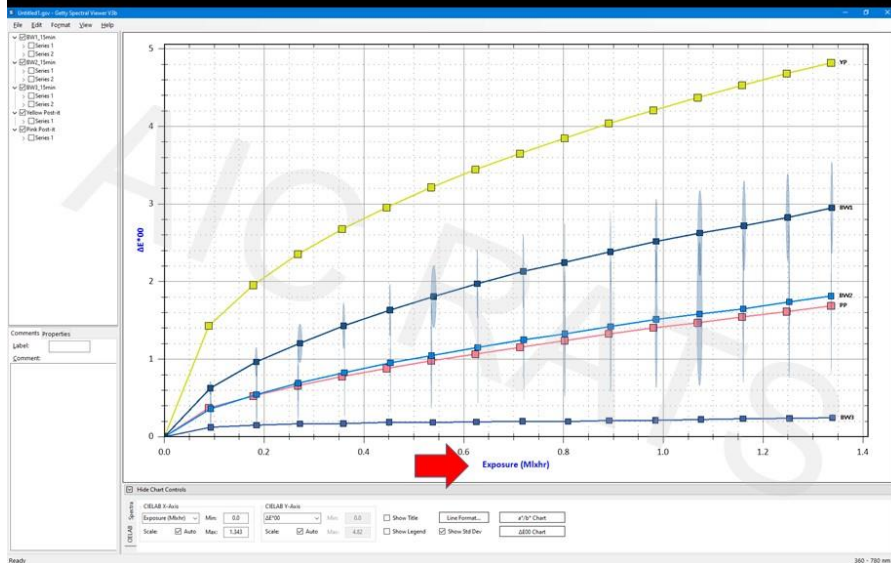
The configurations are embedded in the document for future reference, and are also added to a list accessible to all users on the computer.

SpectralViewer v.3 (SV3) - MFT Configuration



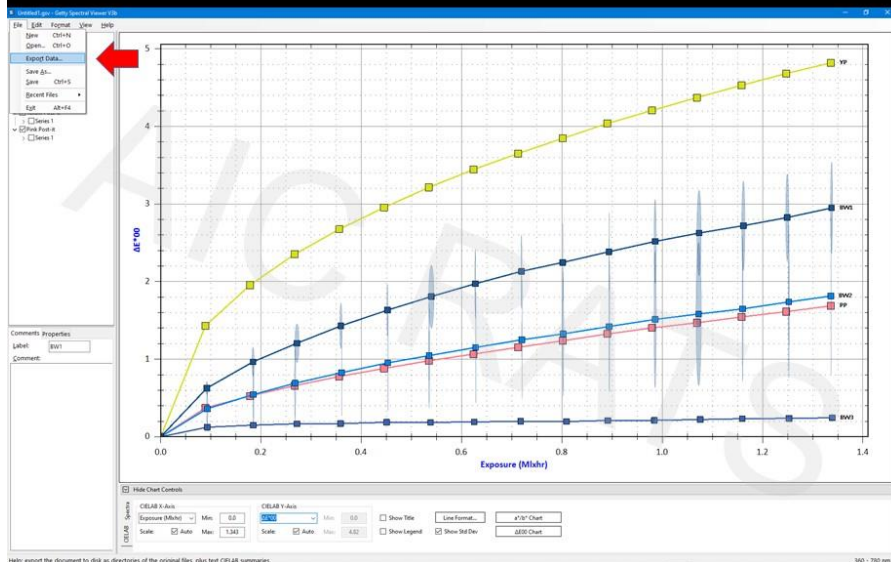
A configuration can be selected from the list and applied to a particular survey.

SpectralViewer v.3 (SV3) - MFT configuration



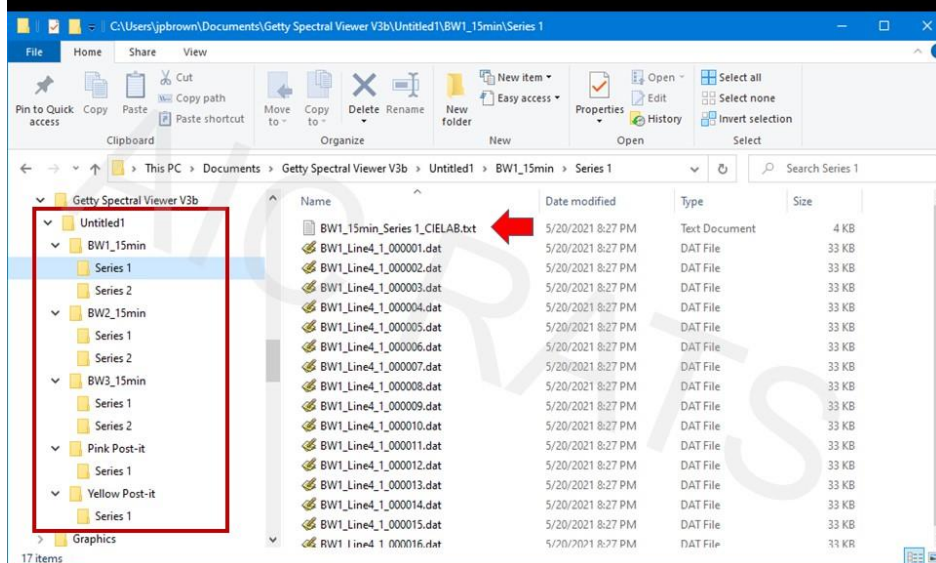
Surveys with an MFT configuration that includes power and spot diameter values can be compared using the calculated exposure values.

SpectralViewer v.3 (SV3) - data export



Spectral data can be exported to disk as spectral files for further analysis...

Spectral Viewer v.3 (SV3) - data export

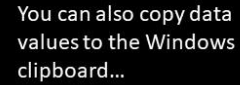


... in a neatly organized folder structure, with a text file in each folder containing the CIELAB values for the survey or series.

SpectralViewer v.3 (SV3) - data export

Example of CIELAB data for a survey....

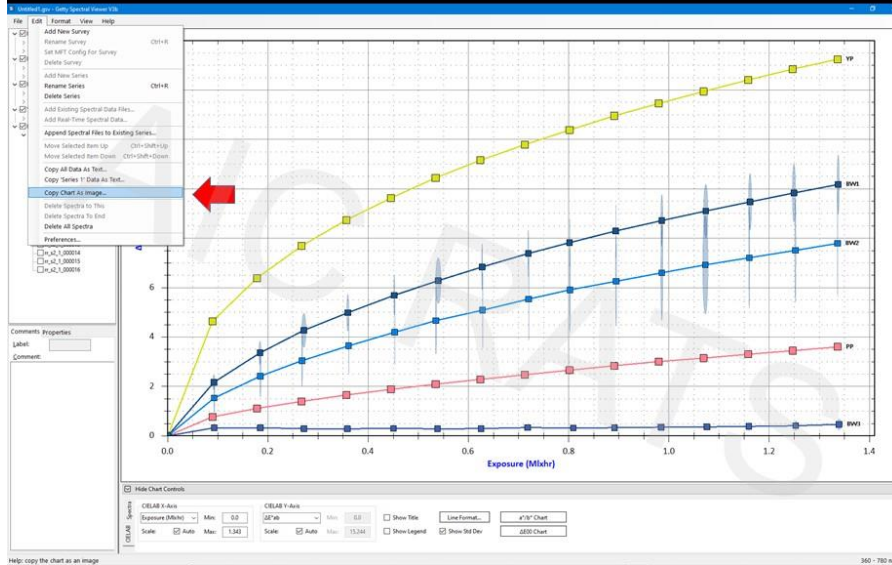
file name	Elapsed time (min)	Exposure (Mlxhr)	L*	a*	b*	C*	h	ΔE*ab	ΔE*94	ΔE*00
BW1_line4_1_000001.dat	0.0	0.0	46.5274	5.5697	-47.8521	48.1751	276.639	0.0	0.0	0.0
BW1_line4_1_000002.dat	1.0167	0.0906	47.0038	4.084	-46.0477	46.2284	275.0684	2.3854	1.081	0.6875
BW1_line4_1_000003.dat	2.05	0.1826	47.3523	3.3422	-45.019	45.1429	274.2459	3.6971	1.6956	1.0993
BW1_line4_1_000004.dat	3.0833	0.2746	47.5849	2.7896	-44.1329	44.221	273.6169	4.7623	2.1618	1.3825
BW1_line4_1_000005.dat	4.0167	0.3578	47.8183	2.4023	-43.5272	43.5934	273.159	5.5139	2.5235	1.6384
BW1_line4_1_000006.dat	5.0667	0.4513	48.0186	2.0225	-42.9108	42.9584	272.6986	6.2628	2.8693	1.8699
BW1_line4_1_000007.dat	6.1	0.5434	48.2198	1.6928	-42.3541	42.3879	272.2887	6.9371	3.1885	2.0932
BW1_line4_1_000008.dat	7.0333	0.6265	48.3995	1.4232	-41.8783	41.9024	271.9464	7.509	3.4621	2.289
BW1_line4_1_000009.dat	8.0667	0.7185	48.5587	1.1679	-41.4181	41.4346	271.6152	8.0559	3.7178	2.4671
BW1_line4_1_000010.dat	9.0	0.8017	48.6762	0.969	-41.022	41.0335	271.3531	8.5108	3.9199	2.6006
BW1_line4_1_000011.dat	10.0333	0.8937	48.7955	0.7159	-40.5641	40.5704	271.0111	9.0453	4.1541	2.7488
BW1_line4_1_000012.dat	11.0833	0.9872	48.9363	0.5349	-40.2155	40.219	270.762	9.4589	4.3559	2.9004
BW1_line4_1_000013.dat	12.0167	1.0704	49.0306	0.3454	-39.8649	39.8664	270.4964	9.8669	4.5362	3.017
BW1_line4_1_000014.dat	13.0667	1.1639	49.1262	0.1778	-39.4911	39.4915	270.258	10.2826	4.7129	3.1297
BW1_line4_1_000015.dat	14.0	1.247	49.1979	0.0094	-39.1431	39.1431	270.0138	10.6722	4.8732	3.2243
BW1_line4_1_000016.dat	15.0333	1.3391	49.3286	-0.1513	-38.8478	38.8481	269.7768	11.0297	5.0548	3.3669



SpectralViewer v.3 (SV3) - data export

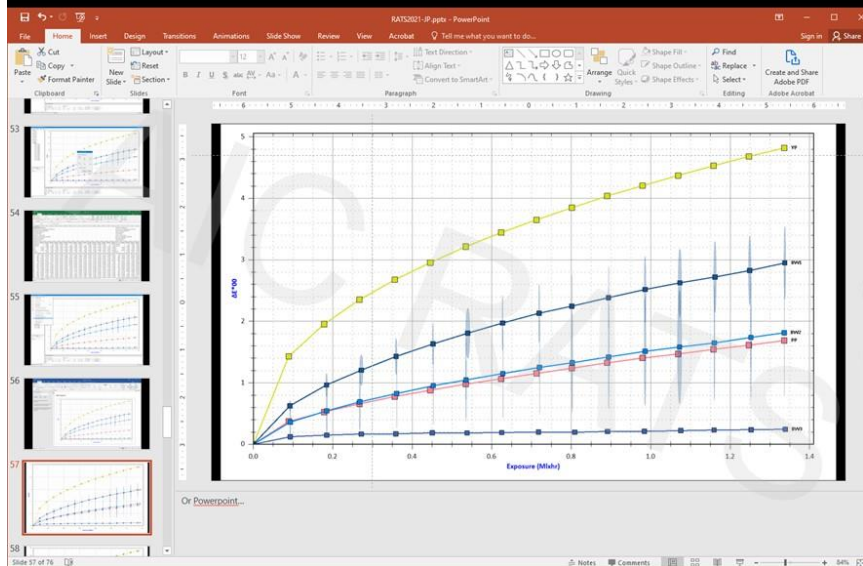
...and paste the copied data directly into programs that accept tab-separated text (such as MS Excel).

SpectralViewer v.3 (SV3) - data export



You can also copy the current chart to the clipboard as an image...

SpectralViewer v.3 (SV3) - data export



...and paste it directly into programs such as MS PowerPoint or MS Word.

SpectralViewer v.3 (SV3) – change summary

Features	Getty Spectral Viewer 2 (2008)	SpectralViewer 3beta (2021)
Read spectra	one spectrometer type (Control Development)	<i>and</i> two more (Ocean Optics, RGBP/Broadcom)
	fixed acquisition time interval	variable time interval, manual shutter support
View CIELAB	after spectral acquisition	during spectral acquisition
	elapsed time vs $L^*a^*b^*$ and ΔE^*	<i>and</i> exposure, C^*h
	x-axis is always elapsed time	arbitrary x- and y-axes (can do a^*/b^* plot, etc.)
	color shift in ΔE^*_{ab} , ΔE^*_{94} (ΔE^*_{00} in v.2.1)	<i>and</i> ΔE^*_{00}
	see uncertainty in $L^*a^*b^*$, ΔE^*	<i>and</i> time, exposure, C^*h
	uncertainty shown on y-axis ($\pm 0.5 \sigma$ of population)	<i>and</i> on x-axis ($\pm 1 \sigma$ of sample for both axis)
User interface	format data lines individually	<i>and</i> automatically/collectively
	[no export options]	export spectra, CIELAB, ΔE^*
	copy data to clipboard item-by-item	<i>and</i> collectively (MS Excel-compatible)
	preserve spectral data files	<i>and</i> truncate/smooth spectral data files
	simple to operate	<i>and</i> easy to navigate
File format	read-write .gci file	read .gci file, read-write .gsv file

Finally, here's a summary of the differences between SV2 and the current beta version of SV3.

Time's short, so I'm not going to read them all out – you can review it on the video if you wish.

Acknowledgments

- Vincent Beltran, Savannah Novencido, Lionel Keene (Getty Conservation Institute)
- Dan Kaping, Erin Murphy, Stephanie Black (Field Museum)
- Paul Lane (Photo Source)
- All the alpha testers!!!
- Federica Pozzi, RATS Program Committee, the AIC conference staff.

If you would like more information about an open source MFT of your own,
email: jacoblthomas@gmail.com

If you have a software feature request, or would like to help with beta testing
email: jpbrown@fieldmuseum.org

Bibliography

- Liang, Hadia, Rebecca Lange, Andrei Lucian, P Hyndes, Joyce Townsend, Stephen Hackney. 2011. Development of portable microfading spectrometers for measurement of light sensitivity of materials. In ICOM-CC 16th Triennial Conference Preprints, ed. J. Bridgland,
- Instytut Fotonowy, 2020. <https://www.fotonowy.pl/products/micro-fading-tester/?lang=en>. Accessed September 27, 2020.
- Whitmore, Paul, Xun Pan, and Catherine Baillie. 1999. Predicting the fading of objects: identification of fugitive colorants through direct non-destructive lightfastness measurements. *Journal of the American Institute of Conservation* 38: 395–409.

Principals on Paper: Using FTIR Spectroscopy and Chemometrics for Non-Invasive Media Analysis

Julie Wertz, Leonie Müller, Arthur McClelland, Penley Knipe

Original Abstract

The identification of media in paper-based artworks is often challenging due to the minimal amounts of material present and the potential impact of sampling on most objects. X-ray fluorescence spectroscopy (XRF) is a valuable non-invasive tool to identify many pigments, but it does not reliably detect elements lighter than aluminum, and cannot be used for carbon-based (organic) materials like gums, resins, glues, inks, and lake pigments. Raman spectroscopy has some non-invasive applications in this context, but infrared spectroscopy consistently provides more detailed spectra for these materials due to their structure and how it interacts with the instruments. Fourier transform infrared (FTIR) instruments come in a variety of configurations, some of which can be used for non-invasive analysis of artworks. Instrument interfaces, like attenuated total reflectance (ATR), diffuse reflectance, or specular reflectance, will influence the data collected and require corresponding reference spectra for interpretation.

FTIR spectra show the total response of all materials present. This means mixed materials, a highly likely occurrence, can be difficult to fully characterize due to potential overlapping peaks and minor components being overwhelmed in the mixture. Slight variations in spectra, which may have significance, can be overlooked by the human eye while major differences can be distracting without saying much. Chemometrics, the application of statistical methods to chemical data, is a way to analyze spectra using algorithmic processing of known and unknown samples.

In this paper, the application of chemometric techniques like principal component analysis (PCA) is explored using FTIR spectral collected from a set of prepared references. These references include a wide varieties of blank papers and inks, such as including iron gall, bistre, and lampblack, that are prepared in-house. We present the samples analyzed, the resulting statistical modeling, and what potential benefits and limitations identified during this investigation. The aim of this work is to determine to what extent it is possible to extract more information about media from works of art that cannot be sampled by using non-invasive analysis.

This work was performed in part at the Center for Nanoscale Systems at Harvard University, a member of the National Nanotechnology Coordinated Infrastructure Network, NSF award no. 1541959.

Elucidation of Natural Organic Red Colorants on Paper via Microsampling and Surface Enhanced Raman Spectroscopy

Lyndsay Kissell, Trine Quady, Samantha Springer, Jeannie Kenmotsu, Tami Lasseter Clare

Original Abstract

Definitive chemical analysis of natural colorants is an ongoing challenge for a variety of objects the amount of colorant is small and has frequently undergone chemical changes as a result of environmental exposure. In Japanese nishiki-e (brocade) prints of the 18th century, natural colorants were used to produce heavily bound, thinly printed inks on fine papers. This important historical period of mass produced, profusely colored and elaborately produced prints marks a decisive shift in the visual and material qualities of Japanese printmaking. Of particular interest in this study is the wide range of pink, red, and orange colors that appears in these works. Historically available organic red colorants are Safflower, Sappan, or Madder inks. Recent studies have suggested the contemporaneous usage of those three and the mixing of colorants to produce a variety of hues.

In this work, a microsampling tool was developed to collect colorant particulate, on the order of 5-10 μm in size, from the surface of prints. This microsampling tool utilizes a small hydrogel surface in contact with the print for one minute to mechanically collect colorant without using harsh solvents nor unnecessarily extended sampling times. By applying silver nanoparticles onto the small samples retained on the hydrogel, a plasmon resonance effect is induced and the Surface Enhanced Raman spectroscopy (SERS) can be performed.

Advantages of SERS over other analytical techniques include extreme sensitivity to analyte molecules, suppression of interfering molecular fluorescence, and unique chemical fingerprints resultant from the molecular structure. Additionally, through extensive analysis of laboratory-produced standards, including accelerated aging techniques, spectral (and in turn molecular) changes may be identified. Successful identification of organic red colorants, after fading or color shifting due to exposure, is demonstrated. This method is also shown to elucidate mixtures of red colorants. This methodology has been applied to works attributed to Suzuki Harunobu in the collection of the Portland Art Museum to better understand the use of individual colorants and colorant mixtures in mid-18th c. Japanese printmaking.